

Russian Original Vol. 36, No. 4, April, 1974

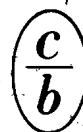
October, 1974

SATEAZ 36(4) 323-432 (1974)

SOVIET ATOMIC ENERGY

АТОМНАЯ ЭНЕРГИЯ
(ATOMNAYA ENERGIYA)

TRANSLATED FROM RUSSIAN



CONSULTANTS BUREAU, NEW YORK

SOVIET ATOMIC ENERGY

Soviet Atomic Energy is a cover-to-cover translation of *Atomnaya Énergiya*, a publication of the Academy of Sciences of the USSR.

An agreement with the Copyright Agency of the USSR (VAAP) makes available both advance copies of the Russian journal and original glossy photographs and artwork. This serves to decrease the necessary time lag between publication of the original and publication of the translation and helps to improve the quality of the latter. The translation began with the first issue of the Russian journal.

Editorial Board of *Atomnaya Énergiya*:

Editor: M. D. Millionshchikov

Deputy Director
I. V. Kurchatov Institute of Atomic Energy
Academy of Sciences of the USSR
Moscow, USSR

Associate Editor: N. A. Vlasov

A. A. Bóchvar

N. A. Dollezhal'

V. S. Fursov

I. N. Golovin

V. F. Kalinin

A. K. Krasin

A. I. Leipunskii

V. V. Matveev

M. G. Meshcheryakov

P. N. Palei

V. B. Shevchenko

V. I. Smirnov

A. P. Vinogradov

A. P. Zefirov

Copyright © 1974 Plenum Publishing Corporation, 227 West 17th Street, New York, N.Y. 10011. All rights reserved. No article contained herein may be reproduced, stored in a retrieval system, or transmitted, in any form or by any means, electronic, mechanical, photocopying, microfilming, recording or otherwise, without written permission of the publisher.

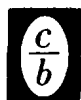
Consultants Bureau journals appear about six months after the publication of the original Russian issue. For bibliographic accuracy, the English issue published by Consultants Bureau carries the same number and date as the original Russian from which it was translated. For example, a Russian issue published in December will appear in a Consultants Bureau English translation about the following June, but the translation issue will carry the December date. When ordering any volume or particular issue of a Consultants Bureau journal, please specify the date and, where applicable, the volume and issue numbers of the original Russian. The material you will receive will be a translation of that Russian volume or issue.

Subscription
\$87.50 per volume (6 Issues)

Single Issue: \$50
Single Article: \$15

Prices somewhat higher outside the United States.

CONSULTANTS BUREAU, NEW YORK AND LONDON



227 West 17th Street
New York, New York 10011

4a Lower John Street
London W1R 3PD
England

Soviet Atomic Energy is abstracted or indexed in *Applied Mechanics Reviews*, *Chemical Abstracts*, *Engineering Index*, *INSPEC-Physics Abstracts* and *Electrical and Electronics Abstracts*, *Current Contents*, and *Nuclear Science Abstracts*.

Published monthly. Second-class postage paid at Jamaica, New York 11431.

SOVIET ATOMIC ENERGY

A translation of *Atomnaya Énergiya*

October, 1974

Volume 36, Number 4

April, 1974

CONTENTS

Engl./Russ.

ARTICLES

Role of Fast Reactors in the Structure of Developing System of Nuclear Energetics

– V. N. Bolbolovich, Yu. I. Koryakin, G. B. Levental', S. Ya. Chernavskii,

N. A. Baskakova, and T. P. Chernysheva 323 251

MHD Conversion of Energy from Pulsed Thermonuclear Reactors

– E. P. Velikhov, V. S. Golubev, and V. V. Chernukha 330 258

Electron Heating in Magnetic Traps for Spiral Electron Beam Interaction with

Plasma – B. S. Akshanov 333 261

Effect of Changes in the Nonuniformity of Energy Evolution in the Fuel of Thermal

Reactors on the Temperature Distribution in the Fuel Elements

– V. S. Yamnikov, L. L. Malanchenko, and V. I. Solyanyi 341 269

Corrosion Resistance of Steels of the Ferritic Austenitic Class and Possibility of

Using Them in Nuclear Power Systems – V. V. Gerasimov, A. I. Gromova,

V. N. Belous, V. A. Gosteva, and É. G. Fel'dgandler 345 273

Slowing-Down of Neutrons in the Presence of Inelastic Scattering – Yu. A. Medvedev,

E. V. Metelkin, and G. Ya. Trukhanov 349 277

BOOK REVIEWS

T. A. Germogenova, V. P. Mashkovich, V. G. Zolotukhin, and A. P. Suvorov

– The Albedo of Neutrons – Reviewed by B. R. Bergel'son 354 281

Spectra of the Prompt Neutrons Arising from the Spontaneous Fission of ^{252}Cf , ^{244}Cm ,and ^{240}Pu – Z. A. Aleksandrova, V. I. Bol'shov, V. F. Kuznetsov,

G. N. Smirenkin, and M. Z. Tarasko 355 282

ARTICLES

Effective Neutron Absorption Cross Sections for Californium, Einsteinium, and

Fermium in the Central Channel of the SM-2 Reactor – V. A. Anufriev,

V. D. Gavrilov, Yu. S. Zamyatnin, and V. V. Ivanenko 359 286

BOOK REVIEWS

L. A. Il'in, G. V. Arkhangel'skaya, Yu. O. Konstantinov, and I. A. Likhtarev

– Radioactive Iodine in the Problem of Radiation Safety – Reviewed by

Yu. V. Sivintsev 363 290

REVIEW

Some Problems of Interaction of Casing Steels with Sodium Heat-Transfer Agent

– A. G. Ioltukhovskii 365 291

BOOK REVIEWS

B. I. Taratorin – Stress Simulation Nuclear Reactor Designs – Reviewed by

A. F. Gurov 375 300

CONTENTS

(continued)

Engl./Russ.

ABSTRACTS

Dose Distributions in Biological Tissue from Superhigh-Energy Nucleon Beams – I. M. Dmitrievskii, E. L. Potemkin, and V. V. Frolov	376	301
Absorbed-Dose Depth Distribution in Tissue-Equivalent Absorber for Quasiisotropic Incidence of 1 MeV Electrons – R. Ya. Strakovskaya, G. N. P'yankov, and I. R. Entinzon	377	302
Electron Microscopic Study of Oxide Films on Zirconium Alloys – T. Kh. Margulova, T. I. Malova, V. A. Dmitriev, and V. M. Ryabov	378	303
Effect of Coherent Scattering on the Spatial Distribution of the Intensity of γ -Radiation from a Point Monodirectional Source – A. M. Kol'chuzhkin, A. I. Ksenofontov, A. M. Panchenko, V. N. Potapov, and V. V. Uchaikin	379	303

LETTERS TO THE EDITOR

Heat Exchange in the Interpipe Space of the Intermediate Heat Exchanger of a BOR-60 Installation – V. I. Kondrat'ev, L. K. Kruplin, and V. F. Masnyi	380	305
Forming of the Structure of Vibration-Compacted Uranium Dioxide in Fuel Elements during Full-Scale Tests in a Fast BOR-60 Reactor – E. F. Davydov, V. N. Syuzev, A. A. Petukhov, and M. M. Antipina	382	306
Effect of Thermal Conductivity of Surface Layer on Contact Thermal Resistance – V. V. Kharitonov, L. S. Kokorev, and Yu. A. Tyurin	385	308
Effect of Degree of Perfection of Structure of Graphite on the Changes of Its Dimensions during Neutron Irradiation – Yu. S. Virgil'ev, I. P. Kalyagina, and V. G. Makarchenko	388	310
Absorption Spectra for Thin Films of Zirconium Dioxide – Kh. V. Shalimova, T. Kh. Margulova, T. I. Malova, M. M. Malov, and S. M. Klimova	391	312
The Prospects of Research on γ -Fields of Rocks and Soils on the Earth's Surface with the Aid of Semiconductor Detectors – V. A. Ionov, Yu. E. Kazakov, I. M. Nazarov, S. I. Patrakeev, V. N. Sorokin, and Sh. D. Fridman	393	313
Using Thermoluminescence of Ruby for the Dosimetry of γ -Radiation – M. S. Yunusov, A. N. Tsoi, K. M. Muminkhodzhaev, and V. Ya. Khaimov-Mal'kov	396	315
Influence of Neutron Irradiation upon the Characteristics of Fully Depleted Silicon Surface Barrier Detectors – M. É. Kaganskaya, O. P. Fedoseeva, and B. I. Sinitsyn	399	317
Half-Life of Am^{241} – V. G. Polyukhov, G. A. Timofeev, P. A. Privalova, and P. F. Baklanova	402	319
Effective Charge of Fission Fragments – A. M. Miterev and E. A. Borisov	404	320
Energy Dependence of Average Number of Prompt Neutrons in Pu^{241} Fission – N. P. D'yachenko, N. P. Kolosov, B. D. Kuz'minov, A. I. Sergachev, and V. M. Surin	406	321
Investigation and Test of the Magnetic System of the Jupiter-1M Electromagnetic Trap – A. V. Georgievskii, V. E. Ziser, O. A. Lavrent'ev, M. G. Nozdrachev, and D. P. Pogozhev	408	323

INFORMATION

Twenty-Five Years of the Engineering Physicochemical Faculty – B. V. Gromov and Ya. D. Zel'venskii	411	325
---	-----	-----

CONFERENCES AND MEETINGS

International Conference on Open Traps – V. A. Chuyanov	413	326
Results of the First International Symposium of Plasma Chemistry – Yu. N. Tumanov	416	328
Fourth International Symposium on Distillation of Saline Water – O. I. Martynova, V. G. Shatsillo, and V. B. Chernozubov	418	329
Regular Session of Technical Committee 45 of MEC – V. V. Matveev and V. S. Zhernov	421	330

CONTENTS

(continued)

	Engl./Russ.	
International Symposium on Nuclear Electronics – A. N. Sinaev.....	424	332
V Foratom Congress – M. Matushek and P. Strugar	426	333
BRIEF COMMUNICATIONS	429	335
BOOK REVIEWS		
N. G. Gusev, L. R. Kimel', E. E. Kovalev, V. P. Mashkovich, B. G. Pologikh, and A. P. Suvorov – Protection from Ionizing Radiations. Volume II.* Protection from Radiations of Nuclear Engineering Installations – Reviewed by S. G. Tsypin..	430	336

The Russian press date (podpisano k pečati) of this issue was 3/29/1974.
Publication therefore did not occur prior to this date, but must be assumed
to have taken place reasonably soon thereafter.

ARTICLES

ROLE OF FAST REACTORS IN THE STRUCTURE OF
DEVELOPING SYSTEM OF NUCLEAR ENERGETICS

V. N. Bolbolovich, Yu. I. Koryakin,
G. B. Levental', S. Ya. Chernavskii,
N. A. Baskakova, and T. P. Chernysheva

UDC 621.039.526

Fast reactors have already been at the center of attention of specialists on planning the development of nuclear energetics (NE) for a long time. However, there is no unanimous point of view on the significance of these reactors as yet. Some specialists see the prospect of NE in the improvement of thermal reactors and discovery and development of cheap deposits of natural uranium and thorium; other start from the limited nature of the stock of natural nuclear fuel and relate their prognosis to the introduction of fast reactors. In recent years a new view point has been noticed, i.e., to consider the system of interconnected thermal and fast reactors as the most promising. It should be noted that investigators holding the last point of view often differ on less general questions; when and in what scales APS with fast reactors should be introduced, what should be their technical-economical indices etc.

There exist several reasons for such diversity (for example, different instruments of investigation, different hypotheses on the future states of NE system etc). In view of this it is advisable to investigate the possible role of fast reactors under different assumptions about the conditions and characteristics of NE systems. The present work is devoted to this problem; some of the results are discussed below. The authors started from the premises that the role of fast reactors is determined not only by their own characteristics but also by the characteristics of thermal reactors and also by the external conditions of development of NE. The investigation was carried out on a mathematical model intended for the determination of the optimum structure of the nuclear energetics being developed from the point of view of minimum structure of the nuclear energetics being developed from the point of view of minimum total expenditure [1, 2].

As yet there is no standard terminology in the problems of prognosis of nuclear energetics. In the present work we adopted the following definitions.

Original list of APS in year t is the list of APS with those types of reactors which by their technical potentialities can be introduced in operation in that year.

Deciding list of APS is the list of APS with those types of reactors which according to the given rule of taking decisions must be put into operation in year t . Another variant of the deciding list is the optimum list.

The structure of APS is characterized by vector S with components x_1, x_2, \dots, x_n , where n is the dimensionality of the list; x_i is the fraction of power of i -th type reactors of the total power of NE in year t . The structures of established and introducable powers are distinguished.

The sequence of structure at the investigated period is called the dynamic structure or the strategy of development of the system.

It is evident from the above definitions that the most important is the concept of original list based on the concept of the type of nuclear reactor. A special feature of this typology is the division of thermal reactors into two variants differing in the operating time of the secondary fuel (in respect of construction these reactors can be practically identical). For simplification let us refer them to the types of nuclear reactors. The original lists of APS were formed from the five types shown in Table 1.

Translated from *Atomnaya Energiya*, Vol. 36, No. 4, pp. 251-257, April, 1974. Original article submitted December 24, 1973.

© 1974 Consultants Bureau, a division of Plenum Publishing Corporation, 227 West 17th Street, New York, N. Y. 10011. No part of this publication may be reproduced, stored in a retrieval system, or transmitted, in any form or by any means, electronic, mechanical, photocopying, microfilming, recording or otherwise, without written permission of the publisher. A copy of this article is available from the publisher for \$15.00.

TABLE 1. Types of Nuclear Reactors

Reactor	Nuclear fuel	Symbol
Thermal with water cooling operating in regime		
a) burner	Enriched uranium	TB
b) converter-operating time accruer	The same	TC
Fast liquid-metal breeder reactor	Plutonium	BR
Fast liquid-metal converter	Enriched uranium	BC
Thermal burner with water cooling	Plutonium	TBF

TABLE 2. Hypotheses of Growth of NE Power

Hypothesis	Total NE power, relative units			Mean annual rate of growth of NE power, %		
	1980	1990	2000	1980-1990	1990-2000	2000-2010
First	1	3	8	11,6	10,3	10
Second	1	3,7	10	13,9	10,6	10
Third	1	4,3	11,7	15,8	10,4	10

An analysis shows that in the next 20-30 yrs APS with thermal burner-reactors will become one of the most important technical means in NE (here no distinction has been made between frame-type and channel-type reactors because of the absence of significant difference between their technical-economic characteristics for the problem of prognosis); therefore TB reactors were included in all the variants of the original lists.

Two groups of hypotheses of development of nuclear energetics differing in the types of reactors were examined. In the first group the original list was formed only from thermal reactors; the second was formed from both thermal and fast reactors. In the first group three variants of the original list of APS were considered; single-component (TB); two-component (TB + TBP); three-component (TB + TBP + TC).

At present it is not clear when a mass-scale introduction of full-scale fast reactors into operation will begin. It is most likely that they will be introduced in mid-eighties. However, in view of the possibility of more accelerated utilization because of the difficulties of resolving the thermal problem or slowing down of the pace of utilization in the second group of hypotheses the start of widespread introduction of fast reactors was varied from 1981 to 1995.

Thus in the hypotheses of the second group the basic list included three (TB + TBP + TC) and later five types of reactors (TB + TBP + TC + BR + BC) up to the start of the introduction of fast reactors.

For the purpose of taking the existing uncertainty in the technical-economic indices of fast reactors into consideration different hypotheses of relative increase of the cost of these reactors compared to thermal reactors were considered. It was assumed that the capital investment in APS with fast reactors will be 10-50% higher than that in APS with thermal reactors.

Fast reactors operating in the converter regime for all the service period are not economical; therefore the time of their operation as converters was restricted to 10 yrs and later these reactors were switched over to the breeder regime. In the present work channel-type reactors with graphite retarder and water cooling were as considered as reactors of TC type.

The parameters of TC type have not been well substantiated as yet; therefore, for the determination of the optimum time of operation of plutonium four modifications having different indices in respect of coefficient of operating time and depth of depletion were included in the basic lists.

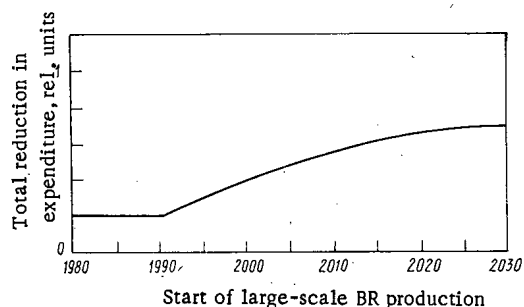


Fig. 1

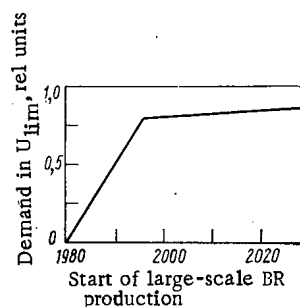


Fig. 2

Fig. 1. Effect of time of introduction of BR on the total reduced expenditure on NE.

Fig. 2. Effect of different times of widespread introduction of BR on the integral need of natural uranium.

Three hypotheses of the growth of NE power were considered. The computational data for these hypotheses are given in Table 2. The tempos of growth of NE power of all electrical power up to the end of the period under consideration decrease.

The conditions of inclusion of different types of APS in the electric power systems are of great interest. As elements of these systems APS may compete with the traditional types of power stations in the variable part of the graph of the load, but APS are a part of the NE system and their use in the variable regime leads to a low yield of the secondary nuclear fuel and in the presence of economical APS using plutonium it leads to a restriction of their introduction. The annual number of hours of use of APS (H) is 5700-6300; the maximum possible number of hours of use of all types of APS is 7000 h, while the minimum is 4500 h.

A tendency of gradual introduction of new technical means into NE was simulated in the present work. This was done with the use of restrictions on the introduced power of fast reactors after the start of their widespread introduction. The computations were carried out on a mathematical model with nonuniform time scale; the period of computation was taken equal to 50 yrs starting from 1980.

In the development of nuclear energetics only on the basis of APS with thermal reactors the needs of natural uranium are extreme and in this sense the analysis of such a strategy is significant. The case where the plutonium turned out is not used in the NE system and the resources of natural uranium are unlimited was considered in the present work. Since the expenditures cited for the investigated TC are somewhat higher than for ordinary thermal reactors (because of increased fuel component) and there is not consumer of plutonium in the APS system (and hence its value is zero), in this case TC do not enter into the optimum structure of the APS system being developed only on thermal burner-reactors.

In accordance with the growth of the output of electrical energy by the APS system the need for natural uranium increases over the years of the computational period, which is evident from the following data:

Period	Uranium consumption, rel. units
1981-1985	1
1986-1990	1.9-2
1991-1995	2.8-3
1995-2000	4-4.5

However, the effect from the use of plutonium only in thermal reactors is relatively small. In particular, the economy of the total demand of natural uranium in NE due to the use of plutonium in TR up to year 2000 is only 10-12%.

The use of plutonium is most efficient in fast reactors. Below we discuss the results of computation for the second group of hypotheses in which fast reactors are included in the basic lists.

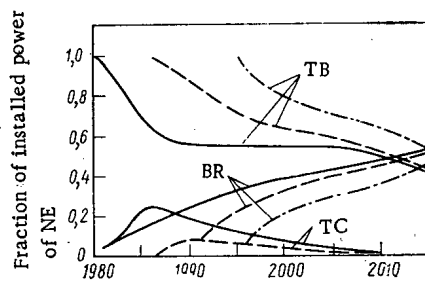


Fig. 3

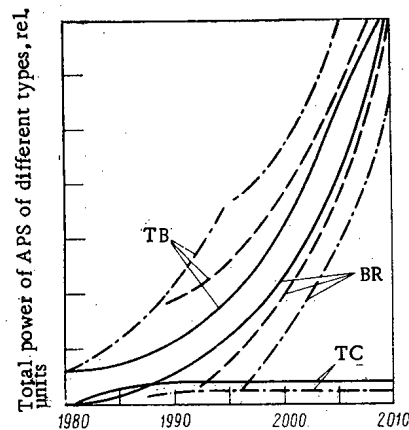


Fig. 4

Fig. 3. Structure of installed power of APS as a function of the start of introduction of BR: —) 1981; ---) 1991; -.-) 1996.

Fig. 4. Effect of the start of widespread introduction of BR on the total power of APS of different types: —) 1981; ---) 1991; -.-) 1996.

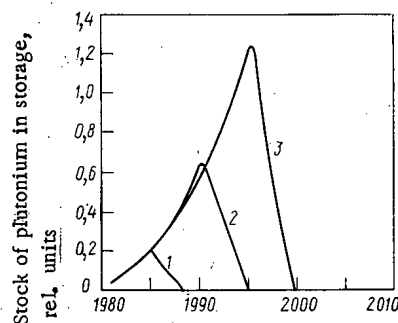


Fig. 5. Stock of plutonium in storage in APS system as a function of the period of introduction of BR: 1) 1986; 2) 1991; 3) 1996.

The dynamic structure of NE in the presence of fast reactors is largely determined by the margin of economy of fast reactors expressing the difference of intrinsic and closing expenditures in the system. This margin in turn depends on the relationships of fast and thermal reactors both in respect of the fuel component and specific capital investments.

The largest uncertainty exists in the indices of specific capital investments. In view of this the effect of possible increase of specific capital investment in APS with fast reactors in comparison with thermal reactors was investigated. The range of the investigated values of this factor (we denote it by α) lies within the limits 1-1.6.

The effect of α on the structure of APS is related to the action of other factors, of which the most important are the breeding factor of BR and the possible limitations on the resources or the cost of natural uranium. For equal capital investments in BR and TB the margin of economy of fast breeder reactors is determined

by the relation of the fuel components, wherein the contribution of breeders in the structure is maximum and their margin of economy is such that in the optimum list APS with TC also enter besides TB. The APS with TC, even though they have larger intrinsic expenditure, enter into the optimum list due to their large turn out of plutonium; their contribution depends on the amount of margin of economy of BR.

A decrease of the margin of economy of BR results in a decrease of the contribution of TC, in a decrease of output of plutonium in the system, and in a slower introduction of BR due to the limitations on plutonium. In the range $\alpha = 1-1.2$ the effect of this relation is still small and does not lead to an appreciable decrease of the contribution of BR. A further increase of α results in the elimination of reactors of TC type from the optimum list (for example, starting from mid eighties with the introduction of BR this occurs for $\alpha = 1.25-1.3$), in a stronger effect of the limitations on uranium, and in a decrease of the contribution of BR in the optimum structure. The values $\alpha = 1.5-1.6$ are critical for the inclusion of BR in the optimum lists in accordance with the conditions of competition in the NE system with thermal burners.

Thus, for the adopted initial information for $\alpha = 1-1.3$ the closing type of APS in the NE system are TC, for $\alpha = 1.3-1.6$ the closing equipment are fast breeders. As well known, the definition of the type of closing equipment is a very important question for the characteristic of a system of developing energetics.

From an analysis of the effect of the time of beginning of widespread introduction of BR (t_0) on the total expenditure on NE during the entire computational period (Fig. 1) and on the need for natural uranium (Fig. 2) it follows that if the introduction of BR starts in 1981-1991, the optimum total expenditures in a

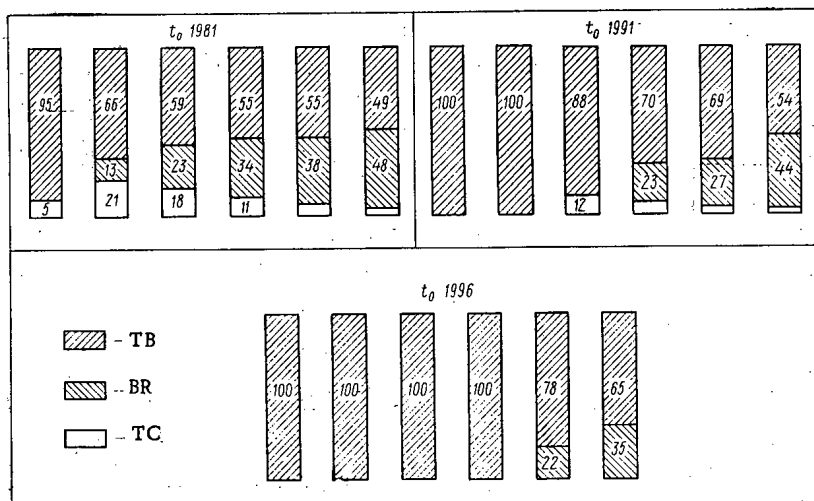


Fig. 6. Effect of the start of widespread introduction of BR on structure of APS (%) in characteristic time intervals.

TABLE 3. Structure of Installed Power of APS

Average No. of hours of APS, h/years	TB %				BR %				TC %			
	1981	1985	1990	2000	1981	1985	1990	2000	1981	1985	1990	2000
5700	96	70	62	59	4	12	22	35	—	18	16	6
6000	96	66	58	54	4	13	23	39	—	21	19	7
6300	93	61	33	37	5	14	26	48	2	25	41	15

period of 50 yrs (starting from 1980) will be practically independent of the variation of the start of introduction.

The delay of introduction of economical BR to 1996 is associated with predicting a significant detriment to the national economy. On the basis of these data it is possible to speak of a zone of "indifference" of NE toward the start of introduction of BR according to the criterion of reduced expenditures. This zone covers the period 1981-1991. Within this zone the following rule operates: it is necessary to facilitate earlier introduction of BR, since this

would create greater uniformity in the operation of the machine-building industry and will facilitate a more intensive improvement of the indices of BR due to accumulation of larger experience with their earlier introduction. Furthermore, an earlier introduction of BR results also in a decrease of the demand of uranium, as seen from Fig. 2.

The delay of the beginning of introduction of BR to 1991 leads to an increase of consumption of natural uranium up to 2000 by about 15% in comparison with the variant of introduction in 1981. With the introduction of BR only from 1996 the demand of natural uranium increases roughly by 25-30%.

In all the investigated variants the use of BR in the development of energetics permits a significant economy in the total expenditure in the development of NE and the demand of natural uranium compared to the development of NE based only on thermal reactors. Even the conservative hypothesis ($t_0 = 1996$) gives an appreciable saving in the total expenditures; the demand for natural uranium over the entire computed period is smaller by a factor of 1.8-2. Without economical BR the development of NE is connected with significant detriment to the national economy; therefore the need for the exploitation of liquid-metal BR of the insurance variant which are being developed at present in the USSR should be taken into consideration (for example, BR with gas heat-transfer agent). Under certain conditions these reactors could be later on considered also competitive. Of course, it should be considered that the development of the insurance variant has as its goal the increase of reliability in the program of development of powerful BR, which must not lead to a decrease of the means of investigation and appropriation of liquid-metal BR, but to the evolution of other means based on this variant. Otherwise the effect of the insurance variant would be opposite to the expected effect of increase of reliability in the breeder program.

The effect of the beginning of introduction of BR into the optimum structure of APS is shown in Fig. 3 for three hypotheses: optimistic, according to which fast reactors can be introduced on a large scale not earlier than 1981, cautious (1991), and conservative (1996).

With the delay of widespread introduction of BR the APS system will undergo some structural changes; this will be primarily manifested in a decrease of the contribution of BR which would result in a decrease of the role of TC in the development of NE.

Investigations have shown that for the variation of the start of introduction of fast reactors in the range 1981-1991 the APS system in the optimum variant must be developed with three types of nuclear reactors, TB, BR, TC.

The largest structural differences in variants with $t_0 = 1981$ and $t_0 = 1991$ are observed in the period before 2000. Thus the contribution of BR at 1990 level is $\sim 23\%$ in the second, i.e., in the first case the total power of BR will be approximately one and a half times larger. However, at the level of 2000 due to the earlier introduction of BR in 1981 compared to 1991 their power will differ already by a factor of 1.2, while in 2010 it will differ only by a factor of 1.1.

It follows from Figs. 3 and 4 that the accuracy of our ideas of the structure of the NE system as a function of the beginning of the introduction of BR changes over the years of the computational period. This initial uncertainty in regard to the beginning of introduction of BR is associated with a certain uncertainty about the ideas of the structure at 1990 level, but after this our ideas on the structure at 2000 level can be regarded as more definite in this aspect. Of course, they are less accurate than the ideas about the structure in the period up to 1980. Later on (after 2000) the action of other factors leads to a decrease of the accuracy of the ideas about the structure.

In the first years of widespread introduction of BR the rate of growth of the installed power will be very large; later it will decrease remaining higher than the rates of growth of the entire power of APS. The later the start of introduction of BR, the higher are the economically advantageous rates of growth of the power with BR especially in the first five years of their operation. This is due to the fact that in delaying the introduction of BR the stock of plutonium in the NE system toward the time of introduction is larger, which offers the possibility of a large-scale introduction of BR immediately after the termination of the stage of mastering of fast reactors. This is confirmed by Fig. 5, in which the effect of the parameter t on the dynamics of change of plutonium reserves in the system is shown.

The nature of the change of plutonium stocks in NE system under the condition of competitive capability of BR is as follows: up to the time t_0 an accumulation of plutonium occurs and the maximum reserve in the system is obtained in the year preceding the year of widespread introduction of BR; afterwards in course of three to five years the plutonium reserve falls to zero.

The maximum plutonium reserve in the NE system is larger for later introduction of BR. Thus, for their introduction from 1996 the maximum reserve is larger than for the introduction in 1991 by a factor of two, and six times larger than for the introduction in 1986.

The acceleration of the start of widespread introduction of BR leads to the need of increasing the total power of TC and of shifting the periods of their introduction toward the beginning of the period, wherein the main role of TC reduces to the maintenance of the high tempos of introduction of power full BR.

Till recently the question about the effect of the scales of development of NE on the contribution of BR to the optimum power structure had not been completely clarified. Computations showed that the change of the total power of NE in the year 2000 by 20% (see Table 2) with subsequent intensive growth of the power has practically no effect on the optimum structure. The contribution of BR for their introduction in early eighties lies in the following ranges: 17-20% in 1990 and 32-35% in 2000, i.e., it changes insignificantly. The rates of growth of BR power are higher than the rates of growth of NE as a whole. Thus under the second hypothesis (see Table 2) for NE the mean annual rate of growth in 1980-1990 was $\sim 14\%$ and 10.6% in the next 10 yrs; for BR the corresponding figures are ~ 33 and $\sim 18\%$. The optimum expenditures on the system and the demand of natural uranium are proportional to the scale of development of NE.

A very important problem, that has not been investigated so far, is the estimate of the decrease in the efficiency of APS during their use in the variable part of the graphs of electrical load due to under-production of plutonium. In order to study this problem we analyzed three hypotheses of use of the NE system in the electrical power systems of the country, differing in the average annual number of hours of use of power H equal to 5700, 6000, and 6300 h/yr. The results of the estimate of the effect of H on the optimum structure of NE are shown in Fig. 6.

As follows from these results, in the indicated range of variation of H APS with three types of nuclear reactors enter into the optimum list: TB, BR, and TC. The last of these is introduced during the period 1981-1990, after which the growth of the power of TC stops. Thus the decision about the need of introduction of APS with three types of reactors into the system under the conditions indicated above is invariant

to the change of the average number of hours of APS in the range 5700-6300 h/yr. In this range an increase of H leads to a larger production of plutonium and, hence, to a larger introduction of BR into the system.

A widespread introduction of APS with BR is in turn associated with the increase in the importance of plutonium in NE, which causes the displacement of the part of thermal burner-reactors from the structure of APS by thermal producer-reactors. If for $H = 5700$ h/yr in the period 1981-1990 TC type reactors are used only in the base part of the graph (newly introduced reactors are kept in mind), then for $H = 6300$ h/yr it becomes economically efficient to use a part of the introduced TC even in the variable part of the graph of the load in 4500 h/yr regime, so that in the period 1986-1990 the introduction of new APS with thermal burner-reactors stops and in all newly introduced APS with thermal reactors operation in the regime of production is envisaged. Thus an increase of the average number of hours of use of APS leads to an increase of the contribution of BR to the total installed power (Table 3).

A change of the average number of hours of use of APS in the range 5700-6000 h/yr has a relatively small effect on the structure of APS up to 1985. Thus, in 1985 the contribution of APS with TB to the installed power is 60-70%, for APS with BR 12-14%, and for APS with TC 18-25%.

After 1985 the optimum structure of APS changes insignificantly for a variation of H in the range 5700-6000 h/yr.

An increase of the average annual number of hours of use of APS from 6000 to 6300 h/yr leads to an increase of the mean annual rates of growth of the power of APS with BR from 16 to 17%, which gives an increase of the power of these APS by 25-26%.

The total reduced expenditures in absolute magnitude naturally increase with the average number of hours of use of APS. However, a relatively smaller rate of expenditure is observed compared to the increase of production of electrical energy, which is accounted for by the improvement of the structure of NE due to the increase of the contribution of BR leading to an increase of the efficiency of the NE as a whole. The increase of the efficiency of the entire NE in the presence of increase of H is accompanied also by a decrease of the demand of natural uranium in the system. Investigations showed the large significance acquired by the positioning of APS in the base part of the load graph in estimating the efficiency of the NE as a whole. The analysis indicates that fast reactors, being an efficient means of increasing the economic factor of NE and of the solution of its fuel problem, should occupy a prominent place in the optimum structure of APS before the year 2000.

LITERATURE CITED

1. N. A. Dollezhal' et al., Atomnaya Energiya, 31, No. 3, 187 (1971).
2. A. D. Virtser, G. B. Levental', and S. Ya. Chernavskii, Atomnaya Energiya, 33, No. 6, 955 (1972).

MHD CONVERSION OF ENERGY FROM PULSED THERMONUCLEAR REACTORS

E. P. Velikhov, V. S. Golubev,
and V. V. Chernukha

UDC 621.039:621.362

Recently in several countries different methods of pulsed heating of a thermonuclear plasma have been investigated. Several of these methods permit significant reduction of the portion of neutron flux and thermonuclear energy which is dissipated into the structural components of the reactor by means of a special blanket which boils off upon heating. Among these methods we may include "microexplosions" with laser [1] or electron-beam [2] ignition, and pinch systems with liners (e.g., the theta pinch [3]).

Conversion of thermonuclear to electrical energy is possible in various ways. A pulsed thermonuclear generating station using laser triggering and a steam turbine generator is considered in [4]. In the present paper the possibility is considered of using some types of conduction and induction MHD generators for possible generating stations of power ~ 10 GW. The reactor for such a station is a specially cooled chamber in which pulsed energy is released. Its magnitude is limited below by the need to maintain a high energy level, and above, by the technical and economic possibilities for building an explosion chamber. For power production the range of energy output of interest is 10^{10} to 10^{12} J. The thermonuclear portion of the structure includes a blanket which absorbs the bulk of the released energy and produces the unstable fuel component (tritium).

Because of convective cooling of the working fluid in the chamber the maximum temperature of a thermonuclear cycle does not exceed 2-3 eV. The maximum plasma pressure depends on the degree of loading of the chamber by the explosion. Shock heating of the gas in the chamber leads to an allowable pressure not exceeding ~ 1 kbar. A higher pressure level may be attained by deformation of the shock wave from the explosion.

Such high working fluid parameters are possible in principle for a high-efficiency thermodynamic cycle, particularly if a monatomic gas is used. However, a series of requirements for the blanket, for the chamber fill gas, and for the coolant introduced into the working volume, as well as considerations of convenience in closing the contour of the working fluid, and the thermodynamic cycle (as a rule, a Rankine cycle) in many cases make preferable the use of alkali metal vapor (Li, Na, K) as a working fluid.

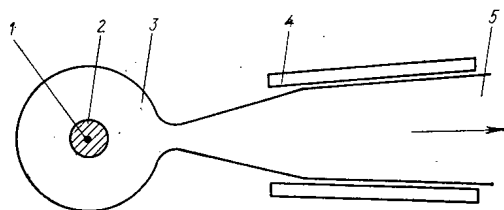


Fig. 1. Diagram of a conduction MHD generator for a pulsed thermonuclear reactor: 1) thermonuclear charge; 2) evaporating blanket; 3) reactor chamber; 4) MHD generator magnet; 5) MHD generator channel.

Calculations for several types of MHD generators which permit evaluation of the difficulties in the way of attaining high conversion efficiencies for pulsed thermonuclear reactors are presented below.

Conduction Plasma MHD Generator

Application of quasistationary MHD generators for energy conversion from a pulsed thermonuclear reactor has the special difficulty, connected with the nonstationary flow of working gas from the combustion chamber, that on one hand the efficiency is lowered, and on the other the problem of matching the current to the load is complicated.

Translated from *Atomnaya Energiya*, Vol. 36, No. 4, pp. 258-260, April, 1974. Original article submitted September 24, 1973.

© 1974 Consultants Bureau, a division of Plenum Publishing Corporation, 227 West 17th Street, New York, N. Y. 10011. No part of this publication may be reproduced, stored in a retrieval system, or transmitted, in any form or by any means, electronic, mechanical, photocopying, microfilming, recording or otherwise, without written permission of the publisher. A copy of this article is available from the publisher for \$15.00.

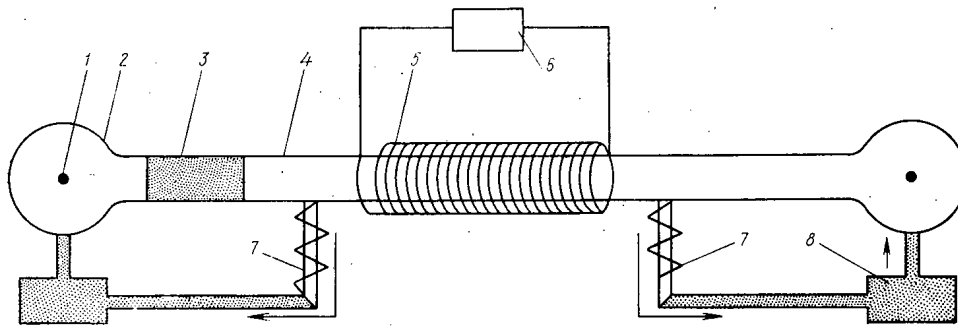


Fig. 2. Conceptual diagram of an inductive MHD generator for a pulsed thermonuclear reactor: 1) thermonuclear charge; 2) explosion chamber; 3) piston; 4) expansion channel; 5) solenoid; 6) load; 7) heat exchanger-condenser; 8) liquid metal reservoir and apparatus for injection of reactor charge with blanket.

The greatest efficiency may be obtained with variable flow parameters during the course of the cycle. As an example, we take the parameters of a supersonic Faraday MHD generator (Fig. 1) with continuous electrodes with the following conditions: working fluid, lithium; energy output from pulse, 10^{11} J; average MHD generator electrical power during the pulse, 10 GW; maximum chamber pressure, 1 kbar; maximum temperature of the thermodynamic cycle, 1 eV; adiabatic flow from the chamber; the flow regime in the MHD generator is constant with static plasma temperature along the channel, decreasing to 0.35 eV as the chamber is emptied; the coefficient of loading ($K = 0.85$) is constant in time; permissible reduction in Mach number by a factor of 2; channel length 5 times exit width; reversible expansion.

The utilization of the internal energy of the plasma as it flows from the chamber through the MHD channel was optimized. This determined the initial statistical temperature (~ 0.5 eV) and the entry Mach number, $M_0 = 4$. This requires constant braking length, which then leads to the necessity of regulating the magnetic field (in our example, to 40%). The following values were obtained: radius of the spherical explosion chamber ~ 4.5 m; effective utilization of plasma enthalpy in the chamber ~ 0.8 ; efficiency of MHD conversion ~ 0.5 ; total efficiency (after deduction of the heat of vaporization) ~ 0.4 ; time of flow from chamber ~ 4.5 sec; maximum power 25 GW; maximum voltage (approximately constant along the generator channel) 8.5 kV; magnetic Reynolds number across the channel width 0.4; critical cross section 0.025 m^2 , entry cross section 0.35 m^2 , exit cross section 2 m^2 , channel length 7 m; braking length 2 m; maximum (magnetic) induction 1.2 T.

In the present example heat loss to the chamber walls due to radiant thermal conduction, hydrodynamic turbulence, and free convection were not included. The last of these is the most significant. For $T = 2$ eV the cooling time is an order of magnitude larger than the effective escape time, i.e., the calculated efficiency is ultimately attainable and the temperature the maximum permissible.

The variation of the gas flow (or electric current) in time requires special electrical matching with the load. If we require it to be constant, then the variable must be the efficiency of conversion. Because of the variation in gas outflow, the average efficiency decreases by 1.5-2 times. Some improvement in thermal efficiency is possible, at the price of more complicated construction, using a disk-shaped Faraday MHD generator.

We note some difficulties with building such a high temperature MHD generator. The assumption that work can be done when the Mach number changes by a factor of 2 still requires experimental verification, although it seems satisfactory. Obtaining a smooth flow may require special technical apparatus (contoured channel; pumping off of boundary layer; etc.). The problem of flow stability with respect to acoustic perturbations is eased somewhat as the Hall number in these conditions is much less than 1. The level of volume Joule heat yield is 1 kW/cm^3 , which does not cause a separation of the electron temperature from that of the neutrals; hence the plasma is in equilibrium. The (current) density in the conduction MHD generator is $\sim 10^2 \text{ A/cm}^2$ and the electric field strength is $\sim 10^2 \text{ V/cm}$, which lie within experimentally investigated limits. Although crude estimates of heat losses to the chamber walls may be made, it is necessary to conduct experiments to accurately take account of them and special methods are needed (e.g., injection through porous walls) to protect the walls from thermal destruction.

Inductive MHD Generator

For energy released in pulses a more logical idea seems to be the use of a pulsed inductive MHD generator, for example, with a conducting piston periodically compressing the magnetic field of a solenoid (Fig. 2). Here a two-chamber system is shown which uses the explosion energy to drive a piston which is then partially slowed down in a magnetic field whose energy greatly exceeds that of the piston. As a piston it is best to use a metal conductor since in the case of a plasma conductor the conversion efficiency is less. This is due to the insufficient heating (3-5 eV) and conductivity of the skin-layer, as well as to the limit on the minimum temperature of the working gas.

The energy put into the magnetic field requires a specially chosen load when the field and piston are interacting. One of the simplest electrical circuits is shown in Fig. 2. It is assumed that engineering solutions will be found which will permit cooling of a metal piston and ensure its stability under acceleration so that it will move through the solenoid as a single piece. The conversion efficiency of blast energy into electricity is determined by the efficiency of pushing and braking of the piston.

At characteristic temperatures, the dimensions and times of thermal losses to the walls are small and the expansion of the working gas is nearly adiabatic (in particular, for this case, the thermal losses due to true convection do not exceed 1%). Losses from friction, dependent on the piston construction, were not included.

An efficiency of piston drive up to 0.8 may be obtained by using metal vapor (Na, K) as a working gas. After the piston has been driven, the vapor will condense as a spray of liquid metal. The degree of condensation is determined by the density of vapor in the chamber necessary to produce the next explosion. Joule losses fall with increasing energy output Q , in the pulse as $Q^{-1/6}$ (in the domain of Q of interest to us, they do not exceed 20%).

As typical parameters, for an inductive MHD generator with average electrical power 5 GW, a sodium piston and working gas, we take the following: pulse energy $\sim 7 \cdot 10^{10}$ J; time between pulses ~ 12 sec; maximum pressure and temperature in the chamber ~ 1 kbar and 1.1 eV; volume 300 m^3 ; minimum and maximum speeds of piston ~ 30 and 100 m/sec ; mass of piston $\sim 16 \text{ kt}$; solenoid magnetic field $\sim 4.5 \text{ T}$; energy 10^{12} J , length $\sim 65 \text{ m}$, diameter $\sim 13 \text{ m}$; degree of expansion ~ 200 ; efficiency of piston drive ~ 0.7 ; Joule losses ~ 0.1 ; overall efficiency of conversion of blast energy to electrical ~ 0.6 . Similar efficiencies occur if potassium is used.

Therefore, a conduction plasma MHD generator for a pulsed thermonuclear reactor seems physically realizable. Its efficiency is comparable with a steam turbine generator. Its use is justified either as a direct converter or in conjunction with a steam turbine. The inductive piston MHD generator exceeds the steam turbine generator in efficiency, and may be of interest in power generation from pulsed thermonuclear reactors.

LITERATURE CITED

1. J. Nuckolls et al., Nature, Vol. 239 (1972), p. 139.
2. E. Winterberg, Nucl. Fusion, Vol. 12 (1972), p. 353.
3. J. Boris and R. Shanny, Proc. of 2nd Topical Conf. on Pulsed High-Beta Plasmas. Garching, BRD, P-G10 (July, 1972).
4. L. Booth, Central Station Power Generation by Laser-Driven Fusion, LA-4858-MS, Vol. 1 (1972).

ELECTRON HEATING IN MAGNETIC TRAPS FOR SPIRAL ELECTRON BEAM INTERACTION WITH PLASMA

B. S. Akshanov

UDC 533.9.07

Following the publication of theoretical results [1, 2] in which were discovered beam instabilities due to beam interactions with a plasma and the completion of experiments on the interaction of an electron beam with a plasma in a uniform magnetic field [3, 4] which showed the possibility of heating and producing electrons with energies exceeding the injection energy, considerable interest in this phenomenon arose with the object of using it, along with the methods of turbulent heating proposed by E. K. Zavoiskii [5-7], to efficiently heat plasmas in magnetic traps.

The first work on plasma heating with electron beams and confinement in magnetic traps was done earlier at Kharkov [8, 9] and Oak Ridge [10, 11]. Long-lived ($\tau \approx 0.1$ sec), hot electron ($T_e \approx 100$ keV) plasmas, with density $n_e \approx 10^{11}$ cm $^{-3}$ and cold plasma background density $n \approx 10^{12}$ cm $^{-3}$, were produced in magnetic mirror traps. Ion temperature regimes of the order of several keV were obtained, and the conditions for creating a completely ionized hot plasma were found [8, 9, 12-24].

The broad spectrum of oscillation observed in these and later works pointed to strong turbulence and to the possibility of accelerating the plasma electrons by means of stochastic RF fields near the cyclotron resonance [15]. The complexity of such plasmas makes it impossible to explain the electron heating by a single experiment or a single physical mechanism. This is supported by reports with different (although some works agree among themselves) treatments of the mechanism for electron heating in magnetic traps when a beam interacts with the plasma [16-24]. Even the question of which electrons are heated (beam or plasma) receives contradictory answers in different cases. A single opinion does not exist on which oscillations are responsible for electron heating. One of the reasons for this situation, in all probability, is the experimental conditions. Only a nonlinear theory can explain the magnitude of the electric fields generated during the development of instabilities, heating, and plasma containment. Furthermore, in the regimes studied in the present paper (when $\omega_{Oe} > \omega_{Be}$ and $\omega_{Oe} < \omega_{Be}$, where ω_{Oe} and ω_{Be} are the plasma and cyclotron frequencies, respectively) stochastic heating occurs, which, as is known, cannot be exhaustively described by a linear or phenomenological theory.

To clarify the heating mechanism it is convenient to study the interaction of a powerful "spiral" electron beam with plasma in a magnetic trap for $\omega_{Oe} > \omega_{Be}$, $\omega_{Oe} < \omega_{Be}$ and with precise determination of the working conditions.

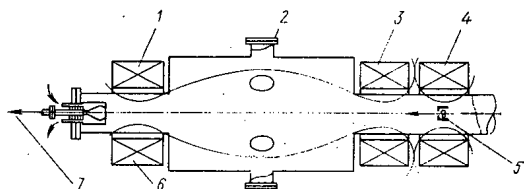


Fig. 1. Schematic drawing of apparatus: 1, 3) main field coils (B_2 , B_3); 2) diagnostic ports; 4) cusped field coils (B_1); 5) electron gun; 6) collector; 7) transfer tube to electrostatic and magnetic analyzers.

Experimental Arrangement and Method of Measurement

This study was carried out on an apparatus (Fig. 1) having the following parameters: magnetic field in center of trap 1-5 kG, at mirrors 3-15 kG (mirror ratio $R = 3$). The distance between the mirrors was 40 cm. The plasma vessel was made of stainless steel. The working gas was hydrogen which was fed in continuously through a palladium leak valve. The apparatus could be operated in either pulsed or continuous mode. In the pulsed mode it was

Translated from *Atomnaya Energiya*, Vol. 36, No. 4, pp. 261-268, April, 1974. Original article submitted May 3, 1973.

© 1974 Consultants Bureau, a division of Plenum Publishing Corporation, 227 West 17th Street, New York, N. Y. 10011. No part of this publication may be reproduced, stored in a retrieval system, or transmitted, in any form or by any means, electronic, mechanical, photocopying, microfilming, recording or otherwise, without written permission of the publisher. A copy of this article is available from the publisher for \$15.00.

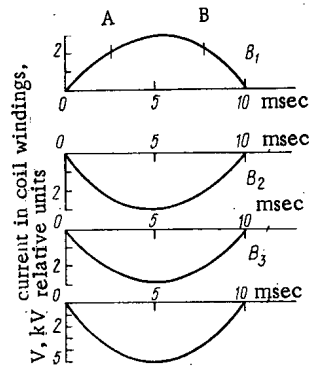


Fig. 2

Fig. 2. Oscilloscope trace showing the increase in number of fast electrons with energy 30 keV leaving the magnetic trap along field lines at the time the accelerating potential V and magnetic field B cross values such that the pitch of the spiral is a minimum ($B_0 = 3$ kG).

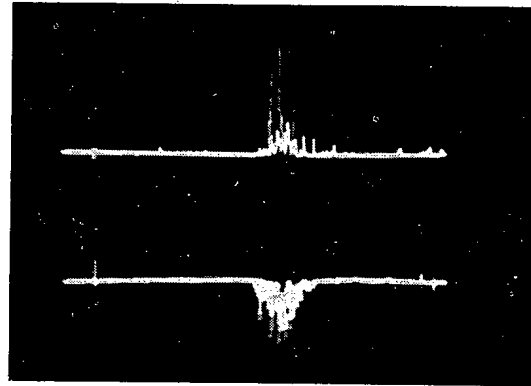


Fig. 3

Fig. 3. Oscilloscope traces of x-radiation (top) and of the corresponding burst of oscillations (bottom) at frequency $f_3 = 350-480$ MHz, $B_0 = 1$ kG, $V = 10$ keV, $I = 5$ A. Pulsed mode. Duration of scan 20 nsec.

possible to supply the cathode of the electron gun either with a rectangular negative pulse of duration 2 msec or with a half sinusoid of duration 10 msec. In the experiments the injection energy was varied between 1-10 keV and the beam current between 1 and 5 A. For injection a spiral beam was used, the pitch and corresponding transverse velocity of which could be changed by varying the magnetic field in the cusp field (B_1). The pitch of the spiral beam is defined by [25],

$$h = 2\pi R_L \sqrt{1 - r_0^2/R_L^2} \quad (1)$$

where R_L is the electron Larmor radius; r_0 the injection radius. The minimum pitch of the spiral occurs for $r_0 \approx R_L$. This experiment investigates a plasma with parameters $T_e \approx 100$ keV, $n_e \approx 10^{11}-3 \cdot 10^{11} \text{ cm}^{-3}$, $n \approx 10^{12}-10^{13} \text{ cm}^{-3}$, $\tau \approx 0.1$ sec. The plasma diagnostics are described essentially in [14].

Heating of Beam and Plasma Electrons

Electron heating in the magnetic trap depends strongly on the pitch of the spiral beam. The presence of a significant transverse component of velocity leads to a sharp increase in the effectiveness of the beam interaction with the plasma, to a broadening of the frequency spectrum, and to an increase of more than an order of magnitude in the amplitude of the oscillations. A similar effect is described in [19]. The experimentally observed high efficiency of build-up of oscillations upon increasing the transverse velocity component of the beam is in agreement with theory [26] from which it follows that with an increase in $v_{T\perp}$, for example, the growth rate of the cyclotron instability increases.

The effect of the pitch of the spiral beam on the number of accelerated particles in the beam is shown in Fig. 2. The oscilloscope trace was obtained for pulsed supply to the magnetic field coils and gun. The magnetic field and accelerated beam pulses had half-sinusoidal form and were chosen so that during the pulse the condition $h \approx 0$ occurred twice (points A and B) in Fig. 2. From the trace it is clear that to these two times there correspond characteristic bursts of fast electrons. At these times the most effective capture by the spiral wave of the electron beam and most effective acceleration of the electrons occur.

Investigations of the possibility of accelerating the plasma electrons have shown that hot electrons are observed in the whole radial cross section of the plasma, and their temperature is higher in the central

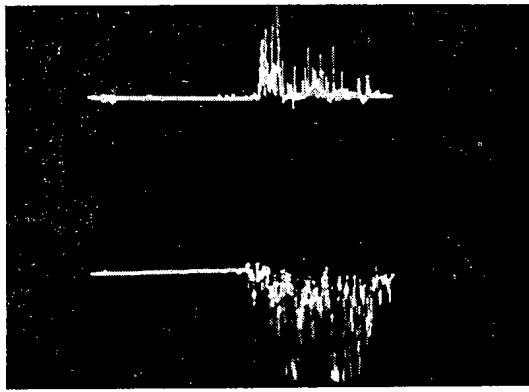


Fig. 4

Fig. 4. Oscilloscope traces of x-radiation (top) and the corresponding burst of RF oscillations (below) at frequency: $f = 2.86 \cdot 10^{10}$ Hz, $B_0 = 5$ kG, $V = 10$ keV, $I \approx 5$ A. Pulsed mode. Duration of scan 10 nsec.

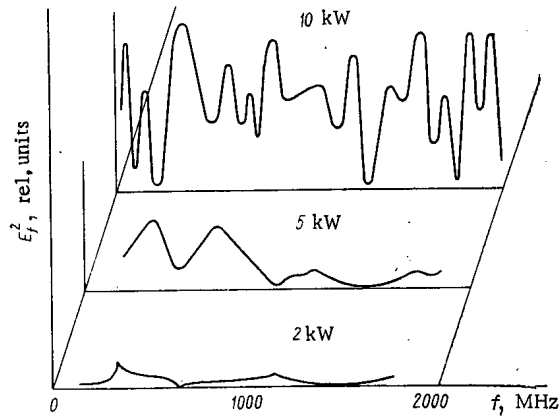


Fig. 5

Fig. 5. A set of spectra of oscillations for stationary injection of beams of different power ($\omega_{Oe} > \omega_{Be}$).

region than in the periphery [14]. The image of the plasma in its own x-rays supports the observation that hot electrons exist throughout the plasma cross section, and not only on the edge. Another factor supporting the possibility of heating the plasma electrons is the randomness of the resultant oscillations, since in this case the electrons could be accelerated with almost thermal velocities [15].

Therefore, when a spiral beam is injected, the electrons, heated to a high temperature, exist not only on the periphery of the plasma volume as shown in [16] but throughout the plasma. This gives reason to assert that, apparently, the electrons from both beam and plasma are involved in the process of acceleration and heating.

General Characteristics of the Spectra of Oscillations in the Regime of Effective Electron Heating

During the course of these experiments it was established that in the two closely studied regimes ($\omega_{Oe} > \omega_{Be}$ and $\omega_{Be} > \omega_{Oe}$) the intense electron heating is due to oscillations of two different kinds. Thus, for $\omega_{Oe} > \omega_{Be}$ (magnetic field in the center of the trap ~ 1 kG) the frequencies $\omega < \omega_{Be}$ have the largest amplitudes.

A correlation measurement was made between the x-radiation and the frequency spectrum of the excited oscillations (Fig. 3) where there was shown to be a single burst of x-rays and oscillations occurring at the times A and B (see Fig. 2). It was found that for $\omega_{Oe} > \omega_{Be}$ the x-rays occur with excitation of frequencies $\omega = \omega_3$ or $\omega = \omega_3$, where ω_3 is the frequency of the spiral waves or of the so-called atmospheric whistlers [27] defined by the equation

$$\omega_3 = |\omega_{Be} \cos| \frac{k^2 c^2}{\omega_{Be}^2} . \quad (2)$$

For $\omega = \omega_3$ it is found that the oscillations have a radial magnetic component. The generation of such waves in such traps was first noted in [17]. These oscillations are possible only when $\omega_{Oe}^2 \gg \omega \cdot \omega_{Be}$; $\omega_{Bi} \ll \omega \ll \omega_{Be}$. The growth rate for the waves [28] for $\omega_{Oe} > \omega_{Be}$ was substantial: $\sim 2 \cdot 10^8 \text{ sec}^{-1}$. According to [29] spiral waves are most efficiently excited when the angle between the propagation direction of the wave and the beam is near $\pi/2$, i.e., when the beam has a large transverse velocity component.

However, there was not always (rather, it seems, for the same experimental conditions) observed a correlation between the heating and these waves. Often heating is associated with oscillations $\omega \lesssim \omega_3$. This phenomenon may be explained by two competing processes in such a plasma, both of which produce oscillations of close frequencies. On one hand, efficient excitation of spiral waves is possible; on the other, probably lower hybrid oscillations, $\omega = \sqrt{\omega_{Bi} \cdot \omega_{Be}}$, which usually arise because of a reduction in the frequency of Langmuir oscillations due to an increase in the angle between the direction of the oscillations and the magnetic field.

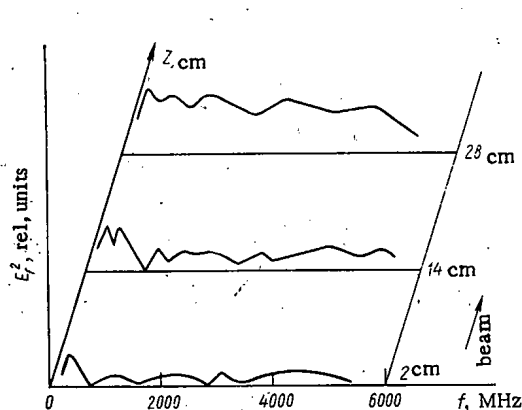


Fig. 6

Fig. 6. Spectral distribution of oscillations along the magnetic trap for beam power ~ 2 kW for stationary conditions ($\omega_{Oe} > \omega_{Be}$).

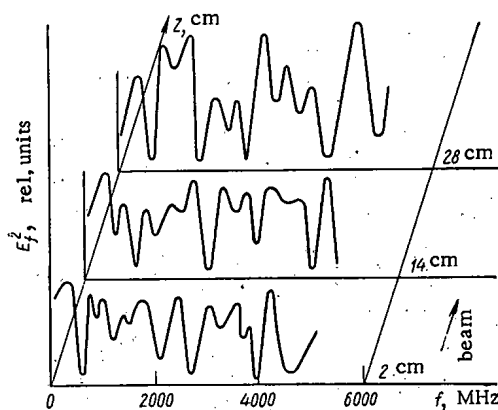


Fig. 7

Fig. 7. Spectral distribution of oscillations along the magnetic trap for beam power ~ 10 kW for stationary conditions ($\omega_{Oe} > \omega_{Be}$). The center of the trap is at $Z = 14$ cm.

For electron heating with $\omega_{Oe} < \omega_{Be}$ and a magnetic field in the mirrors of order 10 to 15 kG correlations were observed between heating and oscillations near (or slightly less than) the electron cyclotron frequency, i.e., lying within the limits $\omega_{Oe} < \omega < \omega_{Be}$. In Fig. 4 are shown oscilloscope traces of the burst of x-rays and the corresponding burst of RF oscillations (the bursts occur at times A and B of Fig. 2). This condition may be connected with the development of an instability due to a normal or anomalous Doppler effect for which, in this case, the growth rates are very large [28]. Thus, for an anomalous Doppler effect the growth rate is

$$\text{Im } \omega = \frac{\omega_{Oe} \cdot \omega_{pb}}{2\omega_{Be}}, \quad (3)$$

which is of the order 10^8 sec^{-1} (here ω_{pb} is the beam plasma frequency).

Correlation is observed between x-radiation and oscillations responsible for heating, at frequencies lower than the calculated electron cyclotron frequencies. The reason for this may be both induced scattering and decay of the excited waves which lead to nonlinear growth of waves on the lower frequency side of the spectrum [26].

Extensive spectral analysis of oscillations was carried out under the conditions $\omega_{Oe} > \omega_{Be}$ and $\omega_{Be} > \omega_{Oe}$. The greatest amplitude in the spectrum for $\omega_{Oe} > \omega_{Be}$ is found in the band corresponding to the spiral waves and to the lower hybrid frequency and for $\omega_{Be} > \omega_{Oe}$ it is found at a frequency slightly lower than the electron cyclotron frequency.

Frequency Change in Time and the Dependence of the Spectrum of Oscillations on Beam Power

Time-resolved study of the oscillations assists in understanding the process of acceleration and heating of electrons in the magnetic trap. If the oscillations are analyzed in time, then it appears that the intermittent burst of oscillations, during which acceleration of electrons is observed, is a collection of wave packets of duration 10^{-7} to 10^{-9} sec [22, 23]. A given packet with a definite frequency is randomly replaced by another.

It is natural to propose that the observed frequency change in time of the oscillations is associated with nonlinear phenomena which transfer energy from one part of the spectrum to others. One such phenomenon is the interaction of longitudinal and transverse waves [26], in which it is important that the nonlinear wave interaction depends on the square of the field amplitude and usually leads to transformation from one type of wave to another. This latter condition may limit the field amplitude, for example, because of transformation of waves from an unstable region to a damped one. We might then expect that with an increase in beam power the width of the spectrum would increase and the length over which the nonlinear wave interaction occurs would decrease. This conclusion was supported by the present experiments.

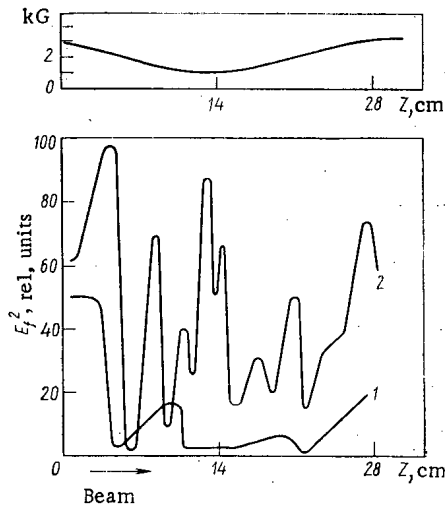


Fig. 8

Fig. 8. Power distribution of oscillations at $f = 400$ MHz along the length of the trap for beam power of 3 kW (1) and ~ 10 kW (2). The conditions are stationary, and $\omega_{Oe} > \omega_{Be}$. (The upper part of the figure shows the magnetic field distribution along the length of the magnetic trap.)

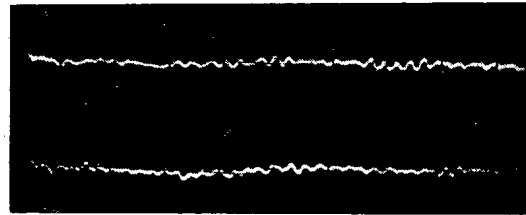


Fig. 9

Fig. 9. Typical oscilloscope traces of oscillations taken during strong x-ray emission for $\omega_{Oe} > \omega_{Be}$.

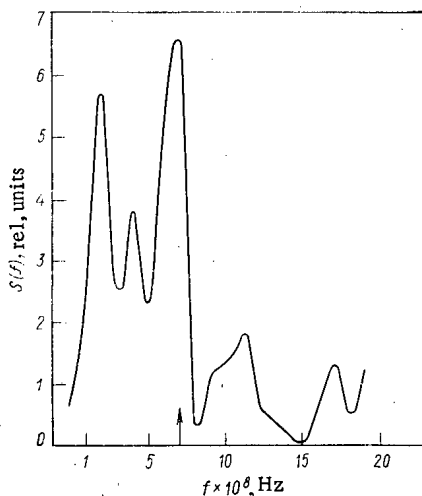


Fig. 10. Integrated spectrum of oscillations from the trace of Fig. 9.

In Fig. 5 a series of integrated spectra are shown which were taken under stationary operating conditions for the electron gun by a calibrated channel analyzer for different values of entrant (beam) power. Analysis of the resulting spectra shows that as the power is increased the spectrum widens and the amplitude of the oscillations increases. As is clear from these observations, the coupling efficiency and, thus, the strength of the oscillations, increase with increasing beam power and pressure of the working gas. In this case there exists some limiting value of beam power and gas pressure beyond which the growth in power of the oscillations is sharply slowed down. Evidently this is connected with the occurrence of some nonlinear effects which lead to a limitation in the amplitude of the oscillations and to nonlinear conversion of longitudinal waves into other kinds of waves which can freely leave the plasma.

In Figs. 6 and 7 are shown the distribution of the oscillations along the axis of the magnetic trap for various beam powers. It is evident that there is a significant change in the spectrum along the length of the apparatus, as well as in the width and amplitude of oscillations dependent on the applied power. Upon increasing the power, along with the general growth in amplitude of the oscillations, the region of wave excitation and absorption seemingly spreads itself along the length of the apparatus and for high power the distribution of oscillations is nearly uniform along the length of the apparatus (Fig. 8). Consequently there is a possibility not only of rapid excitation but of equally rapid dissipation of oscillation. It should be noted that measured amplitudes of the oscillations in electric field for large applied powers reached 2-3 kV/cm. The experimental results show that intense stochastic oscillations are observed and their characteristics are largely determined by the power of the spiral beam.

In concluding this section it should also be noted that the observed bursts of instabilities are, as a rule, accompanied by strong oscillations in the plasma electron density and, therefore, by fluctuations in the plasma frequency. As a result, the plasma frequency also changes in a random way. Sharp fluctuations in the plasma density correspond to ejection of fast electrons along the trap axis.

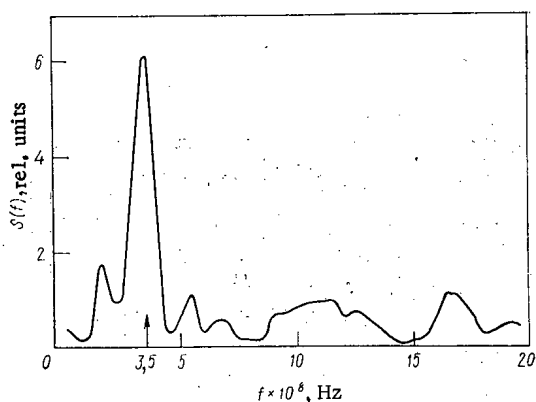


Fig. 11. Instantaneous spectrum of oscillations from the trace of Fig. 9.

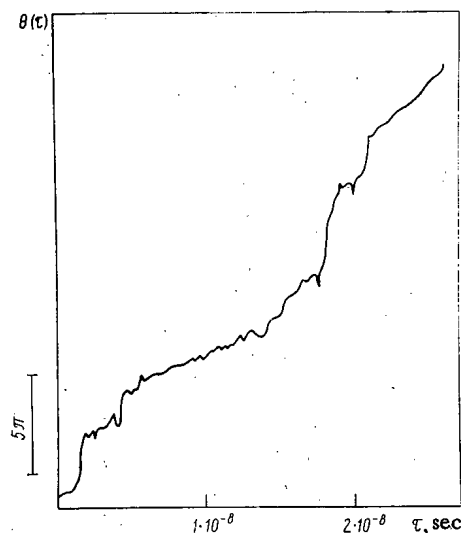


Fig. 12. Phase change of the oscillations as a function of time.

Correlation Analysis of the Oscillations Excited by the Beam

For more complete analysis of the oscillations a space-time correlation method [30, 31] was used. Figures 9, 10, and 11, respectively, show oscilloscope traces of the oscillations, an integrated and an instantaneous spectrum of the oscillations during intensive x-ray emission. It is clear that in the instantaneous spectrum there are oscillations of frequency $f = 350$ MHz which correspond to spiral waves. The correlation time, obtained from the autocorrelation function of the oscillations, is of order $\tau_k \approx 5 \cdot 10^{-9}$ sec. In Fig. 12 is shown a plot of the phase change in time of the oscillations, where discontinuities in the phase of the electric field are clearly visible. The magnitude of these phase discontinuities is $30-180^\circ$. The average time for the phase shift is $\sim 1.5 \cdot 10^{-9}$ sec.

Determination of the joint correlation function of oscillations received by antenna probes placed in the chamber at different distances from one another permitted evaluation of the phase velocity. When $\omega_{Oe} > \omega_{Be}$, f or probes separated by 2 and 4 cm and standing 5, 7, and 9 cm from the center of the trap, the signal delay time was 1 nsec; hence, the phase velocity of the oscillations was

$$v_\phi = \frac{\Delta z}{\Delta \tau} = 2 \cdot 10^9 \text{ cm/sec.}$$

Therefore, correlation analysis of the oscillations has confirmed that for $\omega_{Oe} > \omega_{Be}$ electron heating is due to oscillations with frequency near that of the spiral waves (see Fig. 11). The integrated spectrum, as also that measured by the analyzers, was practically continuous, but the oscillations were strongly nonlinear.

The Mechanism of Electron Heating in the Magnetic-Mirror Trap

Knowing all the basic characteristics of the fields of the stochastic oscillations, it is easy to estimate the temperature of the electrons accelerated by these fields. According to [15], the change in electron temperature due to cyclotron heating by stochastic fields is given by

$$T - T_0 = \frac{e^2}{2m} \sum_k \frac{\tau_k}{1 + (\omega_k \pm \omega_{Be})^2 \tau_k^2} \int_0^{\tau_k} |E_k|^2 dt, \quad (4)$$

where T_0 is the initial electron temperature; τ_k the correlation time of the oscillations; $\int_0^{\tau_k} |E_k|^2 dt$ the energy of oscillations with wave vector k ; e and m the charge and mass of the electron. After a series of simplifications, Eq. (4) and the experimental values are substituted into it we obtain $T_e \approx 3 \cdot 10^5$ eV. The measured

electron temperature is $T_e \approx 1 \cdot 10^5$ eV, which is near the calculated value. This gives reason to consider that the stochastic mechanism plays an important role in accelerating and heating electrons. However, this does not exclude a role for induced scattering of waves by electrons. For two waves the condition for induced scattering may be written in the form

$$\omega_1 - \omega_2 = (k_1 - k_2) v_0. \quad (5)$$

The expression for the force δF acting on a particle shows that the force depends on the product of the amplitude of the two waves and is constant in time [26] if the resonance condition (Eq. (5)) holds.

During study of the oscillations it was found that among the intermittent oscillation packets, there occur fairly often packets for which the frequency of the oscillations remains constant for a long time (up to 0.1 sec) and coherent along the length of the apparatus. From this it follows that along with stochastic acceleration of electrons and induced scattering of waves on electrons there occurs resonance acceleration, or capture of electrons by large amplitude waves. In this case the captured particles may be either plasma or beam electrons. It is noted that the most efficient electron heating in traps with interacting beams occurs when ω_{Oe} and ω_{Be} are close. As is known, in such interactions the electrons are accelerated due to the development of beam instabilities in the fields of oscillations which are excited within a given range Δv_ϕ of phase velocities, roughly corresponding to the velocities of the beam particles. However, as a result of decay processes and induced scattering transformation of oscillations from the range Δv_ϕ to other ranges is possible. Consequently oscillations and waves occur in a whole range of frequencies. Both processes make it possible for particles to fall into a resonance with waves induced by the growth of a given instability. The most intense heating occurs with induced scattering which leads to transformation of oscillations from the original range into another accompanied by a reduction in frequency and in k . The rate of heating may be estimated [26] by

$$\frac{\delta\omega}{\omega} W \frac{1}{\tau}, \quad (6)$$

where τ is the transformation time in the spectrum over some frequency difference $\delta\omega$ and W is the energy of the turbulence. For given oscillations there exists a threshold particle velocity above which the particles may be accelerated. Thus, plasma oscillations accelerate only those particles of $v > v_{Te}$. But, for example, low frequency oscillations may initially accelerate particles. It should be noted that the distribution of oscillations in phase velocity may have a significant influence on electron heating in the beam and plasma. Thus, for example, from [26] it follows that the efficiency of acceleration of particles whose velocity exceeds by many times the phase velocity of the oscillations depends not only on the energy of longitudinal oscillations but also very strongly on the distribution of the oscillations in phase velocity $\sim v_\phi^3$.

CONCLUSIONS

As a result of the interaction of a powerful spiral beam with a plasma, short bursts of instability arise which have large growth rates. These instabilities excite oscillations, the spectrum of which changes over times of 10^{-7} to 10^{-9} sec. In this case conditions are created, where in a given time interval either purely stochastic or ordered acceleration and heating of electrons occurs, which may permit heating of not only the beam electrons but those of the plasma as well.

An RF field of substantial magnitude (2-3 kV/cm) accelerates the particles of the beam and the plasma, so that some of the particles are accelerated to energies higher than the limiting value of energy for containment in the trap. These particles rapidly escape the plasma, creating density oscillations almost synchronous with the RF bursts.

Nonlinear interactions of the oscillations complicate the development of instabilities. In particular, they lead to shifts in the frequencies responsible for heating to frequencies lower than resonance. The fields of the excited oscillations have short correlation times ($\sim 1 \cdot 10^{-9}$ sec) and have a random character, but the interaction of the oscillations strongly changes their characteristics.

The nonlinear interactions appear fairly strongly since they are proportional to the power of the oscillations (which in this case is substantial). One of the important nonlinear effects is the redistribution of the energy of the oscillations into several types of oscillation and its transformation from regions of emission to regions of absorption accompanied by heating of particles. In several cases the nonlinear interactions lead to a growth in the phase velocity of waves, and there is then a sharp increase in the efficiency with which the particles are accelerated. The broadening of the phase velocity and frequency spectrum of the waves leads to the same effect.

The general picture of the heating mechanism remains practically unchanged for $\omega_{Oe} < \omega_{Be}$ from what it is as for $\omega_{Oe} > \omega_{Be}$. The only difference is with which oscillations the beam and plasma basically interact in the given conditions of the experiment (usually $\omega < \omega_{Be}$). In the $\omega_{Oe} > \omega_{Be}$ and $\omega_{Oe} < \omega_{Be}$ cases, the oscillations responsible for heating are, respectively, the spiral waves and those near the electron cyclotron frequency.

One of the practically important results of this experiment is that the plasma parameters can be comparatively easily controlled by means of continuous control of the transverse component of the beam velocity as developed in [8].

In conclusion I wish to thank Ya. B. Fainberg and E. A. Kornilov for useful criticism and valuable advice, and V. P. Zeidlits for computer calculations.

LITERATURE CITED

1. A. I. Akhiezer and Ya. B. Fainberg, Dokl. Akad. Nauk SSSR, Vol. 69 (1949), p. 555.
2. D. Bohm and E. Gross, Phys. Rev., 75, 1851 (1949).
3. Ya. B. Fainberg et al., Atomnaya Energiya, 14, No. 3, 249 (1963).
4. A. K. Berezin et al., in: Plasma Physics and the Problems of Controlled Thermonuclear Fusion [in Russian], Vol. 3, Izd. AN UkrSSR, Kiev (1963), pp. 125-138.
5. M. V. Babykin et al., in: International Conference on Plasma Physics and Controlled Thermonuclear Fusion, IAEA, Salzburg, Lecture No. 209 (1961).
6. M. V. Babykin et al., Zh. Eksperim. i Teor. Fiz., 43, No. 411 (1962), p. 1976.
7. E. K. Zavoiskii and L. I. Rudakov, Plasma Physics [in Russian], Znanie, Moscow (1967).
8. K. D. Sinel'nikov and B. S. Akshanov, in: Plasma Physics and Problems of Controlled Thermonuclear Fusion [in Russian], Vol. 4, Naukova Dumka, Kiev (1965), pp. 403-410 (Lecture at the IV Conference on Plasma Physics, Kharkov (1963)).
9. B. S. Akshanov, Yu. Ya. Volkolupov, and K. D. Sinel'nikov, in: Magnetic-Mirror Traps [in Russian], Naukova Dumka, Kiev (1965), pp. 18-40.
10. I. Alexeff and R. Neidigh, Phys. Rev., 136, 689 (1964).
11. I. Alexeff et al., in: Conf. on Plasma Physics and Controlled Nuclear Fusion Research, Culham (1965), Paper CN-21/102.
12. B. S. Akshanov et al., Zh. Eksperim. i Teor. Fiz., 35, No. 12, 2232 (1965).
13. B. S. Akshanov, Yu. Ya. Volkolupov, and K. D. Sinel'nikov, ZhTF, 34, No. 4, 608-611 (1966).
14. B. S. Akshanov et al., Atomnaya Energiya, 23, No. 3, 201-208 (1967).
15. F. G. Bass, Ya. B. Fainberg, and V. D. Shapiro, Zh. Eksperim. i Teor. Fiz., 49, 329 (1965).
16. L. P. Zakatov et al., ZhTF, 54, No. 4, 1088 (1968).
17. A. N. Karkhov, Dissertation [in Russian], Moscow (1970).
18. F. Bottiglioni et al., EUR-CEA-FC-460, Fontenay-aux-Roses, France (1968).
19. E. A. Kornilov et al., in: Interaction of Charged Particle Beams with Plasma [in Russian], Naukova Dumka, Kiev (1965), pp. 36-44.
20. E. A. Kornilov, E. V. Lifshits, and O. F. Kovpik, Usp. Fiz. Nauk, 14, No. 4, 573-581 (1969).
21. V. T. Astrelin, N. S. Buchel'nikova, and A. M. Kudryavtsev, in: Proc. Third European Conf. on Contr. Fusion Plasma Physics, Utrecht (1969), p. 92.
22. R. A. Demirkhanov et al., Zh. Eksperim. i Teor. Fiz., 63, No. 5, 1653-1663 (1972).
23. R. Neidigh et al., in: Third Conf. on Plasma Physics and Contr. Nucl. Fusion Res., Novosibirsk (1968), Paper CN-24/L-2.
24. H. Hopman, The Electron Cyclotron Instability in a Beam-Plasma System, Rotterdam (1969).
25. K. D. Sinel'nikov et al., see [8], pp. 388-402.
26. V. N. Tsytovich, in: Nonlinear Effects in Plasma [in Russian], Nauka, Moscow (1967); V. N. Tsytovich, in: Theory of the Turbulent Plasma [in Russian], Nauka, Moscow (1971).
27. V. L. Ginzburg and A. A. Rukhadze, in: Waves in a Magnetoactive Plasma [in Russian], Nauka, Moscow (1970).
28. M. F. Gorbatenko, ZhTF, 52, 1070 (1963).
29. A. B. Kitsenko and B. A. Gapontsev, see [19], pp. 131-136; A. B. Kitsenko and K. N. Stepanov, Usp. Fiz. Nauk, 6, 297 (1961).
30. B. P. Levin, in: Theoretical Basis of Statistical Radio Engineering [in Russian], Sovetskoe Radio, Moscow (1966).
31. E. A. Kornilov et al., Pis'ma v Zh. Eksperim. i Teor. Fiz., 4, 147 (1966); A. K. Berezin, Ya. B. Fainberg, and I. A. Bezyazychnyi, Pis'ma v Zh. Eksperim. i Teor. Fiz., 7, 156 (1968).

EFFECT OF CHANGES IN THE NONUNIFORMITY OF ENERGY EVOLUTION IN THE FUEL OF THERMAL REACTORS ON THE TEMPERATURE DISTRIBUTION IN THE FUEL ELEMENTS

V. S. Yamnikov, L. L. Malanchenko,
and V. I. Solnyanyi

UDC 621.039.517.5

It is well known that the nonuniformity of energy evolution over the cross section of the fuel in thermal reactors has a considerable effect on the temperature distribution in the fuel elements [1, 2]. The nonuniformity of energy evolution is due to the nonuniform distribution of the neutron and fissile-isotope flux across the cross section of the fuel. In thermal power reactors, rod-type fuel elements with low fuel enrichment are usually employed, these being assembled into fuel assemblies or cassettes. The neutron distribution over the fuel cross section will depend on the disposition of the fuel element in the assembly and that of the assembly in the reactor. The screening of the neutron field in fuel elements with low fuel enrichment is insignificant in the early stages of a campaign and has no serious effect on the temperature field in the elements. However, during the operation of the reactors plutonium accumulates in the fuel, a considerable proportion of this being formed in the resonance absorption of delayed neutrons by the ^{238}U nuclei. A considerable proportion of the resonance neutrons are absorbed by the outer layers of the fuel, so that during the campaign there is a substantial redistribution of fissile isotopes over the cross section of the fuel. Furthermore, the absorption of the resonance neutrons depends on the construction of the reactor, the assembly of the fuel elements, and the positioning of these in the assembly. For example, the resonance integral of a fuel element from the outer row of an assembly consisting of 18 fuel elements is 20% greater than that of a fuel element from the inner row [3]. Along the perimeter of the fuel element there is also a nonuniform absorption of the resonance neutrons and hence a nonuniform build-up of fissile isotopes.

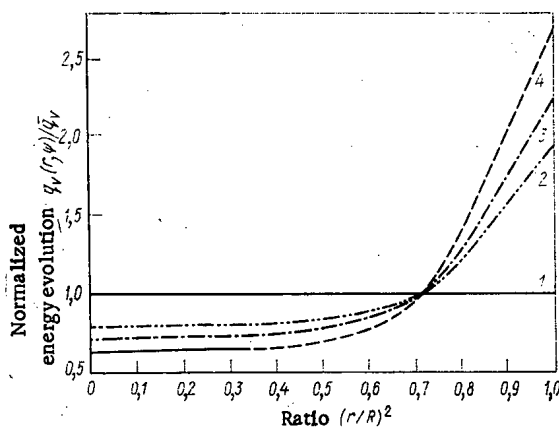


Fig. 1

Fig. 1. Distribution of energy evolution over the cross section of the fuel without burn-up (1) and with a burn-up of 7.5 (2), 15 (3), and 30 MW·day/kg U (4).

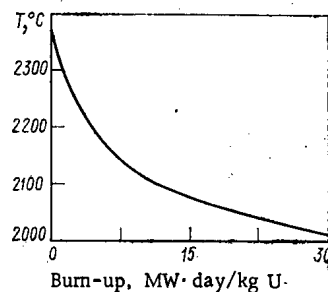


Fig. 2

Fig. 2. Change in the temperature in the center of a VVER-1000 fuel element as burn-up proceeds.

Translated from *Atomnaya Energiya*, Vol. 36, No. 4, pp. 269-272, April, 1974. Original article submitted May 11, 1973.

© 1974 Consultants Bureau, a division of Plenum Publishing Corporation, 227 West 17th Street, New York, N. Y. 10011. No part of this publication may be reproduced, stored in a retrieval system, or transmitted, in any form or by any means, electronic, mechanical, photocopying, microfilming, recording or otherwise, without written permission of the publisher. A copy of this article is available from the publisher for \$15.00.

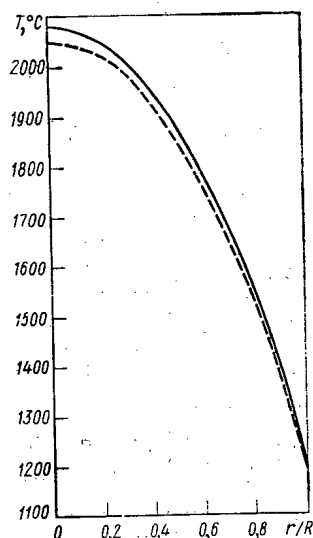


Fig. 3

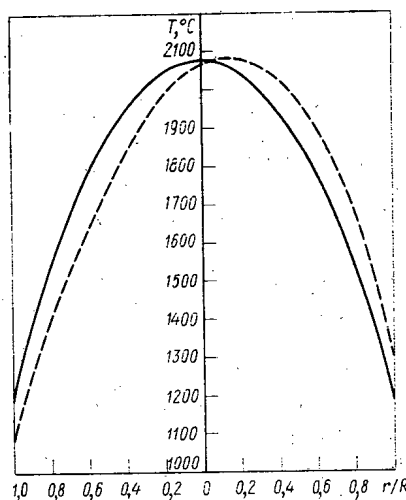


Fig. 4

Fig. 3. Effect of an error in φ (committed when determining the probability of avoiding resonance absorption as a function of the cross section of the fuel) on the temperature distribution in the fuel element: —) value of T calculated by Eq. (8); ---) surface part of the resonance integral in Eq. (8) increased by 20%.

Fig. 4. Effect of the misalignment of the neutron field and the nonuniform distribution of the probability of avoiding resonance absorption around the perimeter and across the cross section of the fuel on the temperature distribution in the fuel for a burn-up of 15 MW · day/kg U: —) symmetrical field of energy evolution in the fuel (see Fig. 1, curve 3); ---) asymmetrical field of energy evolution in the fuel.

Figure 1 shows the typical change in the distribution of energy evolution over the cross section of a fuel element in the course of the campaign due to the nonuniformity of the neutron field and the nonuniform accumulation of ^{239}Pu and ^{241}Pu . The effect of the nonuniformity of the energy evolution on the temperature distribution in the fuel element has been studied in great detail in [2]. However, the equation proposed in [2] for the distribution of energy evolution over the cross section of the fuel element does not allow for the accumulation of ^{239}Pu and ^{241}Pu .

The field of energy evolution existing during the campaign (Fig. 1) may be expressed in the form

$$\frac{q_v(r, \psi)}{\bar{q}_v} = \left[a_1 + a_2 \left(\frac{r}{R} \right) \cos \psi \right] \left[b_1 + b_2 \left(\frac{r}{R} \right)^p \right] = A_1 + A_2 \left(\frac{r}{R} \right)^p + A_3 \left(\frac{r}{R} \right) \cos \psi + A_4 \left(\frac{r}{R} \right)^{p+1} \cos \psi, \quad (1)$$

where $q_v(r, \psi)$ is the density of energy evolution at a particular point in the fuel (W/cm^3); \bar{q}_v is the mean energy-evolution density in the fuel (W/cm^3); $A_1 = q_v(0)/\bar{q}_v$; $A_2 = q_v(R)/\bar{q}_v - A_1$; $A_3 = \mu A_1$; $A_4 = \mu A_2$; $\mu = (q_v(R)_{\text{max}} - q_v(R)_{\text{min}}) / (q_v(R)_{\text{max}} + q_v(R)_{\text{min}})$; μ is a coefficient depending on the alignment of the field; p is a positive whole number depending on the form of distribution of the energy evolution; ψ is the polar angle. Using a method similar to that of [2] we may derive a solution to the heat-conduction equations for the fuel:

$$\frac{\partial^2 T}{\partial r^2} + \frac{1}{r} \cdot \frac{\partial T}{\partial r} + \frac{1}{r^2} \cdot \frac{\partial^2 T}{\partial \psi^2} + \frac{q_v(r, \psi)}{\lambda_r} = 0; \quad (2)$$

and for the can

$$\frac{\partial^2 T'}{\partial r^2} + \frac{1}{r} \cdot \frac{\partial T'}{\partial r} + \frac{1}{r^2} \cdot \frac{\partial^2 T'}{\partial \psi^2} = 0, \quad (3)$$

where $q_v(r, \psi)$ is described by Eq. (1). Allowing for the boundary conditions

- a) for $\psi = 0, \pi, 2\pi \dots \frac{\partial T}{\partial \psi} = 0, \frac{\partial T'}{\partial \psi} = 0$;
 b) for $r/R = 0$ T is a finite quantity
 c) for $r = R - \frac{\partial T}{\partial \left(\frac{r}{R}\right)} = \frac{\alpha_{gap} R}{f} (T_R - T'_a)$;
 d) for $r = R_b - \frac{\partial T'}{\partial \left(\frac{r}{R_b}\right)} = \frac{\alpha_T R_b}{\lambda_{can}} (T'_b - T_T)$;
 e) for $r = R \approx R_a \frac{\lambda_f}{k \lambda_{can}} \frac{\partial}{\partial \left(\frac{r}{R}\right)} = \frac{\partial T'}{\partial \left(\frac{r}{R_b}\right)}$

the solution takes the form

$$T = T_c - \frac{\bar{q}_s R}{k \lambda_f} \left[\frac{A_1}{2} \left(\frac{r}{R}\right)^2 + \frac{2A_2}{(p+2)^2} \left(\frac{r}{R}\right)^{p+2} + \frac{A_3}{4} \left(\frac{r}{R}\right)^3 \cos \psi + \frac{2A_4}{(p+3)^2 - 1} \left(\frac{r}{R}\right)^{p+3} \cos \psi \right] + k_1 \left(\frac{r}{R}\right) \cos \psi; \quad (4)$$

$$T' = T_T + \Delta \bar{T} - \frac{\bar{q}_s R_b}{\lambda_{can}} \ln \frac{r}{R_b} + \Delta \bar{T} \left[\gamma_1 \left(\frac{r}{R_b}\right) + \delta_1 \left(\frac{r}{R_b}\right)^{-1} \right] \cos \psi, \quad (5)$$

where T_c is the temperature in the center of the fuel, determined from the formula

$$T_c = \frac{\bar{q}_s R}{k \lambda} \left[\frac{A_1}{2} + \frac{2A_2}{(p+2)^2} \right] + \Delta \bar{T}_{gap} - \frac{\bar{q}_s R_b}{\lambda_f} \ln k + \Delta \bar{T} + T_T; \quad (6)$$

\bar{q}_s is the averaged thermal flux on the outer surface of the can (W/cm²); λ_f, λ_{can} are the thermal conductivities of the fuel and can respectively (W/cm · deg); α_T is the heat-transfer coefficient from the coolant to the can (W/cm² · deg); R is the radius of the fuel surface (cm); R_a, R_b are the inner and outer radii of the can (cm); k is the ratio of the inner radius of the can to the outer; T_T is the temperature of the coolant (°C); T'_a, T'_b are the temperatures of the can at the inner and outer radii respectively (°C); $\Delta \bar{T}_{gap} = \bar{q} / \alpha_{gap} k$; $\Delta \bar{T} = \bar{q}_s / \alpha_T$.

The coefficients γ_1 and k_1 are found from the system of equations

$$\left(1 + \frac{\alpha_{gap} R}{\lambda_f}\right) k_1 - \frac{\Delta \bar{T} k \alpha_{gap} R}{\lambda_f} \left[1 + \frac{1}{k^2} \cdot \frac{\lambda_{can} + \alpha_T R_b}{\lambda_{can} - \alpha_T R_b}\right] \gamma_1 = \frac{\alpha_{gap} R}{\lambda_f} \Delta \bar{T}_{gap} \left[\frac{A_3}{4} \left(\frac{\alpha_{gap} R}{\lambda_f} + 3\right) + \frac{2A_4}{(p+3)^2 - 1} \right];$$

$$k_1 + \Delta \bar{T} \frac{k \lambda_{can}}{\lambda_f} \left[\frac{1}{k^2} \cdot \frac{\lambda_{can} + \alpha_T R_b}{\lambda_{can} - \alpha_T R_b} - 1 \right] \gamma_1 = \frac{\alpha_{gap} R}{\lambda_f} \Delta \bar{T} \left[\frac{3}{4} A_3 + \frac{2(p+3) A_4}{(p+3)^2 - 1} \right], \quad (7)$$

and

$$\delta_1 = \frac{\lambda_{can} \alpha_T R_b}{\lambda_{can} - \alpha_T R_b} \gamma_1.$$

Thus in order to determine the change in the temperature distribution in the fuel and the can we must find the change in the distribution of energy evolution during the campaign. For this purpose we require to know the neutron flux distribution and to calculate the change in the concentration of the fissile isotopes (²³⁵U, ²³⁹Pu, ²⁴¹Pu) over the cross section of the fuel during the campaign. The chief difficulty lies in determining the distribution of the absorption of delayed neutrons across the fuel cross section. The resonance integrals were measured in [3, 4] for both individual fuel elements and assemblies situated in various media (air, D₂O, H₂O) as well as the distribution of resonance absorption across the cross section of the fuel elements.

These results were used to determine the manner in which the probability of escaping resonance absorption was distributed over the fuel cross section of a water-moderated, water-cooled reactor with fuel in the form of UO₂

$$\varphi = \exp \left\{ - \frac{N^8 R^2}{S \gamma} 2.32 \cdot 10^{-24} \right. \\ \times \left\{ 4.57 + [8.08 - 1.02 \cdot 10^{-22} (RN^8)] \right. \\ \left. + e^{\frac{3.72 \cdot 10^{6,6}}{(RN^8)^{0,3}} \left(\frac{r}{R}\right)^2} \frac{1 + 0.0175 \sqrt{T_f}}{1.32} \Pi_r \Pi_a \right\} \left. \right\}; \quad (8)$$

$$\varphi = \exp \left\{ - \frac{N^8 R^2}{S \gamma} 2.32 \cdot 10^{-24} \left\{ 4.57 + [8.08 - 1.02 \cdot 10^{-22} (RN^8)] \right. \right. \\ \left. \left. + \frac{(RN^8)^{0,3}}{3.72 \cdot 10^{6,6}} \left(1 - \frac{3.72 \cdot 10^{6,6}}{(RN^8)^{0,3}}\right) \frac{1 + 0.0175 \sqrt{T_f}}{1.32} \Pi_r \Pi_a \right\} \right\}, \quad (9)$$

where N^8 is the number of ^{238}U atoms in 1 cm^3 of UO_2 ; S is the area of the water in the active zone (cm^2); γ is the specific gravity of the water under the working conditions of the active zone (g/cm^3); T_f is the temperature of the fuel ($^\circ\text{K}$); Π_r , Π_a are correction factors allowing for the specific construction of the reactor and the fuel assembly.

In deriving Eqs. (1), (4), and (5), two assumptions were made:

- 1) the thermal conductivity of the fuel was independent of temperature;
- 2) there was no redistribution of the plutonium so formed over the fuel cross section. Calculations of the temperature field in a fuel element of the VVER-1000 type were presented as an example. The construction of the fuel elements and its working conditions were indicated in [5].

Figure 2 shows the change in temperature in the center of the fuel during the campaign. The corresponding curves of energy distribution over the radius of the fuel element are presented in Fig. 1. We see from Fig. 2 that the redistribution of energy evolution over the fuel cross section leads to a considerable fall in the maximum and average temperatures of the fuel. In order to estimate the effect of any inaccuracy in the surface part of the resonance integral on the temperature redistribution during the campaign, we made a calculation with a 20% increase in the surface part of the resonance integral, regarding the average resonance integral as constant. The results of the calculation are presented in Fig. 3, from which we see that the inaccuracy introduced into the calculation in determining the ϕ distribution from Eq. (8) has very little effect on the temperature calculations.

As already indicated, the fuel element may operate under conditions in which the neutron field is misaligned with respect to the cross section of the fuel element, while the probability of escaping resonance absorption is unevenly distributed around its perimeter. In order to illustrate the effect of these factors, we calculated the temperature distribution in the fuel for $\bar{q}_s = 158\text{ W}/\text{cm}^2$ and a burn-up of $15\text{ MW} \cdot \text{day}/\text{kg U}$. The results are presented in Fig. 4.

The assumptions made in the derivation of Eqs. (4) and (5) have no serious effect on the results of the calculations, since it is well known that the temperature dependence of the thermal conductivity of UO_2 diminishes with increasing dose of irradiation, while the diffusion coefficient of plutonium in uranium dioxide is low at temperatures of under 1400°C , so that a redistribution of plutonium in the outer layers of the fuel is not to be expected.*

The foregoing calculations lead to the following conclusions:

1. The nonuniform accumulation of fissile isotopes over the cross section of the fuel element during the campaign must certainly be allowed for in the thermal calculation, as it has a major effect on the temperature distribution in the fuel element.
2. Equations (5) and (6) enable us to allow for the effect of the redistribution of the fissile isotopes (^{235}U , ^{239}Pu) over the cross section of the fuel during the course of the campaign on the fuel temperature distribution.
3. The redistribution of energy evolution over the fuel cross section for a burn-up of $30\text{ MW} \cdot \text{day}/\text{kg U}$ in VVER-1000 fuel elements reduces the temperature in the center of the fuel by about 350°C .
4. The misalignment of the field of energy evolution over the fuel element has no appreciable effect on the maximum or average temperature of the fuel.

LITERATURE CITED

1. B. Lastman, Radiation Phenomena in Uranium Dioxide [Russian translation], Atomizdat, Moscow (1964).
2. R. Nijsig, Nucl. Engng. and Design, No. 4, 1 (1966).
3. E. Helstrand, J. Appl. Phys., 28, No. 12, 1493 (1957).
4. C. Orth, Nucl. Sci. and Engng., 9, No. 4, 417 (1961).
5. A. S. Zaimovskii et al., Atomnaya Energiya, 30, 226 (1971).

*The possibility of a redistribution of plutonium taking place at higher temperatures is not considered in the present investigation.

CORROSION RESISTANCE OF STEELS OF THE FERRITIC AUSTENITIC CLASS AND POSSIBILITY OF USING THEM IN NUCLEAR POWER SYSTEMS

V. V. Gerasimov, A. I. Gromova,
V. N. Belous, V. A. Gosteva,
and É. G. Fel'dgandler

UDC 621.039.553.36;620.193.47.7

The construction of atomic (nuclear) power stations is now being widely pursued. There is accordingly a great desire to replace the expensive austenitic steel 0Kh18N10T with more economical steels of at least as good a corrosion resistance. Materials capable of replacing 0Kh18N10T steel include two-phase steels of the ferritic-austenitic class with low nickel contents such as EP-53, EP-54, EP-214, EP-26, and others. It is well known that these steels have a higher resistance to corrosion cracking than 0Kh18N10T, and under certain conditions they also have a high resistance to intercrystallite corrosion. In mechanical properties, technological convenience, and weldability, EP-53 and EP-54 steels are no less favorable than Kh18N10T, and in some cases are even better [1-7].

In this investigation we shall consider the corrosion behavior of the ferritic-austenitic steels indicated under the conditions obtaining in nuclear power stations and shall determine their suitability for reactor building.

We tested samples of EP-53, EP-54, EP-214, and EP-26 steels (compositions indicated in Table 1) in the as-supplied state for continuous and intercrystallite corrosion and corrosion cracking. The experiments were carried out under static conditions in autoclaves made of 0Kh18N10T steel, using existing techniques [8], and also under dynamic conditions during the running of various nuclear power installations and loops. In all cases when determining the rate of continuous corrosion of the materials we used the gravimetric method. The tendency toward intercrystallite corrosion was estimated in accordance with All-Union State Standard 6032-58, using the "A" and "AM" methods with induction heating. The resistance of the steels to corrosion cracking was tested in boiling 42% solutions of magnesium chloride and in saturated steam with a high concentration of oxygen and chlorine ions.

Results of the Tests and Discussion

The possible development of intercrystallite corrosion and the development of corrosion cracking in steels depends on the state of the material itself and on the properties of the corrosive medium. The latter depend both on internal factors (chemical composition of the material, technology of its production) and on external factors (composition of the medium, temperature, degree of stress, etc.).

TABLE 1. Chemical Composition of the Steels (wt. %)

Steel	C	Cr	Ni	Mn	Si	Ti	Mo	P	S	N ₂
EP-53	0,08	21	4,9	0,8	0,8	0,025	—	—	—	—
EP-54	0,08	21	5,5	0,8	0,8	0,3	3,1	—	—	—
EP-214	0,09	22	3,5	0,8	—	0,3	—	—	—	—
EP-26	0,1	17-20	1,5-2,5	4-6	0,8	—	—	0,03	0,03	0,8
Kh18N10T	0,11	17-19	9,0-11,0	1,0-2,0	0,8	0,4	—	0,03	0,02	—

Translated from *Atomnaya Energiya*, Vol. 36, No. 4, pp. 273-276, April, 1974. Original article submitted February 1, 1973.

© 1974 Consultants Bureau, a division of Plenum Publishing Corporation, 227 West 17th Street, New York, N. Y. 10011. No part of this publication may be reproduced, stored in a retrieval system, or transmitted, in any form or by any means, electronic, mechanical, photocopying, microfilming, recording or otherwise, without written permission of the publisher. A copy of this article is available from the publisher for \$15.00.

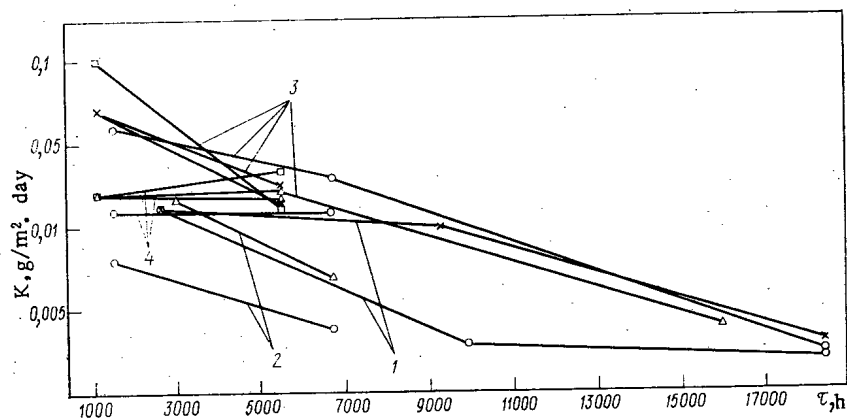


Fig. 1. Corrosion rate of ferritic-austenitic steels in a medium with a high pH value: ○) Kh18N10T; ×) EP-53; △) EP-54; □) EP-26; 1) water-steam mixture [$O_2 = 0.01$ mg/kg, pH = 8.8 (NH_4OH), $Cl' = 0.05$ mg/kg, $t = 285^\circ C$, $v = 6$ m/sec]; 2) saturated steam ($O_2 = 0.91$ -12.3%, $H_2 = 70.4$ -78.2%, $v = 30$ -50 m/sec, $t = 265^\circ C$, $p = 30$ kg/cm²; 3) in water with an irradiation of 10^{13} neutrons/cm²·sec [$O_2 \leq 0.02$ mg/kg, $Cl' \leq 0.5$ mg/kg, pH = 9.2-9.7 (NH_4OH), $t = 300$ -330°C, $v = 4$ m/sec]; 4) in water (composition as indicated for curve 3).

TABLE 2. Results of Tests on the Corrosion Cracking of the Steels under Laboratory Conditions

Type of material	Time to appearance of cracks	
	A	B
OKh18N10T	5-6 min	6 h
EP-53	390 h	900 h
EP-54	—	300 h

Note: Level of reduced stresses ~ 30 kgf/mm². A) 42% $MgCl_2 + 5\%$ $FeCl_3$, boiling solution, $t = 153$ -154°C; B) steam-air medium (film of $FeCl_3$ was deposited on the samples), $t = 100$ -110°C.

Investigations showed that, in the as-supplied state, steels EP-53 and EP-54 were not inclined to intercrystallite corrosion (on testing in accordance with All-Union State Standard 6032-58, methods A and AM). Analogous conclusions were drawn by other research workers [9-15]. A study of the resistance of the two-phase steels toward corrosion cracking showed that the resistance of the industrial two-phase steels EP-53 and EP-54 and the single-phase steel EP-26 to this form of damage was no lower than that of OKh18N10T steel, while in certain cases it was even higher. Steels EP-53 and EP-54 exhibited a higher resistance to corrosion cracking than OKh18N10T in a boiling solution of magnesium chloride and ferric chloride and in a steam-air medium (Table 2). Other investigations support this [11, 16, 17].

The resistance of the steels under consideration to continuous corrosion in water at temperatures up to 300°C under static conditions was comparable with that of OKh18N10T steel under the same conditions. Steels EP-53 and EP-54 corroded at practically the same rate and exhibited uniform corrosion (Table 3).

As a result of our testing of the ferritic-austenitic steels EP-53 and EP-54 in deaerated water under static conditions at temperatures of up to 300°C for 500 h, it was found that these steels constituted members of the "extremely-stable" group of materials, as classified by All-Union State Standard 13819-68.

The existence of applied stresses in the metal has no effect on the corrosion rate of the materials under test (Table 4). Under service conditions the corrosion rate of the steels in question at 50°C in water and in a thermal neutron flux up to $5 \cdot 10^{14}$ neutrons/cm²·sec (10^{15} fast neutrons) is comparable with that of OKh18N10T steel and is no greater than 0.03 g/m²·day over 1860 h testing (Table 5). Steels of these types belong to the group of extremely stable materials (class 2 of corrosion resistance on the ten-class scale of All-Union State Standard 13819-68).

The foregoing data as to corrosion resistance indicate that steels EP-53, EP-54, and EP-214 are perfectly suitable for replacing OKh18N10T steel in the servicing ducts of reactors working at up to 80°C with desalinized water.

On increasing the temperature of the water of 300-330°C the corrosion rate rises slightly for both OKh18N10T steel and the steels of the two-phase type (Table 3). However, even at this temperature the

TABLE 3. Rate of Corrosion of Steels under Static Conditions

Medium	Temperature, °C	Pressure, kgf/cm ²	Duration of tests, h	EP-26	EP-53	EP-54	EP-214	OKh18N10T
Desalinized deaerated water	200	16	50	0,09	0,09	0,08	0,09	0,10
			100	0,08	0,06	0,06	0,06	0,04
Desalinized water containing 2mg/liter oxygen	200	16	50	0,24	0,1	0,12	0,12	0,1
			500	0,13	—	—	—	—
			1000	0,01	—	—	—	0,01
Desalinized deaerated water pH=3(HNO ₃)	300	87	50	0,2	0,1	0,12	0,16	0,1
Desalinized deaerated water	300	87	50	0,25	0,20	0,27	0,27	0,2—0,3
			100	—	0,09	0,07	0,07	0,19
			300	—	0,04	0,04	0,03	0,07
			500	—	0,03	0,03	0,02	0,03
			1000	—	—	—	—	0,018
Desalinized deaerated water	300	87	50	0,21	0,13	0,14	0,15	0,15
Desalinized water containing 5, 6-6, 9 mg/liter oxygen	300	150	50	—	0,11	0,07	0,07	—
Deaerated water containing 10mg/liter Cl'	300	87	50	0,25	0,24	0,18	0,11	—

Note: Here and subsequently the corrosion rate is expressed in g/m²·day.

TABLE 4. Corrosion Rate of Steels at 175°C

Steel	Applied stress, kgf/mm ²	A		B
		Period of tests, h		
		4320	5000	16 500
OKh18N10T	16	0,17	0,126	0,081
		0,14	0,155	0,094
EP-53	—	0,152	0,121	0,1
	16	0,162	0,126	0,103
EP-54	—	0,21	0,186	0,137
	16	0,17	0,187	0,138

Note: Pressure up to 20 kgf/cm²; rate of water flow 0,56 m/sec. Composition of water A) O₂=0,15-0,8 mg/liter; H₂O₂=0,6 mg/liter; Cl'=0,02 mg/liter; Fe=0,1 mg/liter; Al=0,1 mg/liter; pH=6,5; B) O₂=0,4-0,5 mg/liter; H₂O₂=3,3-70 mg/liter Cl'=0,018-0,02 mg/liter Fe=0,023 mg/liter; Al=0,002-0,002 mg/liter, pH 5,5.

corrosion rate of the steels is low in absolute magnitude and comparable for all the individual types tested. The high corrosion resistance of these materials in deaerated water with high pH values remains intact under service conditions, with or without irradiation (Fig.1). Under these conditions steels EP-53 and EP-54 belong to the category of extremely stable materials after 4000 h testing according to All-Union State Standard 13819-68. According to tests in water with a pH value close to neutral and with a high oxygen content at ~300°C (Table 6), steels EP-53 and EP-54 do not fall into the category of materials with a lower corrosion resistance than OKh18-N10T steel according to All-Union State Standard 13819-68.

Steels EP-53 and EP-54 behave in a similar way under the working conditions of a loop of the boiling type. Thus in a water-steam mixture, in water, and in saturated

TABLE 5. Corrosion Rate of Steels in Water at 50°C

Medium	Conditions of tests	Rate of water flow, m/sec	Period of tests, h	OKh18N10T	EP-53	EP-54	EP-214
Desalinized deaerated water	No irradiation	—	1650	0,02	0,01	0,01	0,01
Circuit water*	Irradiation with a thermal neutron flux, neutron/cm ² ·sec : 5·10 ¹⁴	8	1650	0,08	0,01	0,01	0,01
		3	1850	0,01	0,01	0,01	0,02
	2,2·10 ¹⁴	—	—	—	—	—	—

*Composition of water: Cl' absent, Fe = 0.29 mg/kg; s/r=31 mg/kg; O₂=10-12 mg/kg; pH=4.3-6.5; activity 10⁻³ Cl/liter of water.

TABLE 6. Corrosion Rate of Steels in Water at 329°C and Pressure 130-132 kg/cm² for 7000 h of Tests*

Condition of tests	0Kh18N10T	EP-53	EP-54
Water of first circuit	0,0007 0,0096†	0,0074 0,0096†	0,0069 —
Active zone (10 ¹² /thermal neutrons/cm ² ·sec)	0,0144	0,0102	0,010

*Composition of water: pH = 5, 8-7, 2; O₂ = 0.08-1.5 mg/liter s/r = 0.8-2.0 mg/liter, v = 1.5 m/sec.

†Corrosion rate of stressed samples (reduced stresses 30 kgf/mm²).

TABLE 7. Corrosion Rate of Steels under the Working Conditions of a Boiling Reactor at 270-285°C and a Pressure of 70 kg/cm²

Conditions of tests	Period of tests, h	0Kh18N10T	EP-53	EP-54
Water (pH = 6.3-7.4; O ₂ = 0.3-0.4 mg/kg)	2 668	0,011	0,023	0,024
	5 900	0,007	0,016	0,015
	10 000	0,013	0,017	0,01
	17 700	0,02p	0,009	0,014
Water-steam mixture (x = 16 ÷ 17%)	2 668	0,0085	0,019	0,024
	5 900	0,003	0,0056	—
	10 000	0,0068	0,0045	0,0054
	17 700	0,003	0,002	0,003
Saturated steam (O ₂ = 7,1 mg/kg)	2 668	0,015	0,018	0,014
	5 900	0,012	0,011	0,017
	10 000	0,014	0,0108	0,010
	17 700	0,006	0,005	0,005

steam, the corrosion rate of the two-phase steels is roughly twice that of 0Kh18N10T (Table 7), the category of corrosion resistance remaining the same.

Thus steels EP-53 and EP-54, like steel 0Kh18N10T, belong to the category of perfectly stable materials (according to All-Union State Standard 13819-68) under the working conditions of water-cooled, water-moderated reactors (desalinized, deaerated water, neutral and high pH) and reactors of the boiling type.

After fairly long holding periods at 400-600°C, the ferritic-austenitic steels may show a tendency toward embrittlement; they should thus not be used in corrosive media above 300°C.

Thus the diffusion-type steels EP-53 and EP-54 have the following advantages over Kh18N10T: a lower nickel content, a higher yield stress, and a greater resistance to corrosion cracking. These steels have a resistance to continuous and intercrystallite corrosion in desalinized water at 80-300°C comparable with that of 0Kh18N10T steel, and may be recommended as construction materials for reactors at temperatures up to 300°C in aqueous media under the same conditions as those in which Kh18N10T steel allows reliable use of the equipment.

LITERATURE CITED

1. E. Thum, Metal Progr., No. 6 (1936).
2. M. B. Shapiro and A. L. Belinskii, Metal. i Term. Obrabotka Metal., No. 7, 10 (1963).
3. D. F. Odesskii and V. M. Vozdvizhenskii, Metal. i Term. Obrabotka Metal., No. 2, 36 (1962).
4. E. A. Kovaleva and I. V. Salli, Metal. i Term. Obrabotka Metal., No. 10, 41 (1963).
5. M. N. Kulakova and N. I. Ignat'eva, Metal. i Term. Obrabotka Metal., No. 3, 53 (1965).
6. F. F. Khimushin, Stainless Steels [in Russian], Metallurgizdat, Moscow (1963).
7. L. Ya. Liberman and M. I. Peisikhis, Properties of Steels and Alloys Used in Boiler-Making [in Russian], Part 2, No. 16 (1966), p. 85.
8. V. V. Gerasimov and A. I. Gromova, in: Corrosion of Reactor Materials [in Russian], Atomizdat, Moscow (1960), p. 191.
9. N. A. Levin and D. G. Kochergina, Zashchita Metal., 1, No. 3, 257 (1965).
10. N. P. Cherkashina, Metal. i Term. Obrabotka Metal., No. 3, 65 (1967).
11. A. A. Babakov, Zashchita Metal., 7, No. 3, 23a (1971).
12. N. I. Ershova et al., Zashchita Metal., 2, No. 1, 83 (1966).
13. A. A. Babakov and M. V. Pridantsev, Corrosion-Resistant Steels and Alloys [in Russian], Metallurgiya, Moscow (1971).
14. D. A. Odesskii and I. Ya. Sokol, Khim. i Neft. Mashinostroenie, No. 2, 21 (1970).
15. A. V. Makarova and E. K. Malakhova, Khim. i Neft. Mashinostroenie, No. 12, 20 (1966).
16. V. N. Gulyaev and I. P. Tsybina, Teploenergetika, No. 10, 44 (1965).
17. V. N. Gulyaev et al., Teploenergetika, No. 12, 32 (1967).

SLOWING-DOWN OF NEUTRONS IN THE PRESENCE OF INELASTIC SCATTERING

Yu. A. Medvedev, E. V. Metelkin,
and G. Ya. Trukhanov

UDC 539.125.523.5

It is essential to know the delayed-neutron spectrum in order to solve a number of problems associated with reactor and shielding physics, geophysics, and related fields [1].

The energy of the neutrons formed as a result of nuclear reactions is usually measured in hundreds of keV – tens of MeV. In the initial instants, corresponding to fairly high energies, the neutrons will be slowed both as a result of elastic scattering at the nuclei of the medium and as a result of inelastic nuclear scattering. So far as the authors are aware, the effect of inelastic scattering on the formation of the delayed-neutron spectrum has never yet been analytically studied.

In this paper we shall present an analytical study of the slowing-down of neutrons, with due allowance for inelastic scattering in a heavy (mass number of the moderator nucleus $M \gg 1$), finite, homogeneous medium, from a stationary source uniformly distributed in space.

Let us assume that, as a result of inelastic scattering, a neutron having energy E' before the collision acquires an energy E :

$$E = E' - \Delta(E') \quad (1)$$

with a probability equal to unity. Here $\Delta(E')$ is the average jump in energy as a result of one inelastic collision.

We shall consider that, in addition to the elastic and inelastic scattering processes (respectively having cross sections Σ_s and Σ_{in}) absorption of neutrons characterized by a cross section Σ_a may also occur. The equation describing the slowing of the neutrons in a homogeneous medium from a stationary, uniformly distributed source, allowing for inelastic scattering, takes the following form [1]:

$$\Phi(\Sigma_s + \Sigma_a + \Sigma_{in}) = \int_0^\infty dE' \Sigma_s(E') P_s(E' \rightarrow E) \Phi(E') + \int_0^\infty dE' \Sigma_{in}(E') P_{in}(E' \rightarrow E) \Phi(E') + q(E), \quad (2)$$

where $\Phi(E)dE$ is the flux of neutrons with energy E in the range dE ; $P_s(E' \rightarrow E)$ and $P_{in}(E' \rightarrow E)$ are the probabilities that a neutron will pass from a state with energy E' into a state with energy E as a result of elastic and inelastic scattering respectively; $q(E)$ is the spectrum of the source.

Depending on the value of the ratio $\Delta(E')/E'$ we may consider two different solutions of the problem in question.

1. Case $\Delta(E')/E' \ll 1$. It is well known that the average energy lost by a neutron having an energy E' before the collision as a result of elastic scattering (for spherically symmetrical scattering in the center of inertia system)

$$\Delta(E') = \frac{\alpha}{2} E'; \quad \alpha = \frac{4M}{(M+1)^2}. \quad (3)$$

Thus for elastic scattering in the case of a heavy moderator the condition $\Delta(E')/E' = \alpha/2 \ll 1$ is also satisfied. Let us unite the processes of elastic and inelastic scattering, i.e., consider that scattering takes place in the moderator with a cross section $\Sigma_s^0 = \Sigma_s + \Sigma_{in}$ and a mean energy jump of $\Delta(E')$, satisfying the conditions (1) and $\Delta(E')/E' \ll 1$. Then Eq. (2) may be written in the form

Translated from *Atomnaya Energiya*, Vol. 36, No. 4, pp. 277-281, April, 1974. Original article submitted May 21, 1973.

© 1974 Consultants Bureau, a division of Plenum Publishing Corporation, 227 West 17th Street, New York, N. Y. 10011. No part of this publication may be reproduced, stored in a retrieval system, or transmitted, in any form or by any means, electronic, mechanical, photocopying, microfilming, recording or otherwise, without written permission of the publisher. A copy of this article is available from the publisher for \$15.00.

$$\Phi(\Sigma_s + \Sigma_a) = \int_0^\infty dE' \Phi(E') \Sigma_s^0(E') \delta[E + \Delta(E') - E'] + q(E), \quad (4)$$

where $\delta(z)$ is the Dirac δ function, while $\Delta(E')$ is the mean energy jump, determined by the relation

$$\Delta(E') = \int_0^\infty dE (E' - E) \frac{\Sigma_s(E') P_s(E' \rightarrow E) + \Sigma_{in}(E') P_{in}(E' \rightarrow E)}{\Sigma_s(E') + \Sigma_{in}(E')}. \quad (5)$$

Carrying out the corresponding integration in (4), we obtain the following equation (regarding $\Delta(E)$ as a monotonic function)

$$\left(\Phi[E - \Delta(E)] \{ \Sigma_s^0[E - \Delta(E)] + \Sigma_a[E - \Delta(E)] \} - q[E - \Delta(E)] \right) \left(1 - \frac{d\Delta}{dE} \right) = \Sigma_s^0(E) \Phi(E). \quad (6)$$

The solution to Eq. (6) was obtained by one of the authors in conjunction with G. V. Fedorovich (when studying the thermalization of electrons in a gas) by expanding the functions in the equation in series and taking account of terms containing derivatives no higher than the first order (here essentially we used the inequality $\Delta(E)/E \ll 1$). The solution of Eq. (6) so obtained takes the form

$$\Phi(E) = \frac{1}{\Sigma_s^0 + \Sigma_a} \left\{ q(E) + \frac{1}{\Delta(E)} \int_E^\infty dE' \frac{q(E') \Sigma_s^0(E')}{\Sigma_s^0(E') + \Sigma_a(E')} \exp \left[- \int_E^{E'} \frac{\Sigma_a}{(\Sigma_s^0 + \Sigma_a)} \frac{dE''}{\Delta} \right] \right\}. \quad (7)$$

Neglecting processes of inelastic scattering and using the expression [1]

$$P_s(E' \rightarrow E) = \frac{1}{\alpha E'} \Theta(E' - E) \Theta[E(1 - \alpha)^{-1} - E'] \quad (8)$$

(here $\Theta(z)$ is a unitary function), we find from Eq. (5) that $\Delta(E) = (\alpha/2)E$, as indicated earlier. Substituting the resultant value of $\Delta(E)$ into Eq. (7) we may easily convince ourselves that the latter coincides with the expression for the neutron flux given in [1] in the absence of elastic scattering, with the sole difference that in [1] the quantity ξ occurs in the final result instead of $\alpha/2$, this being the average change in energy for one elastic collision.

For heavy moderators $\alpha/2 = \xi$ to an accuracy governed by terms of order $1/M$ [1].

2. Case of a large energy jump: $\Delta(E')/E' \ll 1$.

Let us introduce the following extra assumptions:

- 1) the inelastic scattering cross section Σ_{in} differs from zero in the range $[E_1; E^+]$, where E^+ is the energy of the source, which we shall regard as monochromatic;
- 2) the function $y(E') = E' - \Delta(E')$ has an upper limit of E_1 for any E' in the range $[E_1; E^+]$. The meaning of the second assumption lies in the fact that a neutron with energy in the range $[E_1; E^+]$ necessarily passes out of this energy range as a result of one inelastic collision. These assumptions enable us to allow for inelastic scattering by adding the inelastic scattering cross section to the capture cross section in the range $[E_1; E^+]$ and introducing additional neutron sources in the range $E < E_1$. A note as to the possibility of allowing for inelastic processes in this way appears in [2], although without the corresponding calculations.

An equation describing the slowing of the neutrons in the case under consideration will take the form

$$(\Sigma_s + \Sigma_a + \Sigma_{in}) \Phi = \frac{1}{\alpha} \int_E^{E/1-\alpha} \Phi(E') \Sigma_s(E') \frac{dE'}{E'} + \int_{E_1}^{E^+} \Phi(E') \Sigma_{in}(E') \delta[E + \Delta(E') - E'] dE' + S \delta(E - E^+), \quad (9)$$

where $\Delta(E')$ is determined by Eq. (5) with $\Sigma_g = 0$.

In view of the foregoing discussion, it is clear that the solution of Eq. (9) should be sought in the form of the sum of two terms

$$\Phi = \Phi_1 + \Phi_2, \quad (10)$$

one of which Φ_1 satisfies the equation

$$(\Sigma_a + \Sigma_{in} + \Sigma_s) \Phi_1 = \frac{1}{\alpha} \int_E^{E/1-\alpha} \Phi_1(E') \Sigma_s(E') \frac{dE'}{E'} + S \delta(E - E^+). \quad (11)$$

The solution of Eq. (1) is well known [1]:

$$\Phi_1 = \frac{S}{\xi E (\Sigma_s + \Sigma_{in} + \Sigma_a)} \frac{\Sigma_s(E^+)}{\Sigma_{in}(E^+) + \Sigma_s(E^+) + \Sigma_a(E^+)} \exp \left(-\frac{1}{\xi} \int_E^{E^+} \frac{\Sigma_a + \Sigma_{in}}{\Sigma_a + \Sigma_{in} + \Sigma_s} \frac{dE'}{E'} \right) + \frac{S \delta(E - E^+)}{\Sigma_s + \Sigma_a + \Sigma_{in}}. \quad (12)$$

Allowing for (9)-(11), we find that the function Φ_2 satisfies the equation

$$(\Sigma_s + \Sigma_a) \Phi_2 = \frac{1}{\alpha} \int_E^{E/1-\alpha} \Phi_2(E') \Sigma_s(E') \frac{dE'}{E'} + q(E), \quad (13)$$

where $q(E)$ is the source function having the form

$$q(E) = \int_{E_1}^{E^+} \Phi_1 \Sigma_{in}(E') \delta(E + \Delta(E') - E') dE'. \quad (14)$$

In passing from (9) to (13), we have allowed for the following facts. In accordance with the original assumption, the function $y(E') = E' - \Delta(E')$ has an upper limit of E_1 and hence for, $E > E_1$

$$\int_{E_1}^{E^+} \Sigma_{in}(E') \Phi_{1,2}(E') \delta[E + \Delta(E') - E'] dE' = 0.$$

Hence for $E > E_1$ the function Φ_2 satisfies a linear homogeneous equation with a zero initial condition, and hence in this region $\Phi_2 = 0$. If we also allow for the fact that for $E < E_1$ the value of $\Sigma_{in} = 0$ (by hypothesis) we obtain Eq. (13), the solution of which appears thus [1]:

$$\Phi_2 = \frac{q(E)}{\Sigma_s + \Sigma_a} + \int_E^{E_1} G_0(E; E') q(E') dE', \quad (15)$$

where $G_0(E; E')$ is the Green's function of Eq. (13) not including the unscattered neutrons:

$$G_0(E; E') = \frac{1}{\xi E (\Sigma_a + \Sigma_s)} \frac{\Sigma_s(E')}{\Sigma_a(E') + \Sigma_s(E')} \exp \left(-\frac{1}{\xi} \int_E^{E'} \frac{\Sigma_a}{\Sigma_a + \Sigma_s} \frac{dE''}{E''} \right). \quad (16)$$

Allowing for (14), Eq. (15) may be written in the form

$$\Phi_2 = \frac{q(E)}{\Sigma_s(E) + \Sigma_a(E)} + \int_{E_1}^{E^+} dE' \Phi_1(E') \Sigma_{in}(E') G_0[E; E' - \Delta(E')] \Theta[E' - \Delta(E') - E], \quad (17)$$

where Φ_1 and $G_0(E; E')$ are given by (12) and (16). The final result for Φ_2 may be obtained in a simple and obvious form for a number of particular cases.

Let us discuss the behavior of the function $y(E) = E - \Delta(E)$. We assumed earlier that this function had an upper limit of E_1 (for E from $[E_1; E^+]$). Let us assume that it has a lower limit of E_2 . This assumption, essential for subsequent discussions, reflects the fact that the neutrons emerging as a result of inelastic collisions from the energy range $[E_1, E^+]$ cannot acquire an energy less than E_2 . We assume the function $y(E)$ is monotonic. The generalization to the case of the nonmonotonic behavior of the function may be effected in a straightforward manner, and is indicated in the Appendix.

Let us give the final result for the neutron flux in certain particular cases.

1. Absorption is absent, i.e., $\Sigma_a = 0$. Here for $E < E_1$

$$\begin{aligned} \Phi = & \frac{Sh(E^+)}{\xi E \Sigma_s(E)} \exp \left(-\int_E^{E^+} g \frac{dE'}{\xi E'} \right) + \frac{Sg(E^+)}{\xi E \Sigma_s(E)} + \frac{Sh(E^+)}{\xi E \Sigma_s(E)} \left[1 - \exp \left(-\int_{\varepsilon(E)}^{E^+} g \frac{dE'}{\xi E'} \right) \right] \\ & + \frac{Sh(E^+)}{\xi \Sigma_s \varepsilon(E)} \frac{g(\varepsilon)}{\left| 1 - \frac{d\Delta}{dE} \right|_{E=\varepsilon}} \exp \left(-\int_{\varepsilon(E)}^{E^+} g \frac{dE'}{\xi E'} \right), \end{aligned} \quad (18)$$

where $h = \Sigma_s / \Sigma_s + \Sigma_{in}$; $g = \Sigma_{in} / \Sigma_s + \Sigma_{in}$; $\varepsilon(E)$ is a root of the equation

$$E + \Delta(E') - E' = 0. \quad (19)$$

Each term in (18) has a specific physical meaning. The first corresponds to neutrons which have not experienced any inelastic collisions (function Φ_1), the second describes neutrons which, as a result of the first (inelastic) collision, have been driven out of the range $[E_1; E^+]$. The third corresponds to neutrons which have passed out of the range $[E_1; E^+]$ as a result of subsequent inelastic collisions and have thereafter been slowed to an energy E . The last term corresponds to neutrons which by virtue of inelastic collisions in the energy range $[E_1; E^+]$ have immediately acquired an energy E (first term in (17)). This term is determined by the behavior of the function Φ_1 in the range $[E_1; E^+]$ with an additional factor $(\Sigma_{in}(\epsilon)/\Sigma_s(E)) (1/1 - d\Delta/dE)|_{E=\epsilon}$. Clearly for $E < E_2$ Eq. (19) does not have any roots, where $E < E' - \Delta(E')$ and $E' \in [E_1; E^+]$. Hence the expression for the neutron flux with $E < E_2$ takes the form

$$\Phi = \frac{S}{\xi \Sigma_s(E) E}. \quad (20)$$

This is obtained from (18) on replacing $\epsilon(E)$ by E_1 and rejecting the last term. Thus inelastic scattering has no effect on the behavior of the flux in the range $E < E_2$. This conclusion is a consequence of the well-known fact that, in the absence of absorption the character of the neutron spectrum a long way from the lower energy limit of the source spectrum, is independent of the source spectrum.

2. $\Sigma_s = \text{const}$; $\Sigma_{in} = \text{const}$; $\Sigma_a = \text{const}$ for $E > E_1$, $\Sigma_a = 0$ for $E < E_1$.

This case corresponds to the existence of constant absorption in a region characterized by inelastic scattering. The expression for the neutron flux (17) accordingly takes the following form ($E < E_1$):

$$\begin{aligned} \Phi = \Phi_1 + \Phi_2 = & \frac{S \Sigma_{in}}{\xi E \Sigma_s (\Sigma_a + \Sigma_{in})} + \frac{S}{\xi E \Sigma_{tot}} \left[\exp \left(- \int_{E_1}^{E^+} \frac{\Sigma_a + \Sigma_{in}}{\Sigma_{tot}} \frac{dE'}{\xi E'} \right) - \frac{\Sigma_{in}}{\Sigma_a + \Sigma_{in}} \right. \\ & \times \exp \left(- \int_E^{E^+} \frac{\Sigma_a + \Sigma_{in}}{\Sigma_{tot}} \frac{dE'}{\xi E'} \right) \left. \right] + \frac{S \Sigma_s \Sigma_{in}}{\xi E \Sigma_{tot}^2} \exp \left(- \int_E^{E^+} \frac{\Sigma_a + \Sigma_{in}}{\Sigma_{tot}} \frac{dE'}{\xi E'} \right). \end{aligned} \quad (21)$$

For $E < E_2$ Eq. (21) takes the form

$$\Phi = \frac{S}{\xi E \Sigma_s} \left[\frac{\Sigma_{in}}{\Sigma_a + \Sigma_{in}} + \frac{\Sigma_s \Sigma_a}{\Sigma_{tot} (\Sigma_a + \Sigma_{in})} \exp \left(- \int_{E_1}^{E^+} \frac{\Sigma_a + \Sigma_{in}}{\Sigma_{tot}} \frac{dE'}{\xi E'} \right) \right], \quad (22)$$

where $\Sigma_{tot} = \Sigma_s + \Sigma_a + \Sigma_{in}$. For $\Sigma_a = 0$ the results (21) and (22) transform into the corresponding results (18) and (20).

In the present case, in contrast to the previous, owing to the existence of absorption in the range $(E_1; E^+)$ the neutron flux for $E < E_2$ (and hence in the thermal region) depends considerably on the inelastic scattering cross section. For $\Sigma_{in} = 0$ Eq. (22) coincides with the analogous result of [1], while for $\Sigma_a/\Sigma_{in} \rightarrow 0$ - c it coincides with (20). This indicates that for large inelastic scattering cross sections the absorption in the range $[E_1; E^+]$ has only a slight effect on the neutron spectrum for $E < E_2$.

In conclusion, it should be noted that the results obtained in the present investigation enable us to describe the slowing-down of neutrons with due allowance for inelastic scattering in the majority of materials employed in reactor building. Actually for a large energy jump in inelastic scattering processes the neutrons will leave the energy range in which the inelastic cross section differs from zero by virtue of a single inelastic collision. In this case the slowing-down of the neutrons is described by Eqs. (17), (18), and (22). For a small energy jump, the slowing-down process will be described by Eq. (7), which was obtained under reasonably general assumptions.

APPENDIX

Let us consider the case in which the function $y(E') = E' - \Delta(E')$ is not monotonic but as before is characterized by upper and lower limits of E_1 and E_2 . This physically corresponds to the fact that the neutrons acquire the specified energy E ($E_2 \leq E \leq E_1$) by virtue of inelastic scattering at various energies constituting the roots of Eq. (19). It is clear that the value of the function Φ_1 will in this case remain as before, while Eq. (17) for the function Φ_2 will take the form

$$\Phi_2 = \frac{q(E)}{\Sigma_s + \Sigma_a} + \sum_{i=1}^n \int_{e_1^{(i)}}^{e_2^{(i)}} dE' \Phi_1(E') \Sigma_{in}(E') G[E; E' - \Delta(E')], \quad (23)$$

where $[\varepsilon_1^{(i)}; \varepsilon_2^{(i)}]$ are the energy ranges in which the condition $y(E') \geq E$ is satisfied for a fixed E ($E_2 \leq E \leq E_1$) and E' from $[E_1; E^+]$.

The expressions for Φ_2 in the two particular cases considered take the form

$$\Phi_2 = \frac{S_g(E^+)}{\xi E \Sigma_s} \Theta(\varepsilon_0 - E) + \frac{Sh(E^+)}{\xi \Sigma_s} \sum_{i=0}^n \sum_{j=1}^2 \frac{g(\varepsilon_j^{(i)})}{\varepsilon_j^{(i)}} \frac{\exp\left(-\int_{\varepsilon_j^{(i)}}^{E^+} g \frac{dE'}{\xi E'}\right)}{\left|1 - \frac{d\Delta}{dE}\right|_{E=\varepsilon_j^{(i)}}} + \frac{Sh(E^+)}{\xi E \Sigma_s} \sum_{i=0}^n \left[\exp\left(-\int_{\varepsilon_2^{(i)}}^{E^+} g \frac{dE'}{\xi E'}\right) - \exp\left(-\int_{\varepsilon_1^{(i)}}^{E^+} g \frac{dE'}{\xi E'}\right) \right]; \quad (24)$$

$$\Phi_2 = \frac{S \Sigma_{in}}{\xi E \Sigma_s \Sigma_{tot}} \Theta(\varepsilon_0 - E) + \frac{S \Sigma_s \Sigma_{in}}{\xi [\Sigma_{tot}]^2} \sum_{i=0}^n \sum_{j=1}^2 \frac{1}{\varepsilon_j^{(i)}} \exp\left(-\int_{\varepsilon_j^{(i)}}^{E^+} \frac{\Sigma_a + \Sigma_{in}}{\Sigma_{tot}} \frac{dE'}{\xi E'}\right) + \frac{S \Sigma_{in}}{\xi E \Sigma_{tot} (\Sigma_a + \Sigma_{in})} \sum_{i=0}^n \left[\exp\left(-\int_{\varepsilon_2^{(i)}}^{E^+} \frac{\Sigma_a + \Sigma_{in}}{\Sigma_{tot}} \frac{dE'}{\xi E'}\right) - \exp\left(-\int_{\varepsilon_1^{(i)}}^{E^+} \frac{\Sigma_a + \Sigma_{in}}{\Sigma_{tot}} \frac{dE'}{\xi E'}\right) \right], \quad (25)$$

where $\varepsilon_0 = E^+ - \Delta(E^+)$.

The expression for the neutron flux with $E < E_2$ will clearly have exactly the same form as in the case of a monotonic function $y(E')$.

LITERATURE CITED

1. A. Weinberg and E. Wigner, Physical Theory of Nuclear Reactors [Russian translation], IL, Moscow (1961).
2. B. Davison, Theory of Neutron Transfer [Russian translation], Atomizdat, Moscow (1960).

BOOK REVIEWS

T. A. Germogenova, V. P. Mashkovich,
V. G. Zolotukhin, and A. P. Suvorov

THE ALBEDO OF NEUTRONS

Reviewed by B. R. Bergel'son

The monograph is devoted to the problem of the reflection of neutrons from the reactor spectrum or from isotope sources by matter. The authors are famous specialists in the field of computational and experimental research on the transfer of reactor radiation in various media. In particular, the authors have written several papers in which the various techniques of solving albedo problems were considered for neutrons and in which the results of the corresponding calculations were listed. The information compiled in the book is therefore on an advanced level and of immediate interest.

The principal concepts and definitions referring to albedo are introduced in the first chapter. The traditional, but for a book of this kind necessary, description of the interaction of neutrons with the nuclei of a medium is given. A two-group model (in the angular distribution of the reflected radiation) of the albedo problem is formulated in the first chapter. The formulas which were obtained with this model facilitate in a relatively simple manner the calculation of qualitative and, in some cases, even quantitative characteristics of reflected neutrons.

The second chapter is a description of the various methods of solving albedo problems. At the beginning of this chapter, the general boundary-value problem with conditions for the reflection of neutrons at the boundaries of a region under consideration is formulated. It is shown that an "albedo approach" to the solution of the transfer problem in heterogeneous media is possible. Actual calculation methods are then described: the Monte Carlo method, the method of discrete coordinates, the method of the age-diffusion approximation, and the method of the n -th collision. In conclusion of this chapter, the determination of the group constants is considered with proper regard for the specific details of albedo problems. The experimental methods used to investigate fields of reflected radiation are briefly described.

The basic information on the quantitative characteristics of various albedos, i.e., the information which is of greatest interest in practical applications, is presented in the third and fourth chapter of the book. These chapters describe the results (some of which were obtained by the authors of the book) of computational and experimental studies of the reflection of thermal, intermediate, and fast neutrons emitted from various sources by media of different compositions and geometries. Publications which deal with the backscattering of fast neutrons are reviewed and the results are compared.

The section on the yield of capture-type γ radiation is of particular interest and usefulness. However, this problem can be considered only an approximation to albedo problems, and the entire section of the book therefore is beyond the general scope of the book.

The final chapter is an analysis of the development of the reflected neutron field and makes use of the data on the differential albedo considered in the preceding chapters. The dependence upon parameters such as the angle of incidence, the angle of reflection, the energy of the source, the threshold of detection, and the thickness of the reflector is considered.

The authors have undertaken a great work when they generalized and analyzed the theoretical, computational, and experimental data on neutron albedo. The authors have filled a big gap which existed in Soviet and Western literature on the physics of radiation shielding. No doubt that the book will be often used by scientists and engineers in their work on the development of shielding from sources of neutron radiation.

Translated from *Atomnaya Energiya*, Vol. 36, No. 4, p. 281, April, 1974.

© 1974 Consultants Bureau, a division of Plenum Publishing Corporation, 227 West 17th Street, New York, N. Y. 10011. No part of this publication may be reproduced, stored in a retrieval system, or transmitted, in any form or by any means, electronic, mechanical, photocopying, microfilming, recording or otherwise, without written permission of the publisher. A copy of this article is available from the publisher for \$15.00.

SPECTRA OF THE PROMPT NEUTRONS ARISING FROM THE SPONTANEOUS FISSION OF ^{252}Cf , ^{244}Cm , and ^{240}Pu

Z. A. Aleksandrova, V. I. Bol'shov,
V. F. Kuznetsov, G. N. Smirenkin,
and M. Z. Tarasko

UDC 539.185

Terrell showed earlier [1] that the spectrum of prompt fission neutrons could be described to a fair degree of approximation by a single-parameter distribution of the Maxwell type

$$N(E) = \frac{2\sqrt{E}}{\sqrt{\pi\theta^3}} e^{-\frac{E}{\theta}}, \quad (1)$$

where θ is called the hardness parameter of the spectrum, or the temperature parameter, although it has no relationship to the temperature of the nucleus. In this representation the average energy of the spectrum is related to θ in a simple manner:

$$\theta = \frac{2}{3} \bar{E}. \quad (2)$$

This kind of one-parameter representation is convenient for reactor calculations, and the determination of the parameter for the principal fissile isotopes is an important problem.

TABLE 1. Results of the Determination of θ for ^{252}Cf , ^{244}Cm , and ^{240}Pu

Isotope	Range of neutron energy, MeV	Result of θ , * MeV	Measuring methods	Literature cited
^{252}Cf	> 2	$1,402 \pm 0,009$	Photographic plates	[11]
	0,2-7	(1,57)	Time of flight	[12]
	< 4	$1,367 \pm 0,03$	Bramlett counter	[10]
	0,5-6	(1,56 \pm 0,03)	Time of flight	[13]
	0,7-7,5	$1,39 \pm 0,04$	Time of flight	[14]
	0,5-15	(1,522)	Time of flight	[15]
		1,39	Manganese bath	[16]
	0,4-6	$1,48 \pm 0,03$	Time of flight	[8]
		(1,436 \pm 0,016)	Proportional H counter	[17]
	1,5-7	(1,420 \pm 0,015)	^3He counter	[2]
^{244}Cm	0,3-7	$1,37 \pm 0,04$	Time of flight	[9]
	0,5-6	(1,455 \pm 0,062)	^3He spectrometer	[17]
	0,5-6	$1,38 \pm 0,03$	Time of flight	[8]
^{240}Pu	< 4	$1,158 \pm 0,030$	Bramlett counter	[10]
	3-11	$1,24 \pm 0,03$	Scintillation spectrometer	[18]

* The results in brackets are not given directly in the references but are calculated according to Eq. (2).

Translated from Atomnaya Energiya, Vol. 36, No. 4, pp. 282-285, April, 1974. Original article submitted June 5, 1973.

© 1974 Consultants Bureau, a division of Plenum Publishing Corporation, 227 West 17th Street, New York, N. Y. 10011. No part of this publication may be reproduced, stored in a retrieval system, or transmitted, in any form or by any means, electronic, mechanical, photocopying, microfilming, recording or otherwise, without written permission of the publisher. A copy of this article is available from the publisher for \$15.00.

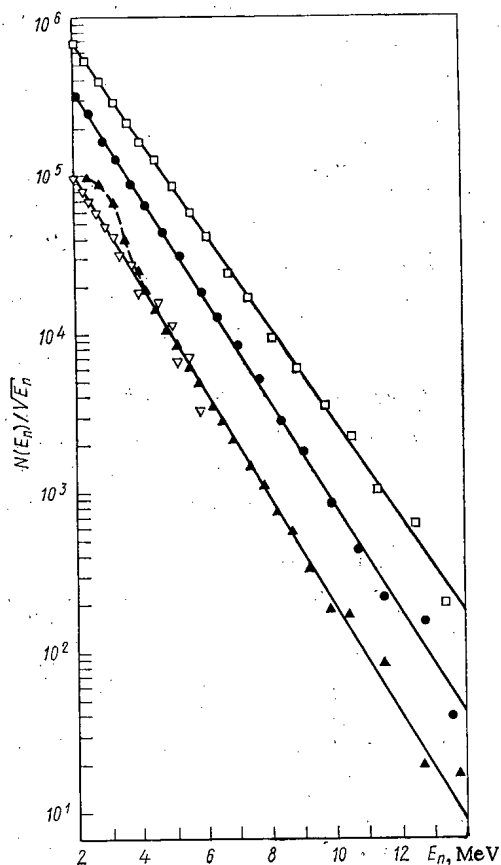


Fig. 1. Energy spectra of fission neutrons: \square ^{252}Cf ; \bullet ^{244}Cm ; \blacktriangle ^{240}Pu (oxide; ∇) ^{240}Pu (bromide).

The discrimination of the γ -quanta was based on the difference in the effective time of deexcitation (scintillation) of stilbene on irradiating the latter with neutrons and γ -quanta. The circuit for discriminating the pulse by reference to their shape was taken from [3].

The degree of "suppression" of the γ -quanta with the discrimination circuit employed reached $\sim 10^4$. Here only recoil protons with energies of over 1 MeV were recorded. The necessity of a high degree of suppression of the γ background arose from the high γ activity of the samples studied and was achieved at the expense of raising the lower threshold of neutron recording. The stilbene crystal had the form of a cylinder 3 cm in diameter and 3 cm high. We used an FEU-13 photomultiplier. The samples of the isotopes studied were placed at a distance of 5 cm along the axis of the crystal. In order to reduce the number of γ -quanta falling into the crystal, a lead plate 1 cm thick was placed between the source and the crystal. The measurements were carried out in a room such that the distance from the source to the walls, floor, and ceiling equaled 5-9 m, thus ensuring that there should only be a small contribution from the scattered neutrons. The stability of the recording apparatus was monitored periodically by reference to the position of the edge of the Compton distribution of a ^{208}Tl reference γ source. Careful selection and conditioning of the photomultiplier and due limitation of temperature fluctuations in the room ($\pm 2-3^\circ\text{C}$) kept the amplification factor of the tract stable to better than 1%.

The processed amplitude distribution was obtained by summing the individual distributions measured over the time intervals (~ 1.5 h) between which the stability was monitored. The neutron spectra of all the isotopes studied were obtained under identical geometrical conditions.

One of the characteristics of stilbene is a nonlinear relationship between the light output and the energy of the recoil protons. Hence very serious attention indeed was paid to the calibration of the energy scale of the spectrometer. The calibration was effected in an electrostatic accelerator using monoenergetic neutrons obtained in p-T, d-d, and d-T reactions. The relationship between the light output and the proton energy is excellently described for the crystal employed by the semiempirical Birks formula [4]

TABLE 2. Characteristics of the Sources Employed

Isotope	Chemical compound	Number of α -particles per fission	Intensity of source with respect to fission neutrons, neutrons/sec
^{240}Pu	PuO_2	$1.9 \cdot 10^7$	$8 \cdot 10^3$
	PuBr_4	$1.9 \cdot 10^7$	$1 \cdot 10^3$
^{244}Cm	Cm_2O_3	$7.7 \cdot 10^5$	$1 \cdot 10^4$
^{252}Cf	$\text{Cf}(\text{NO}_3)_3$	31	$5 \cdot 10^4$

At the present time large amounts of ^{252}Cf have been accumulated; this may constitute a convenient standard neutron source. However, the published data recorded in Table 1 reveal a serious scatter despite the fairly high accuracy of individual results. The majority of these are obtained by the time-of-flight method and a few by means of photographic plates (giving a low statistical accuracy) or by passing through retarding spheres. Two different kinds of detector were used in [2] for recording neutrons: a proportional H counter and a ^3He counter. As regards ^{244}Cm and ^{240}Pu only two or three investigations have been made. It would be desirable to try a method not so far used for these purposes, having a high efficiency, a reliable calibration of the energy scale, and the capacity to work with very strong background fields of γ -quanta. These requirements are satisfied by the one-crystal scintillation spectrometer with discrimination of γ -quanta used in the present investigation.

The prompt neutron spectra associated with the spontaneous fission of ^{252}Cf , ^{244}Cm , and ^{240}Pu were all measured under identical conditions in one experiment. The characteristics of the sources are shown in Table 2.

$$V(E) = \int_0^E \frac{dE'}{1 + kB \frac{dE'}{dx}},$$

where $V(E)$ is the light flash obtained on exciting stilbene with protons having an energy E ; dE'/dx is the slowing-down power of protons with energy E' in stilbene; kB is an empirical parameter (roughly 0.013).

The apparatus spectra were analyzed by the differentiation method [5]:

$$N(E_n) = - \frac{E_n}{1 - \exp[-\Sigma(E_n)d]} \frac{d}{dE} \left[P(E) \frac{dV}{dE} \right]_{E=E_n}.$$

Here $N(E_n)$ is the unknown neutron spectrum; $\Sigma(E_n)$ is the macroscopic cross section for the interaction of neutrons of energy E_n with protons; d is the thickness of the scintillator; $P(E)$ is the apparatus distribution obtained after transforming from the linear light-output scale to the scale of proton energies, in accordance with the calibration of the energy scale; dV/dE is the derivative of the light output with respect to energy.

The foregoing method of analysis is based on representing the apparatus curve for the irradiation of stilbene by monoenergetic neutrons in the form of a "step" dE/E_n , which is permissible if the crystal dimensions are such that only small contributions arise from the multiple scattering of neutrons at hydrogen nuclei in the soft part of the neutron spectra under consideration and from edge effects in the hard part [6]. It is found in practice that a crystal with the dimensions here chosen satisfies the conditions in question for neutron energies of 1-17 MeV. Experimental attention was directed at the following factors, which might cause distortion of the spectrum.

1. Contribution arising from the anisotropy of the light yield of stilbene. In the measurements of the spectra the neutron sources were placed close to the crystal, and the angles of incidence of the neutrons on the crystal during the measurements differed from the angles employed during the calibration of the light yield, when the neutron source was placed a long way from the end of the crystal. The dependence of the light yield on the angle of incidence of the neutrons on the crystal [4] might affect the uniqueness of the calibration curve and the relationship between light yield and energy ruling under specified conditions. This effect was checked in a separate experiment in which the spectra of the fission neutrons of ^{252}Cf were compared for a source close to (~ 2 cm) and a long way from (~ 75 cm) the end of the crystal. The results of the experiments showed that the distance from the source to the crystal actually had little effect on the form of the spectrum.

2. Allowance for superpositions. The integrated loading of the crystal with both neutrons and γ -quanta during the measurements amounted to some $1-1.5 \cdot 10^3$ pulses/sec. It was essential to allow for the contribution of superpositions, since the particles recorded in the crystal, following one another within periods of $\tau \leq 1$ μsec , created superposed $n-n$, $n-\gamma$, or $\gamma-\gamma$ pulses at the output of the photomultiplier, which were passed by the discrimination circuit and coincided in time with the corresponding pulses in the linear channel.

The spectrum of the superpositions was approximately calculated from the formula:

$$\Delta N_k = \sum_{i=1}^p N_i N_j 2\tau; \quad \begin{matrix} i = k - j & \text{for even } k; \\ p = \begin{cases} k/2 \\ \frac{k-1}{2} \end{cases} & \text{for odd } k, \end{matrix}$$

where ΔN_k is the number of superposed pulses in the k -th channel; N_i , N_j is the total load with respect to neutrons and γ -quanta in channels with numbers i and j related by the condition $i + j = k$; τ is the effective resolving time in the discrimination channel.

The spectrum calculated by this formula fell extremely sharply in the large-amplitude direction. Estimates showed that for the loadings chosen the proportion of chance superpositions was no greater than 1% of the number of recorded pulses.

3. Influence of the lead screen (between the source and crystal). This was taken into account by measuring the neutron spectrum of ^{252}Cf with and without the lead. The influence of the screen on the measured spectrum was negligibly small.

4. Contribution of the (α, n) reaction. In the strongly α active oxide sources of spontaneously-fissile isotopes (^{240}Pu), a considerable contribution to the neutron yield came from the (α, n) reaction of the oxygen isotope ^{18}O [7]. For E_n values below 3-4 MeV, in particular, the contribution of the (α, n) reaction was

very considerable for ^{240}Pu . The contribution of the (α, n) neutrons in the soft region was eliminated by making the ^{240}Pu source in the form of plutonium bromide, in which the (α, n) reaction does not take place. The low intensity of this source enabled us to measure the neutron spectrum over a range extending to ~ 6 MeV; however, the range 2-4 MeV did not contain any traces of (α, n) neutrons.

Figure 1 gives a semilogarithmic representation of the spectra so measured for the isotopes in question. The hardness parameters θ for ^{252}Cf , ^{244}Cm , ^{240}Pu are 1.42 ± 0.03 ; 1.33 ± 0.03 and 1.27 ± 0.03 MeV respectively. The straight lines in the figure were drawn through experimental points corresponding to the values of $N(E_n)/\sqrt{E_n}$ by the method of least squares, although the error for θ appeared unjustifiably small. The errors actually indicated here reflect possible inaccuracy in measuring the light-yield curve and correspond to the scatter in θ values obtained on analyzing apparatus distributions with $k_B = 0.012$ and 0.014 .

We see from Table 1 that the results obtained for ^{252}Cf lay close to the latest results, published in 1969-1971. The result obtained for ^{244}Cm agrees excellently with the results of [8, 9], but the only previous data for ^{240}Pu (Bonner [10]) differ substantially from those obtained in the present investigation.

Calculation based on a semiempirical version of Eq. (1)

$$\bar{E} = 0.78 + 0.621 \sqrt{v+1} \quad (3)$$

gives values of the parameter θ for ^{252}Cf , ^{244}Cm , and ^{240}Pu equal to 1.42, 1.33, and 1.26 MeV respectively. Perhaps no particular significance should be ascribed to this good agreement, since the Terrell relationship is too rough, and was obtained on the assumption that the level density parameter a (MeV^{-1}) was independent of the nucleon composition of the nucleus, whereas in fact the mass curve varies considerably from isotope to isotope, and the parameter a varies accordingly.

The authors wish to thank V. G. Zolotukhin for interest in this work, B. A. Efimenko for help in analyzing the results of the measurements, and K. E. Volodin for help in the measurements themselves.

LITERATURE CITED

1. J. Terrell, *Phys. Rev.*, **113**, 527 (1959).
2. H. Werle and H. Bluhm, *Prompt Fission Neutron Spectra*, IAEA, Vienna (1972), p. 65.
3. V. G. Brovchenko and G. V. Gorlov, *Pribory i Tekh. Eksperim.*, No. 4, 49 (1971).
4. *Physics of Fast Neutrons* [in Russian], Vol. 1, Gosatomizdat, Moscow (1963), p. 241.
5. V. A. Dulin et al., *Pribory i Tekh. Eksperim.*, No. 2, 35 (1961).
6. V. G. Zolotukhin, B. A. Efimenko, and G. G. Doroshenko, *Monte Carlo Method in the Radiation Transfer Problem* [in Russian], Atomizdat, Moscow (1967), p. 199.
7. A. G. Khabakhpashev, *Atomnaya Energiya*, **7**, No. 1, 71 (1959).
8. Ju. Samjatnin et al., *Nuclear Data for Reactors*, Vol. 2, IAEA, Helsinki (1970), p. 183.
9. P. M. Belov et al., *Yadernaya Fiz.*, **9**, No. 4, 727 (1969).
10. J. Bonner, *Nucl. Phys.*, **23**, 116 (1961).
11. E. Hjalmar et al., *Arkiv. Fys.*, **10**, 357 (1956).
12. A. Smith and P. Fields, *Phys. Rev.*, **108**, 411 (1957).
13. H. Bowman et al., *Phys. Rev.*, **126**, 2120 (1962).
14. H. Conde and G. Doring, *Phys. and Chem. of Fission*, Vol. 2, IAEA, Vienna (1965), p. 93.
15. J. Meadows, *Phys. Rev.*, **157**, 1076 (1967).
16. L. Green, *Nucl. Sci. and Engng.*, **37**, 232 (1969).
17. F. Herold, *Savannah River Laboratory Report*, DR-949 (1969) (Proc. of a Consultants Meeting, Vienna (1972), p. 18).
18. V. I. Bol'shov et al., in: *Physics of Nuclear Fission* [in Russian], Gosatomizdat, Moscow (1962), p. 127.

ARTICLES

EFFECTIVE NEUTRON ABSORPTION CROSS SECTIONS FOR CALIFORNIUM, EINSTEINIUM, AND FERMIUM IN THE CENTRAL CHANNEL OF THE SM-2 REACTOR

V. A. Anufriev, V. D. Gavrilov,
Yu. S. Zamyatnin, and V. V. Ivanenko

UDC 539.125.5.173

The use of high-flux reactors for the production of transuranic elements has placed the buildup of significant amounts of heavy isotopes of actinide elements on a realistic basis. The possibilities for optimization of buildup are mainly determined by accuracy in the knowledge of the effective cross sections for interaction of neutrons with the nuclei of these elements. At the present time, data on the effective capture and fission cross sections for the isotopes of californium, einsteinium, and fermium are crude estimates and differ considerably [1-3].

To obtain new information, 5 capsules containing 50 targets with trace amounts of ^{252}Cf were irradiated in the central channel of the SM-2 reactor. A diagram of the main nuclear transformations during the irradiation of californium isotopes is shown in Fig. 1.

The initial isotopic composition of the californium was determined by mass spectroscopy, and the irradiated targets were analyzed on an α spectrometer and a 2π flow counter.

Burnup of ^{252}Cf was determined from the change in α activity and in the composition of the α -radiation before and after irradiation. Consideration was given to the additional corrections resulting from the presence in the target of light californium isotopes and from the effect of chains leading to the formation of ^{252}Cf : a) $^{252}\text{Cf} \xrightarrow{n\gamma} \dots \rightarrow ^{253}\text{Es} \xrightarrow{\alpha} ^{249}\text{Bk} \xrightarrow{n\gamma} \dots \rightarrow ^{252}\text{Cf} \rightarrow$; b) $^{252}\text{Cf} \xrightarrow{n\gamma} \dots \rightarrow ^{254}\text{Fm} \xrightarrow{\alpha} ^{250}\text{Cf} \xrightarrow{n\gamma} \dots \rightarrow ^{252}\text{Cf} \rightarrow$; c) $^{252}\text{Cf} \xrightarrow{\alpha} \dots \rightarrow ^{248}\text{Cm} \xrightarrow{n\gamma} \dots \rightarrow ^{252}\text{Cf} \rightarrow$, and also from the contribution of the low-energy fission fragment distribution to the α spectra.

In the first two capsules, californium containing 21% of light isotopes was used. During irradiation of the targets by a flux of $\sim 10^{21}$ neutrons/cm², 6% ^{252}Cf is formed from these impurities which compensates

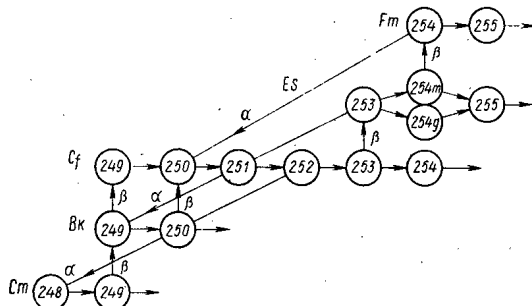


Fig. 1

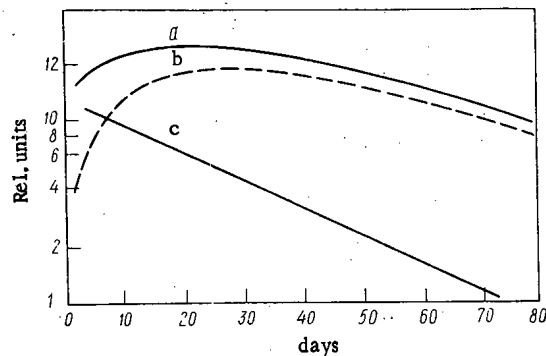


Fig. 2

Fig. 1. Main nuclear transformations in the irradiation of californium isotopes.

Fig. 2. Relation of ^{253}Es and ^{252}Cf activities: a) total (experimental) curve; b) buildup of ^{253}Es from ^{252}Cf ; c) decay of ^{253}Es .

Translated from *Atomnaya Energiya*, Vol. 36, No. 4, pp. 286-289, April, 1974. Original article submitted July 30, 1973.

© 1974 Consultants Bureau, a division of Plenum Publishing Corporation, 227 West 17th Street, New York, N. Y. 10011. No part of this publication may be reproduced, stored in a retrieval system, or transmitted, in any form or by any means, electronic, mechanical, photocopying, microfilming, recording or otherwise, without written permission of the publisher. A copy of this article is available from the publisher for \$15.00.

TABLE 1. Effective Neutron Absorption Cross Sections

Isotope	this work			other authors		
	$\sigma_{n\gamma}$	σ_{nf}	$\sigma_{n\gamma+nf}$	$\sigma_{n\gamma}$	σ_{nf}	$\sigma_{n\gamma+nf}$
^{252}Cf	63 ± 9	$0^* [6]$	63 ± 9	25 [1] 30 [2] 20 [3]	0 [7] 0 [8]	40-50 [4]
^{253}Cf	26	5300 ± 950	5300 ± 950	17,6 [9]		2550 [9]
^{254}Cf	—	—	1400			
^{253}Es	$940 \rightarrow m$ $40 \rightarrow g$	$0^* [6]$	980 ± 90	$338 \rightarrow m$ [5] $13 \rightarrow g$ [5]		
^{254g}Es	—	—	9 000	15 [2] 40 [7]	3060 [10] 2000 [11]	
^{254m}Es	—	—	14 300	40 [7]		
^{254}Fm	—	—	1 400	—		

*Calculated.

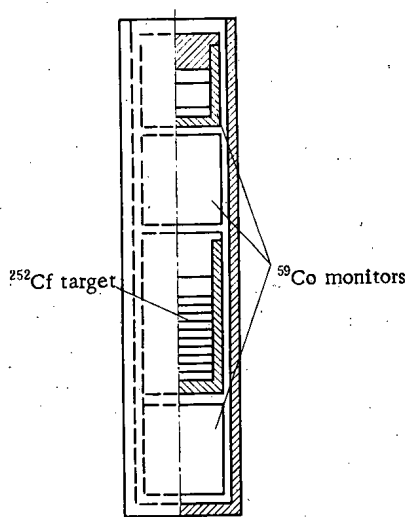


Fig. 3. Ampule.

to a considerable extent for the loss of ^{252}Cf nuclei because of burnup and introduces an error in the determination of cross section values. Subsequently, in order to obtain ^{252}Cf practically free of light isotopes, we used a preliminary irradiation of the californium in a flux $\geq 10^{21}$ neutrons/cm² which ensured burnup of ^{249}Cf , ^{250}Cf , and ^{251}Cf by more than an order of magnitude followed by storage of the targets for a year.

Changes in the amount of ^{252}Cf because of chains *a* and *b* are respectively 0.2 and 0.02% for integral fluxes of $\sim 1.5 \cdot 10^{21}$ neutrons/cm². The effect of chain *c* depends both on the integral flux and on the amount of ^{248}Cm which is built up in the californium before the start of an experiment. For a ^{248}Cm content $\approx 30\%$ relative to ^{252}Cf , calculation of chain *c* yields an additional formation of $^{252}\text{Cf} \approx 0.3\%$. It should be noted that for integral fluxes of $\sim 10^{22}$ - 10^{23} neutrons/cm², the contributions of chains *a* and *c* may reach ~ 10 - 15% of the ^{252}Cf content.

The content of ^{253}Cf , which is a β emitter, was determined from the buildup of its daughter ^{253}Es . Measurements of the α activity of ^{253}Es were carried out on an α spectrometer for a period of 40 days, which made it possible to obtain the variation in ^{253}Es content relative to ^{252}Cf (Fig. 2). The curve shows these changes as a function of time and determines the amount of ^{253}Cf and ^{253}Es in the target at the end of irradiation. Analytic decomposition of this curve into two components made it possible to determine the ^{253}Cf and ^{253}Es contents in targets with trace amounts of emitters to an accuracy of 5-7%. Additional analysis of the californium and einsteinium fractions obtained in a test radiochemical separation confirmed the results of the analytic decomposition with 1%.

The content of the isotopes ^{254m}Es and ^{254}Fm was also determined by decomposition into two components of the curve for the time variation of the amount of ^{254}Fm .

Since the content of ^{254g}Es in the targets was very small, it was determined from the intensity of the α lines in the einsteinium fraction. Radiochemical separation of the californium fraction made it possible to eliminate the effect of the low-energy portion of the ^{252}Cf fission fragment spectrum on the α spectrum of the einsteinium isotopes. Subsequent storage of the Es fraction for a period of four months reduced the ^{253}Es content to such a level that α analysis of the softer α -radiation from ^{254g}Es ($E_\alpha = 6430$ keV) became possible.

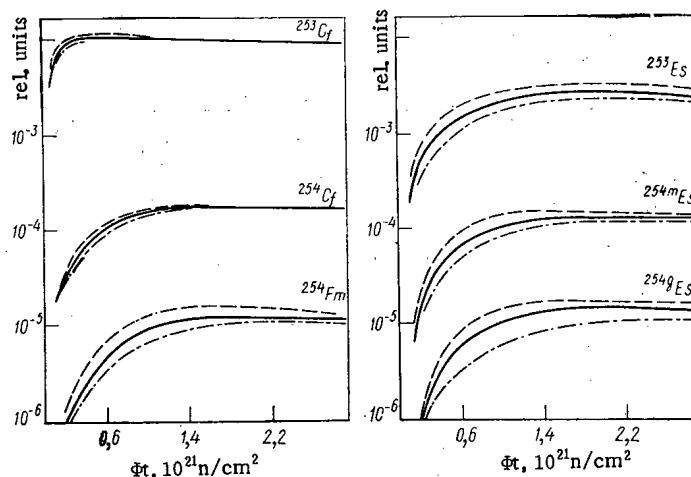


Fig. 4. Isotopic buildup during irradiation of ^{252}Cf ; $\Phi = 1 \cdot 10^{15}$ (—); $0.65 \cdot 10^{15}$ (---), and $1.5 \cdot 10^{15}$ (- · - · -) neutrons/cm² · sec.

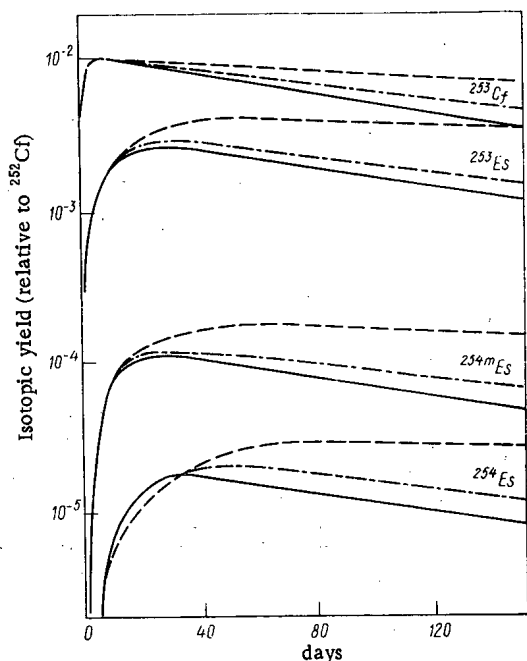


Fig. 5. Isotope buildup during irradiation of ^{252}Cf by a flux of $1.1 \cdot 10^{15}$ neutrons/cm² · sec in various modes; ---) 5 days irradiation and 15 days holding; - · - · -) actual mode; —) continuous irradiation.

The ^{254}Cf content relative to ^{252}Cf was calculated from the ratio of α -decay and spontaneous fission rates before and after irradiation; in this case, a correction was introduced for the presence of other spontaneously fissioning isotopes in the targets.

The cobalt monitors shown in Fig. 3 were used for the measurement of integral fluxes. The amount of ^{59}Co in the monitors was determined by weighing and the induced activity was measured with a Ge(Li) spectrometer. Fluxes were calculated on the basis of an effective cross section $\sigma_{n\gamma}^{59\text{Co}} = 35$ b.

Knowledge of the isotopic compositions of the targets irradiated by various integral neutron fluxes made it possible to calculate $\sigma_{n\gamma}$ and σ_{nf} for these isotopes. However, the determination of the cross sections by solution of a system of two equations hardly makes sense in our case because the capsules were irradiated under somewhat different conditions which could affect the hardness of the neutron fluxes. In calculating the radiative capture cross sections for ^{252}Cf and ^{253}Es , it was assumed the fission cross sections for these isotopes were small in comparison with the radiative capture cross sections [4].

Calculations of the cross sections for all nuclei investigated were performed on the BESM-3M computer by successive approximation and the results are given in Table 1.

Knowledge of the ratio of ^{254m}Es and ^{254g}Es activities and of the total capture cross section for ^{253}Es made it possible to determine the branching ratio for the $(n\gamma)$ reaction in ^{253}Es leading to the isomeric and ground states of ^{254}Es . The branching ratio for the $(n\gamma)$ reaction is approximately 22. This value agrees with the data in [5] in which a value of approximately 26 is given for the branching ratio.

Cross section values for the nuclei ^{254}Cf , ^{254m}Es , ^{254g}Es , and ^{254}Fm should be considered estimates because of the complexity of the analysis (small amounts of material, short half-lives, etc.).

The effective capture and fission cross sections (see Table 1) are considerably larger than indicated by data from other reactors. Obviously, one of the reasons is the hardness of the neutron spectrum from the SM-2 reactor.

Experimental data and calculated curves for the buildup of californium, einsteinium, and fermium isotopes from ^{252}Cf are shown in Fig. 4.

The values of the fission and capture cross sections were used in seeking an optimal irradiation mode for the production of einsteinium isotopes. The curves in Fig. 5 show the buildup of einsteinium isotopes for a continuous irradiation mode and for alternating cycles of irradiation and storage. The yield of einsteinium isotopes can be increased by nearly a factor of two by alternating irradiation and storage cycles.

The use of effective neutron interaction cross sections considerably simplifies all calculations for the buildup of transuranic elements and for the choice of optimal irradiation conditions, and offers an opportunity to estimate the yields of californium, einsteinium, and fermium isotopes for the actual operating mode of the SM-2 reactor where cycles of irradiation and maintenance shutdown of the reactor are alternated. However, the dependence of radiative capture cross sections on the hardness of the neutron spectrum can significantly change the buildup of heavy transuranic elements in reactors with other ratios of thermal and resonance neutrons. Therefore data from measurements of thermal cross sections σ_0 and resonance integrals I_{res} will be less ambiguous.

LITERATURE CITED

1. L. Magnusson, Phys. Rev., 96, 1576 (1970).
2. B. Harvey, Phys. Rev., 95, 581 (1954).
3. J. Halperin, Nucl. Sci. and Engng., 37, 228 (1969).
4. W. Burch, J. Bigelow, and L. King, ORNL-4376 (1969).
5. P. Fields, Nucl. Phys., A96, 440 (1967).
6. A. Prince, Proc. Symp. Sponsored by the New York Metropolitan Section of ANS (October 22, 1968).
7. D. Hughes, BNL-325 (1958).
8. S. Vandenbosch, ANL 6252 (1961).
9. C. Bemis, Nucl. Sci. and Engng., 41, 146 (1970).
10. H. Diamond, J. Inorg. and Nucl. Chem., 30, 2553 (1968).

BOOK REVIEWS

L. A. Il'in, G. V. Arkhangel'skaya,
Yu. O. Konstantinov, and I. A. Likhtarev

RADIOACTIVE IODINE IN THE PROBLEM OF RADIATION SAFETY

Reviewed by Yu. V. Sivintsev

Since the first years of the actual use of nuclear reactors, the problem of radioactive iodine has received the attention of specialists in the field of radiation safety. The volatility at temperatures which are characteristic of reactor operation, high yield in the fission of uranium, a complicated chemistry, and difficulties in the retention of some compounds, high selectivity in the accumulation in a critical organ of low mass are details which characterize the radioactive iodine isotopes among the uranium fission fragments which pose a radiation risk. The need for obtaining low internal irradiation doses of the personnel operating nuclear reactors and of the population living near reactor sites has resulted in a very large number of investigations in the field of radiation sanitation and protective radiation shielding. In view of the continued increase in the number of these publications, it became necessary to have a comprehensive publication. The authors of the monograph had the goal to provide this publication and have successfully dealt with their task. The reader has been provided with an outstanding book in which the results of almost 700 publications and a large number of original investigations of the authors of the monograph were generalized and analyzed.

The first chapter presents a list of data on the main sources from which radioactive iodine isotopes are emitted into an external medium (nuclear reactors, radiochemical plants, and nuclear explosions). The problem of iodine migration in the biosphere is considered in the first chapter.

A critical analysis of the extensive data material has permitted the authors to draw an important conclusion. Inhalation-induced incorporation of radioactive iodine in the human organism rather than contamination of locally produced milk is under certain conditions the main radioactive risk of iodine emission into the biosphere. It was convincingly shown that a situation of this type can arise particularly when methyl iodide is the predominating chemical compound in emissions. Inhalation is also the basic risk in the irradiation of professional personnel.

The third chapter of the monograph is related to this section in a natural way. Dosimetric estimates of the inhalation risk of mixtures of radioactive iodine isotopes are given in the third chapter.

The third chapter includes a qualitative evaluation of the contribution of short-lived iodine isotopes to the total radiation dose and describes in detail the conditions under which the dose of the short-lived isotopes can exceed the dose produced by I^{131} . The reader finds in the same chapter a correct description of both the concept and calculations of the admissible I^{131} emission limit in the controlled release of this isotope into the atmosphere. The chapter includes estimates of the radiation risk of iodine in emissions resulting from emergency situations in nuclear reactors or in local fallout of nuclear explosion products. Particular attention deserves the section on the medical and biological risk of incorporation radioactive iodine. An analysis of the published data is used in this section to evaluate the frequency of cancer development in the thyroid gland. It was shown that the frequency amounts to 10-35 cases per 1 million man-rad for irradiation with radioactive iodine in childhood or infancy.

Unfortunately, the authors did not consider it possible to incorporate in these chapters a section on iodine transport in reactor accidents (from the hot medium to the external medium), which considerably reduces the applicability of the monograph. But one must acknowledge that the term "greatest likely accident" has been successfully employed in place of the more adequate term "possible accident limit." As a

Translated from *Atomnaya Energiya*, Vol. 36, No. 4, p. 290, April, 1974.

© 1974 Consultants Bureau, a division of Plenum Publishing Corporation, 227 West 17th Street, New York, N. Y. 10011. No part of this publication may be reproduced, stored in a retrieval system, or transmitted, in any form or by any means, electronic, mechanical, photocopying, microfilming, recording or otherwise, without written permission of the publisher. A copy of this article is available from the publisher for \$15.00.

consequence, the concept of the most severe accident is unintentionally transformed by the authors into the wrong concept of the greatest probability of the most severe accident or its "representation" (see p. 137).

The multiple approximations of iodine transport in the system "man" has received great attention. In the second chapter, the two-, three-, and four-chamber versions of the models are described in detail and compared according to various criteria. The mathematical apparatus is used in the third chapter in the analysis of problems of normalizing radioactive iodine, and in the fourth chapter for a quantitative evaluation of protecting the thyroid gland by introducing stable iodine. The fact that the radiobiological investigations were optimized is the particular merit of these sections.

The first published results of experiments made with three volunteers for the determination of numerical values of communication constants (see pp. 102-110) and the generalized stationary four-chamber model of the iodine metabolism proposed by the authors of the book for the human organism will certainly receive the reader's attention. The four-chamber models were matched with the recommendations of the International Commission on Radiological Protection and the most probable values of the constants for the population of the European part of the USSR (see pp. 162-163).

Particularly noteworthy in the fourth chapter are interesting investigations of a basis for dosing and of the optimum technique for obtaining stable iodine preparations to protect humans from overexposure. These experiments, which involved 78 volunteer males, made it possible to study the dynamics of unblocking the incorporation of iodine in the thyroid gland. A separate section of the fourth chapter outlines the problems encountered in the protection of pregnant females and the fetus from the effect of radioactive iodine.

Unfortunately, the book sections on problems of biochemistry are loose, because a detailed description of numerous hypotheses and unsuitable methods is redundant, and because these sections are overloaded with a very special terminology. It was hardly worth while to cite in these sections a large number of papers of the forties and fifties in view of the review publications of a later date (particularly, recommendations of the International Commission on Radiological Protection). In some passages, particularly in the third chapter, the reading of the text is difficult because the letter symbols of the notation are ambiguous.

The monograph as a whole, which was written by a group of famous Soviet scientists, is a well-ordered, concise, consistent review of an enormous amount of information on the iodine problem.

REVIEW

SOME PROBLEMS OF INTERACTION OF CASING
STEELS WITH SODIUM HEAT TRANSFER AGENT

A. G. Ioltukhovskii

UDC 621.039.548.535

At present the construction of the fuel element with oxide fuel and casing of stainless chrome-nickel steel of austenite class [1, 2, 52] is chosen as the basic variant for fast reactors with sodium cooling (for investigational as well as industrial reactors). In view of this considerable attention is being devoted to the problems of compatibility of possible casing steels with sodium heat-transfer agent and, in particular, to the interaction with sodium in the case of its contamination by impurities (C, N, O, etc.). This fact is especially important for large industrial reactors of type BN-350, "Fenix," BN-600, PFR, in which it is considerably more difficult than in the experimental reactors to maintain the purity of the heat-transfer agent at the required level, while the conditions of operation for the casings of the fuel element are extremely difficult; the operating temperature with the overheating taken into consideration is 700-720°C, the duration of the operation is from a year (active zone) to several years (zone of regeneration).

Below we discuss some regularities of the interaction of casing steels with sodium heat-transfer agent depending on their alloying and the conditions of operation.

A large amount of information is available [3-11, 50, 51, 53-56] on the effect of the composition and conditions of tests on the resistance to sodium for steels of different classes, nickel alloys, and other materials. Thus, in [3] the point of view of soviet scientists is expressed about the approximate optimum (in respect of compatibility with sodium) composition of stainless chrome-nickel steel intended for casings of fuel elements; 1) the nickel content in steel must be minimum but sufficient to ensure the stability of the structure and composition; 2) the steel must be stabilized by strong carbide-forming elements (niobium or titanium) for binding of carbon in thermodynamically stable carbides and for prevention of decarbonization during contact with sodium; 3) manganese and silicon contents in the steel must be minimum and special

alloying of steel with nitrogen is also inadmissible; 4) it is desirable to introduce molybdenum or tungsten in the composition of the steel.

On the basis of a wide range of investigations carried out in the USSR the steel 0Kh16N15M3B [4, 6] was developed as the basic material for casings of fuel elements of the fast reactors BOR-60 and BN-350. In other countries also steels in different structural states are being already used or are being considered as possible materials; 304, 316, 316L, 1.4988, 12R72HV; besides, the possibility of using nicol-800 and RE-16, containing 30-40% Ni by weight, for the same purposes is also being investigated [1, 2, 10-14].

The study of compatibility of these materials with sodium (especially with the use of such delicate methods of investigation as microprobes, electron microscope, etc.) has shown the correctness of the formulated requirements on the composition of steel, which will be illustrated below.

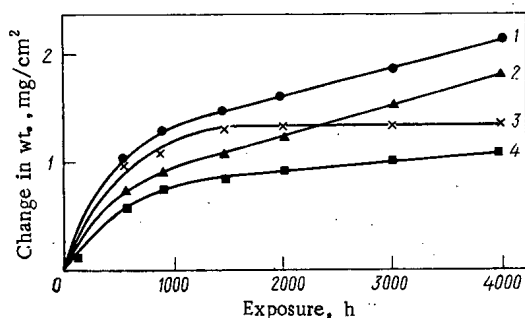


Fig. 1. Change of weight of samples of austenite chrome-nickel steels during exposure in sodium flow ($V = 5$ m/sec): 1) WNR-4981 (0.1 C, 18.6 Cr, 17.6 Ni, 1.65 Mo, 0.12 N); 2) WNR-1.4988 (0.1 C, 16.7 Cr, 14.0 Ni, 1.28 Mo, 0.67 V); 3) 12R72HV (0.1 C, 14.4 Cr, 13.1 Ni, 1.17 Mo, 0.48 Ti, 0.006 B); 4) 316 (0.08 C, 18-20 Cr, 8-11 Ni, 2-3 Mo).

Translated from *Atomnaya Energiya*, Vol. 36, No. 4, pp. 291-300, April, 1974. Original article submitted July 30, 1973.

© 1974 Consultants Bureau, a division of Plenum Publishing Corporation, 227 West 17th Street, New York, N. Y. 10011. No part of this publication may be reproduced, stored in a retrieval system, or transmitted, in any form or by any means, electronic, mechanical, photocopying, microfilming, recording or otherwise, without written permission of the publisher. A copy of this article is available from the publisher for \$15.00.

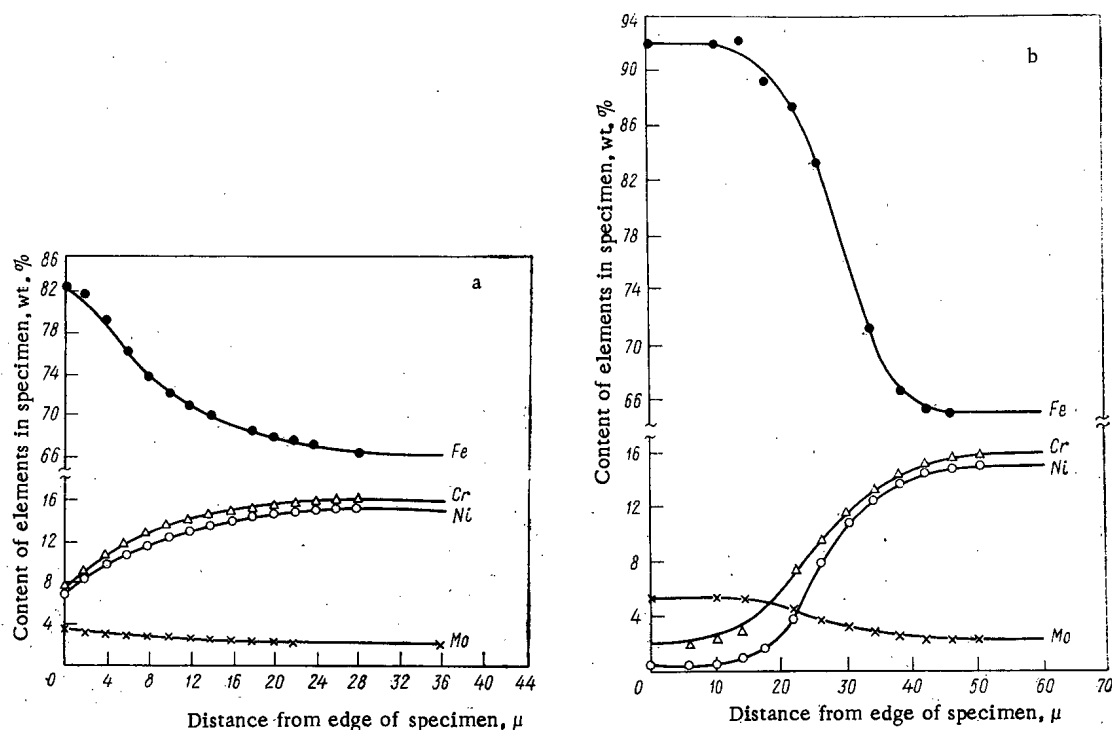


Fig. 2. Change in concentration of elements in steel 0Kh16N15M3B in contact with sodium ($V = 3-5 \text{ m/sec}$; $T_{\text{cold trap}} = 120-130^{\circ}\text{C}$ [6]): a) $T = 650^{\circ}\text{C}$, $\tau = 8000 \text{ h}$; b) $T = 800^{\circ}\text{C}$, $\tau = 7200 \text{ h}$.

Effect of Test Conditions on the Rate of Corrosion of Austenite Chrome - Nickel Steels in Pure Sodium

The exposure of austenite chrome-nickel steels and nickel alloys in a stream of sodium at $600-800^{\circ}\text{C}$ is generally accompanied by losses of the weight of the samples. Typical kinetic curves of the change of weight of different steels [15] during tests in sodium ($T = 700^{\circ}\text{C}$, oxygen content about 10^{-3} wt. \%) are shown in Fig. 1. During the first 1500-2000 h of the tests the losses of weight occur according to the parabolic law and later according to the linear law. A certain difference in the absolute figures of the weight losses in different steels is accounted for by different nickel content in them (see Fig. 1). With the increase of the temperature the rate of corrosion of austenite chrome-nickel steels increases exponentially [9], but the nature of the kinetic curves of corrosion does not change [3, 4, 6]. For similar test conditions ($T = 650-704^{\circ}\text{C}$) the rate of corrosion of nicol-800 ($\sim 300 \text{ wt. \% Ni}$) is three to four times greater than for steel 316 [16], which confirms the negative effect of nickel concentration in the nickel concentration in the material on its durability in sodium.

According to the rate of corrosion in sodium, estimated from the change of weight, all the investigated austenite chrome-nickel steels (with oxygen content of not more than 10^{-3} wt. \%) pertain to the category of completely stable materials up to temperature of 720°C (rate of corrosion $K \leq 0.025 \text{ mm/yr}$). However, nicol-800 and all the more high-nickel alloys have significantly larger K ; this casts doubt on the advisability of using thin-walled parts made from these at temperatures above 700°C .

The rate of corrosion of stainless steels in sodium depends not only on the temperature and length of the tests but also on other factors, for example the velocity of the heat-transfer agent. Up to a certain value of the velocity of the flow ($< 3-4 \text{ m/sec}$) this dependence is close to linear. Afterwards the rate of corrosion remains almost constant. It has been suggested [18] that the rate of corrosion of steel in certain conditions may depend on the diffusion of its components (or oxygen) through the laminar boundary layer of sodium. The thickness of this layer is related to Reynolds number which depends on the velocity of the flow, the diameter of the pipe, and the viscosity of the medium. For certain values of Re the thickness of this layer can be insignificant; then the other stage of corrosion process becomes the controlling factor. In the light of this suggestion the divergence between the results of certain authors (on the effect of the velocity of flow on the rate of corrosion), in which the difference of the diameters of the pipes has been disregarded, becomes understandable.

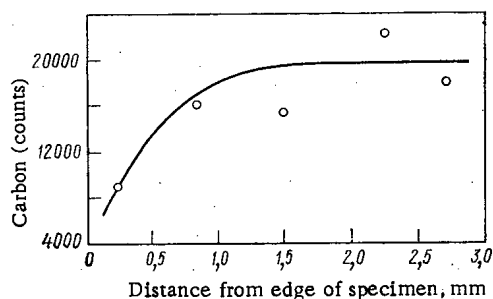


Fig. 3

Fig. 3. Decarbonized steels 316 in contact with sodium flow, $T = 720^{\circ}\text{C}$; $\tau = 10,000$ h; oxygen content about 10^{-3} wt. %. Diameter of aperture diaphragm 70 mm [22].

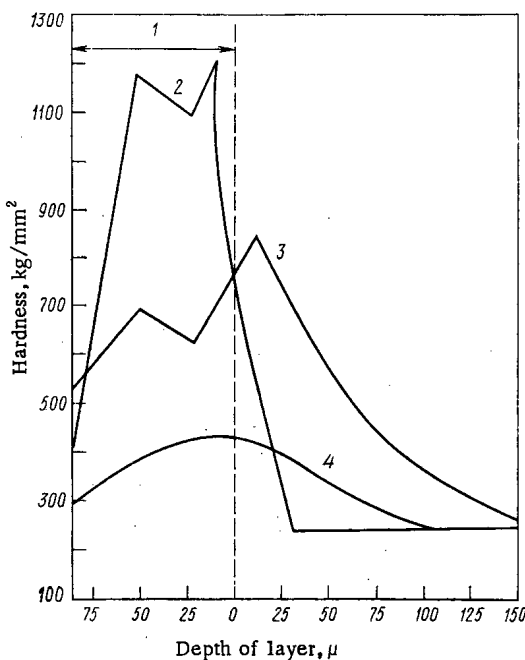


Fig. 4

Fig. 4. Effect of exposure in sodium and vacuum at 593°C on the reduction of hardness of nitrated layer on the surface of steel 304 [26]: 1) nitrated layer; 2) original; 3) 100 h in vacuum; 4) 100 h in sodium.

The increase of the volumetric discharge of the heat-transfer agent causes an increase of the rate of corrosion of steel 316 only by 10% ($T = 704^{\circ}\text{C}$; $Q = 1.9\text{--}3.8$ liter/min) [17]. However, the correctness of this conclusion should be verified at larger flow rates of the heat-transfer agent. There is some information [19] on the acceleration of corrosion of steel 304 in contact with sodium and under simultaneous action of a large thermal flux ($T_{\text{Na}} = 650^{\circ}\text{C}$; ΔT at the wall $\sim 25^{\circ}\text{C}$). The course of the corrosion process is undoubtedly affected by other factors also, in particular, by the degree of nonsaturation of sodium by the components of the steel, which is largely determined by the conditions of falling of the corrosion products into colder regions of the circuit (temperature drop, geometry of the system, velocity of the flow etc.).

In the following sections of the article we shall also discuss the effect of contamination of sodium by impurities on the rate of corrosion of steels.

The rate of corrosion of steel, or the rate of thinning of the casing of the fuel element, determined from the change of weight, is an averaged quantity which does not reflect the entire set of changes that can occur in the metal in contact with sodium. Therefore the stability of steels should be estimated also from the change of the chemical composition, structure, and mechanical properties.

Change of Composition of Austenite Chrome - Nickel

Steels in Contact with Pure Sodium

It has been established by many investigators [3, 6, 17, 20] that during contact with sodium (especially in a nonisothermal circuit) from the investigated steels (at $T \geq 600\text{--}650^{\circ}\text{C}$ and oxygen content not more than 10^{-3} wt. %) the main components Ni, Cr, Mn, and Si are selectively removed ("leached out") and the surface layer becomes rich in Fe and Mo (if the latter is present in the steel). This process occurs particularly intensively in the zone with maximum temperature of the heat-transfer agent. The driving force of the "leaching" process is the gradient of the chemical activity of these elements in the investigated material and the sodium flow, while the controlling stage is the diffusion into the solid metal (at least for long tests).

Investigations showed that the conditions of tests (mainly the temperature) have a significant effect on the rate of progress of this process and on the total depth of the zone with changed chemical composition

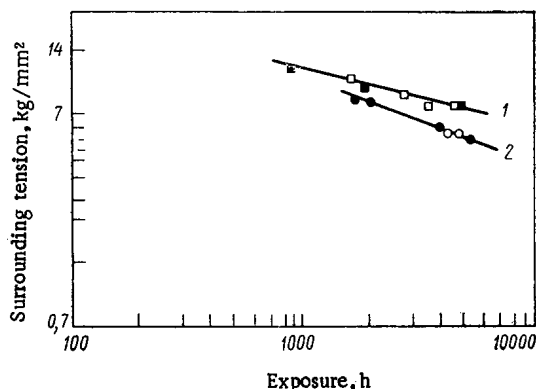


Fig. 5. Long-term durability of steel 316 at 704°C in complex-stressed state in argon (1) and sodium (2). $V = 5.1$ m/sec; oxygen content about 10^{-3} wt. % [2]: ○□) austenization; ●■) coagulation of carbides.

in nonisothermal flow of sodium at $T \geq 650^\circ\text{C}$ is accompanied by their noticeable decarbonization. This phenomenon is especially noticeable when in the circuit there is a formation of more thermodynamically stable carbides than chromium carbide (for example, in the case of use of zirconium inflammable trap [23] or in simultaneous test of high-melting metals (Nb, Ta, V, etc.). However, an assumption has been put forward in [21] that even in a multimetallic circuit made of unstabilized steel (type 316) the transport of carbon is unavoidable due to the need of attaining equilibrium between the activities of carbon in the constructional material and in sodium in the presence of different temperature zones in the circuit. This assumption is substantiated by the results of many studies [17, 21, 22], in which it is shown that for $T \geq 700^\circ\text{C}$ the depth of decarbonized layer can be comparable with the thickness of the casing of the fuel element (Fig. 3).

Earlier it had been assumed that carbon in sodium systems can be transferred to the form of Co [24] or Na_2C_2 [25]. Roy and Wozadlo [21] assert that at sufficiently low concentration of oxygen in sodium ($\leq 10^{-3}$ wt. %) and $T \geq 538^\circ\text{C}$ carbon is transferred to the form of atoms, since thermodynamic computations show the impossibility of existence of CO and Na_2C_2 in such test conditions. They think that the process of decarbonization of steel in a multimetal circuit is associated with the passage of carbide-forming elements (Cr, Mn, Mo, etc.) in sodium in the high-temperature zone of the circuit, accompanied by a lowering of the thermodynamic activity of carbon in the flow and, hence, by a passage of carbon from the steel into sodium. In the low-temperature zone of the circuit chromium and other metals fall off from the oversaturated sodium causing an increase of the activity of carbon and its partial removal from the solution accompanied by the formation of carbides M_2C_6 or M_7O_3 on the surface of the steel. The carbon atoms remaining in the solution combine into molecules or particles and are present in the form of suspension. This carbon can precipitate out in the cold zone of the circuit in the form of elementary carbon and cause carbonization of steel, which is confirmed experimentally. In [21] the concentration of carbon in the hot zone of the circuit ($3 \cdot 10^{-3}$ wt. %) was several orders of magnitude higher than the limit of its solubility; however, in this zone ($T = 704^\circ\text{C}$; $V = 1.5$ m/sec; oxygen content about $5 \cdot 10^{-4}$ wt. %) decarbonization of steel 316 was observed. This permits the conclusion that elementary carbon does not occur in equilibrium with the sodium flow; otherwise the samples of steel must have been carbonized.

It is not excluded that the process of transport of carbon into the sodium system is more complex. For example, it is possible that in sodium those mentioned above as well as other more inert and stable forms of carbon with low activity are present causing neither carbonization of the steel nor changes of the activity of carbon in sodium.

As already shown in [2, 3], steels stabilized by niobium or titanium do not show a tendency to carbonization (at least in the investigated range $600\text{--}800^\circ\text{C}$) and are even carbonized in a number of cases. Apparently, the difference in the activities of carbon in steel and sodium, which is the driving force for the process of decarbonization, is of opposite sign in this case. However, it can be supposed that at higher temperatures, when the amount of carbide-forming elements passing into sodium increases sharply and the thermodynamic activity of carbon in steel also increases, decarbonization of stabilized steel also may start, wherein the presence of stabilizer element must be reflected in the kinetics of the process.

(Fig. 2), which also depends on the length of the tests. It should be noted that in certain conditions the depth of the zone with changed chemical composition may reach 100μ and the content of chromium and nickel at the surface is reduced almost to zero. At those points of the contour, which lie after the zone with maximum temperature (along the direction of the flow), generally a sedimentation of the transport products is observed, which may significantly change the nature and rate of "Leaching." It is announced in [17] that an increase of the flow velocity accelerates the depletion of nickel from the steel but does not affect the removal of chromium. Apparently, this may be characteristic of the first stage of the corrosion process, when the controlling stage is the tearing off of the atoms of easily soluble elements from the surface of the solid body into the liquid or their diffusion in the boundary layer of the liquid.

As established by a number of investigations [3, 21, 22], a long exposure of unstabilized austenite steels

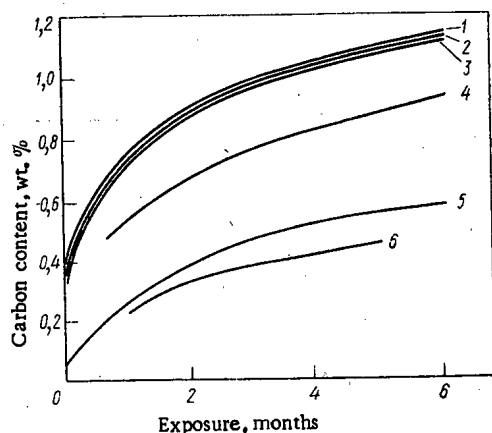


Fig. 6

Fig. 6. Rate of carbonization of steel 316 at 650°C from different sources of carbon [40]: 1) carbon steel; 2) sodium carbonate; 3) oil; 4) carbon black; 5) graphite; 6) acetylide.

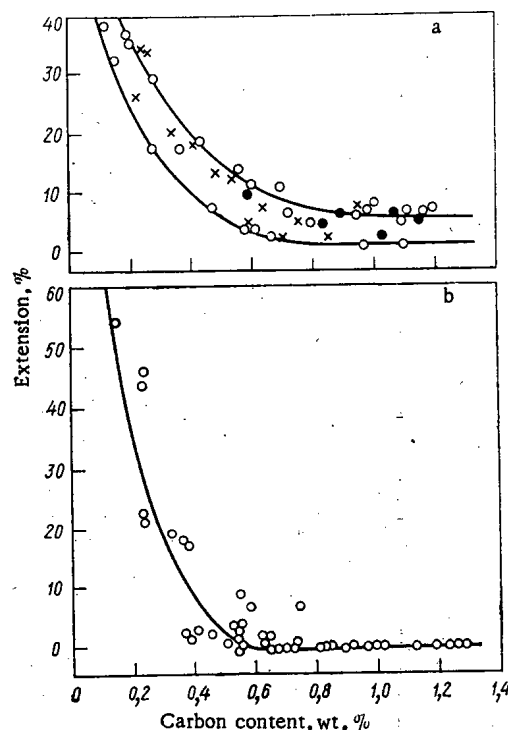


Fig. 7

Fig. 7. The effect of carbonization of steel 316 in sodium on its plasticity in transient explosion [40]. Oxygen content about 10^{-3} wt. %: a) at high temperature: ●) 500°C, ×) 600°C, ○) 650°C; b) at room temperature.

Along with decarbonization in sodium systems denitration of stainless chrome-nickel steels can be observed [26-28]. Thus, after 100 h exposure at 593°C in sodium a resorption of nitrated layer at the surface of steel 304 occurs due to the diffusion of nitrogen deep into the sample as well as due (mainly) to passage into sodium [26] (Fig. 4). An increase of the temperature to 650°C accelerates this process. The mechanism of transfer of nitrogen into sodium systems is not yet clear, but it can be assumed that at higher temperatures it is connected with the solubility of nitrogen in sodium. According to the data of [29] its solubility of nitrogen in sodium. According to the data of [29] its solubility is very low (at 502°C $m = 19 \pm 7 \cdot 10^{-10}$ wt. %, and at 600°C $m = 49 \pm 8 \cdot 10^{-10}$ wt. %). In the range of lower temperatures (up to 200-300°C) the possibility of transfer of nitrogen into sodium through C_2N_2 can be admitted. In the case of contamination of sodium by such impurities as Ca, Li, Be, Zr, Ti it is possible that nitrogen is transferred in the form of nitrides of these metals.

At present it is difficult to say what is the sink for the nitrogen removed from the steel. According to one view [30] it is gaseous purging of sodium over the mirror (for example, in reactor tank); according to others [2] nitrogen can enter into corrosion products (for example, in the form of Cr_2N) precipitating out in the cold zone of the circuit. It is also not clear which is the controlling stage in the process of transfer of nitrogen.

There is information about the removal of boron in contact with sodium ($T = 704^\circ\text{C}$; τ up to 11,000 h; oxygen content less than 10^{-3} wt. %) from steels 316 and 321 [28].

Change of Structure and Mechanical Properties of Austenite Chrome - Nickel Steels in Contact with Pure Sodium

The change of the chemical composition of austenite chrome-nickel steel in contact with sodium is accompanied by a change of its phase state. Thus, a layer with the structure of α -ferrite appears at its

surface (due to removal of γ -stabilized elements); the depth of embedding of this layer depends on the conditions of tests and the original alloying of the metal. Besides this the amount of chromium carbides decreases in the layer and their dispersability increases [2]; also the fallout of grains of σ -phase along the boundaries increases [6, 16, 31]. Some authors have observed the penetration of sodium deep into the steel sample. For example, with an ion microprobe the penetration of sodium into steel 316 to a depth of 40μ after a test in sodium flow at 720°C for 10,000 h has been established [22]; this depth coincides with the depth of the zone of changed chemical composition (in respect of Ni, Cr, Mn, etc.).

Sodium is not a surface-active medium [32]. Therefore, a contact with it, which is not accompanied by a change of the composition and structure of the steels, does not affect their mechanical properties. If the changes of the composition and structure do occur, this causes a change of the mechanical properties of the steel, in particular, of the characteristic of heat resistance. Thus, at 650°C contact with sodium for 3000-5000 h does not cause noticeable changes in the structure of casing steels, as a result of which the heat-resistance characteristics of these steels (304, 316, 0Kh16N15M3B, etc.) in sodium and argon are similar [3, 33, 34]. At the same time a test in similar conditions made on high-nickel alloy 80A having lower stability causes a decrease of the time before disintegration by a factor of four compared to the tests in argon [34]. At 700°C a noticeable reduction of the time before disintegration in sodium is also observed (static conditions, oxygen content about $5 \cdot 10^{-3}$ wt. %) in nicol-800 samples [12], whereas in simultaneously tested samples of stabilized steel 16-13 the period of creep is reduced only by one third (compared to the tests in argon). However, tests with stabilized austenite chrome-nickel steels at $T \geq 700^\circ\text{C}$ showed an appreciable reduction of the time before disintegration; this is indicated, for example, by the characteristics of long-time durability of steel 316 in sodium and argon flows at 740°C [2], shown in Fig. 5. The weakening of steel in sodium can be explained by its decarbonization (after 4840 h of tests the carbon content decreased by 48%). Similar results have been obtained also by other investigators [27, 35, 36].

Effect of Neutron Irradiation on Corrosion of Austenite

Chrome - Nickel Steels in Sodium

For science and technology it is very important to know whether neutron irradiation has any effect on the course of corrosion processes during the contact of austenite steels with sodium. There is no unanimous view on this question. It can be assumed that irradiation must have an effect on the course of diffusion processes in a solid metal (due to the change of state of the lattice, increase of the number of vacancies etc.) and, hence, on selective depletion of its components from the composition of the steel, if diffusion is the controlling stage of this process. In [37] it is communicated that there was no effect of irradiation observed on the rate of corrosion (estimated from the change of weight) of steel 304 in test in EBRII reactor. However, it is well known that at the temperature of this experiment (530°C) selective removal of such elements as Ni, Cr, Mn, etc., from steel is not observed. At the same time the possible acceleration of removal of nitrogen and carbon from the steel under irradiation was not controlled and the change of concentration of these elements in steel has little influence on the change of weight of the samples. Hence the above-mentioned experiment still does not demonstrate the absence of the effect of irradiation on corrosion.

An attempt to estimate the possible effect of irradiation on the rate of corrosion of steel in sodium with the use of an analytical model [31] has generated considerable interest. According to this model the process of corrosion of austenite steel in sodium is assumed to consist of two processes: depletion of the components of steel controlled by diffusion and frontal corrosion of the layer rich in elements that are difficult to dissolve, wherein this corrosion depends linearly on time. It should be mentioned that this model gives a good agreement with the results (without irradiation) with experimental data on corrosion of steel 316 at 650°C . It is concluded that as a result of knocking out of a large number of metallic atoms from the surface of the steel by the flux of fast electrons the frontal corrosion may increase sharply and the time required for change-over to the linear nature of corrosion may get shortened. In the case of formation of a layer of α -ferrite on the surface of the steel (as a result of removal of γ -stabilizing elements) the depth of embedding of this layer under the action of irradiation must decrease, but the layer itself will grow more rapidly. Besides, as the authors of [31] assume, a readjustment of the lattice under the action of irradiation may accelerate the diffusion processes in the steel. Computations show that irradiation can significantly affect the rate and the nature of the course of the corrosion process; however, these computations need experimental verification.

Interaction of Austenite Chrome - Nickel Steels with Impurities in Sodium

All the effects discussed above were observed in tests of materials in sodium relatively free of impurities. The main impurity, which the investigators encountered in the use of sodium as heat-transfer agent, was oxygen. From that time such effective methods of purification of sodium as cold traps have been developed, with which the concentration of oxygen in the heat-transfer agent can be reduced to $5 \cdot 10^{-4}$ wt. % in a few tens of hours even in large industrial systems, which is entirely sufficient for ensuring good corrosion resistance of steels in the chosen temperature range. However, we recall that the increase of concentration of oxygen from $5 \cdot 10^{-4}$ to $25 \cdot 10^{-4}$ wt. % increases the rate of corrosion of steel 316 at 725°C by a factor of almost 10 [11]. Similar results were obtained also for other steels [2, 3, 9, 13, 38, 39]. With the increase of the concentration of oxygen the nature of interaction of the investigated steels with sodium changes: Fe, Cr, and Mn are selectively removed from the surface layer and the layer gets rich in Ni and Mo [3, 37]. Besides the increase of the rate of frontal corrosion oxygen in sodium accelerates intercrystal corrosion which is accompanied by loss of plasticity [3, 10] even in the test of long-term strength.

At present the contamination of sodium by carbon is undoubtedly more hazardous, especially in the process of operation of a reactor because of the difficulty of cleaning the heat-transfer agent and relatively rapid run of the process of carbonization.

Carbonization of austenite steel in I circuit of a reactor may occur from several sources, but the main source is the carbon and other carbonizing impurities in the heat-transfer agent (graphite, mineral oil, carbonate Na_2CO_3 , etc.) whose presence in industrial reactors is inevitable according to the opinion of certain investigators [40].

An experimental verification of carbonization of steel 304 in static sodium showed [41] that up to 565°C this process mainly occurs along the grain boundaries, but at higher temperatures frontal carbonization is also observed. Campbell and Tyzack [42] have proposed a model of carbonization of austenite chrome-nickel steels in sodium at 700°C containing carbon of unit activity. According to this model it is necessary to consider the diffusion of carbon, which is the controlling stage in the growth of the carbonized layer, as well as the fall out of carbides (first enriched by chromium M_{23}C_6 , and later by carbon M_7C_3 and M_3C).

The transfer of carbon into sodium is a multistage process. It is shown in [40, 43] that the controlling stage is the diffusion of carbon into austenite steel. However, there is some evidence [44] that in certain conditions the controlling stage may be also the diffusion of carbon in ferrite of carbon steel which may be its source. Apparently, here the ratios of the areas and thickness of the source and the receiver of carbon will be a deciding factor. However, in a number of cases other stages may be the controlling stages in this process (for example, the stage of transfer of carbon through sodium for sufficiently large distance between the source and the receiver of carbon).

Thorley and Tyzeck [40] did an experimental verification of the effect of carbonization on the mechanical properties of a number of construction materials. Thus, in the test of stabilized steel 18-8-Ti in dynamic sodium at 650°C its carbonization was observed even at low concentrations of carbon, $1 \cdot 2 \cdot 10^{-4}$ wt. %. The increase of the carbon content in steel was reflected only in a decrease of (by a factor of 1.5 in comparison with the tests in argon) the relative elongation at 20°C. The change concentration of oxygen in sodium in the range $5 \cdot 30 \cdot 10^{-4}$ wt. % did not affect the results of carbonization, which is in agreement with the theoretical computations [21]. Earlier Nevzorov and Starkov [43] had shown the accelerating effect of the increase of concentration of oxygen ($5 \cdot 500 \cdot 10^{-3}$ wt. %) in sodium on the process of transfer of carbon. The results of [40] and [43] are not contradictory, since the increase of concentration of oxygen above a certain level changes the mechanism of the process of transfer, making the transfer of carbon through CO or complex oxygen containing compounds of carbon possible.

The carbonizing action of different sources of carbon on steel 316 was also verified [40]. The tests were conducted in static conditions at 650°C. It was established (Fig. 6) that mineral oil, carbon steel (0.36 wt. % C), and carbonate Na_2CO_3 are active graphitizers causing relatively rapid carbonization of steel; carbon black is considerably less active and graphite and acetylide ($\text{NaC}-\text{CH}$) are relatively inert. However, the results of [40] show that the plasticity of the investigated steel at 20°C after six months of contact with "inert" impurities was lowered to 3-5%, i.e., their "inertness" is highly conditional.

Furthermore, Thorley and Tyzack [40] determined the critical value of carbonization for steel 316 causing an increase of the strength and disappearance of plasticity after the test in sodium at 500, 600, and

650°C (the carbon source was carbon steel). It was found that for a carbon content of ~1 wt. % the values of σ_B and $\sigma_{0.2}$ coincide irrespective of the temperature of the test. The plasticity of the steel is more sensitive to the carbon content. Thus, for ~0.7 wt. % C the relative elongation of steel at 20°C is equal to zero (Fig. 7). The plasticity determined at increased temperatures (500–650°C) is close to zero for higher concentrations of carbon (1.0–1.2 wt. %).

Similar results were obtained in the investigations by Luk'yanova et al. [45] in carbonization of steels 1Kh18N10T and 1Kh16N15M3B. The proposed empirical equations relate the change of the mechanical properties of steels with the carbon concentration in them (in wt. %). Thus, for steel 1Kh16N15M3B

$$\begin{aligned}\sigma_B^{20} &= (62.0 + 37.5C) \pm 4.1 \text{ kg/mm}^2, \\ \delta^{20} &= (54.69 - 105.22C + 50.01C^2) \%\end{aligned}$$

It had been shown in an earlier work [20] that the test of steel 316 in moving sodium with increased carbon content at 650°C is accompanied by a decrease of the long-term plasticity by 50–75%, whereas the elongation in transient explosion (after exposure for 4000 h) was reduced by 96%.

The possibility of falling of carbon in the first circuit of the reactor and carbonization of the parts of active zone has been confirmed, for example, by the analysis of the casing of ignition fuel element of reactor EBR II [46] made from steel 304. On the casing corrosion along the grain boundaries and presence of fissures were observed on the side of the heat-transfer agent. A chemical analysis showed increase carbon content. According to the investigators the reason of corrosion is the presence of residues of grease or other carbonizing impurities on the surface of the fuel element before loading in the reactor.

As mentioned already, there is a possibility of transfer of nitrogen in sodium systems; however, published information on this phenomenon is extremely meager. The source of nitrogen in the I circuit of the reactor may be: impurity in the inert gas above the reflector of sodium; nitrogen as alloying element or as impurity in the construction material; diffusion of nitrogen from the atmosphere through the walls of the high-temperature part of the system in sodium and impurities in sodium.

Nitration of steel 304 at 600°C in the case of use of nitrogen as the protective gas in the expansion tank of the sodium circuit was accompanied by a sharp decrease of plasticity of the steel due to the formation of large amount of nitrides of chromium in its structure [47]. It is communicated in [37] that steel with reduced chromium content is less prone to nitration in sodium.

According to the computations of Subbotin et al. [30] in the operation of sodium systems at high temperatures ($T \geq 600^\circ\text{C}$) an increase of the concentration of nitrogen in sodium is possible due to its diffusion from the atmosphere through the walls made of chrome–nickel steels.

It is noted in [48, 49] that after 21,000 h of operation of the sodium circuit in the temperature range 300–800°C (of this 19,000 h at $T \geq 650^\circ\text{C}$) nitration of steel 304 occurred on the side of the heat-transfer agent (from 0.06 to 0.49 wt. %) due to the presence of potassium nitride in sodium.

Cases of contamination of sodium by other impurities (copper [4], sulfur [49]) are also known.

CONCLUSIONS

The results of investigations discussed above show that a considerable amount of experimental data has been accumulated about the compatibility of austenite chrome–nickel steels with sodium heat-transfer agent and this has significantly widened our concepts of the physicochemical characteristics of the construction material – liquid sodium system. Definite steps have been taken toward the development of theoretical ideas about a number of phenomena occurring during the contact of liquid and solid metals. Besides, operation of fast reactors with sodium cooling (for example, BR-5, BOR-60, Rhapsody, etc.) shows that correctly chosen stainless steels of type 0Kh16N15M3B or 316 may be used quite successfully (also in respect of compatibility with sodium of reactor purity) as the material for the casing of the fuel elements of these reactors. However, there are many aspects of the interaction of casing steels with sodium in conditions of operation of industrial reactors that are not sufficiently clear. Thus, the opinion on the mechanism of the process of transfer of carbon, nitrogen, and other impurities in the sodium circuit is varied, which in turn hinders the development of effective methods of coping with this phenomenon and its consequences which can significantly lower the efficiency of the casings of fuel elements. The effect of neutron irradiation on the processes of interaction of steels with sodium and its impurities has remained practically uninvestigated (especially in the range of temperatures higher than 600°C), which may give entirely unexpected effects both in qualitative and quantitative aspects. There is very little information on the effect of the structural state of the metal (austenitization, cold working, mechanical-hermetic processing, etc.) and also of

the size of the grain on the compatibility of steels with moving sodium, which of great practical interest in connection with the search for effective methods of combating swelling of casing steels in a flux of fast neutrons, for example, through the development of a special structure in the steel.

Apparently these questions must be answered by the investigators in the near future in order to pass on to the operation of industrial fast reactors with sodium cooling.

LITERATURE CITED

1. Nucl. Engng. Intern., 8, No.203, 304 (1973).
2. P. Murrey, React. Technol., 15, No.1 (1972).
3. N. P. Agapova, A. G. Ioltukhovskii, and V. V. Romaneev, in: Alkali Metal Coolants, IAEA, Vienna (1967), p. 85.
4. N. P. Agapova et al., in: State and Prospects of Work on the Development of APS with Fast Neutron Reactors, SEV Symposium, Obninsk, Vol.2, FEI (1967), p.457.
5. D. Curinsky et al., Proc. Third UN Intern. Conf., Geneva, Vol.9 (1965), p.550.
6. N. P. Agapova et al., Paper Presented at French-Soviet Colloquium on Fuel Elements for Fast Neutron Reactors, Kadarash, France (1970).
7. B. A. Nevzorov et al., see [5], p.561.
8. E. Brush, Trans. Amer. Nucl. Soc., 8, 412 (1965).
9. A. Thorley and C. Tyzack, see [3], p.97.
10. K. Horton et al., see [3], p.247.
11. N. Nettli et al., in: Selected Papers of the London Conference on Fast Neutron Reactors, Atomizdat, Moscow, No.4 (1967).
12. H. Bohm and H. Schnelder, Nucl. Mater., 24, 188 (1967).
13. P. Heltz, React. Mater., 12, No.3, 181 (1969).
14. O. M. Vishkarev et al., Protection of Metals, 11, No.5, 552 (1971).
15. M. Fevery et al., Conf. on Fast Reactor Technology, Tyrso, England, Rep. No.13 (1971).
16. React. Mater., 12, No.3, 181 (1969).
17. P. Roy and M. Gebhardt, ibid, 13, No.3 (1970).
18. P. Roy and M. Schad, J. Nucl. Mater., 47, 129 (1973).
19. J. Hopfenfeld and D. Darley, React. Mater., 13, No.3, 144 (1970).
20. W. Lee, ibid, 13, No.1 (1970), p.49.
21. P. Roy and G. Wozadlo, Nucl. Technol., 10, No.3, 307 (1971).
22. E. Berkey et al., ibid, 16, No.1, 263 (1972).
23. W. Lee, Nucl. Appl. Technol., 7, No.2, 155 (1969).
24. B. A. Nevzorov, Corrosion of Construction Materials in Sodium, Atomizdat, Moscow (1968).
25. Argonne Nat. Lab. Development, USAEC, Rept. ANL-7513 (1967), p.124.
26. C. Bagnall et al., Trans. Amer. Nucl. Soc., 15, No.1, 234 (1972).
27. K. Natosan et al., React. Technol., 15, No.4, 244, Winter (1972-1973).
28. D. Sandusky et al., J. Nucl. Mater., 46, 225 (1973).
29. React. Mater., 12, No.1, 30 (1969).
30. V. N. Subbotin et al., Physicochemical Bases of the Use of Liquid-Metal Heat-Transfer Agents, Atomizdat, Moscow (1970).
31. J. Anno and J. Walowit, Nucl. Technol., 10, No.1, 67 (1971).
32. V. N. Nikitin, Physicochemical Phenomena in the Interaction of Liquid Metals with Solids, Atomizdat, Moscow (1967).
33. L. Kirschler et al., React. Mater., 13, No.3, 144 (1970).
34. React. Mater., 10, No.4, 231 (1969).
35. R. Amonn, Trans. Amer. Nucl. Soc., 15, No.2, 590 (1972).
36. Atomic Intern. USAEC Rept. NAA-SR-12395 (1967), p.115.
37. W. Berry, Corrosion in Nuclear Applications. Corrosion Monograph Series, J. Wiley and Sons, New York (1971).
38. J. Weeks, React. Mater., 12, No.3, 180 (1969).
39. A. Fleitman and H. Isaacs, React. Mater., 13, No.3, 143 (1970).
40. A. Thorley and C. Tyzack, see [15], Rept. No.11.
41. W. Holcomb, Nucl. Engng. Design, No.3, 264 (1967).
42. S. Campbell and C. Tyzack, see [3], p.159.
43. B. A. Nevzarov and O. V. Starkov, Phys.-Chem. Mechanics of Materials, 3, 257 (1967).

44. F. Litton and A. Morris, *J. Less Common Met.*, **22**, No. 1, 71 (1970).
45. I. N. Luk'yanova et al., *Atomnaya Energiya*, **32**, No. 4, 852 (1972).
46. M. Ruther et al., *React. Mater.*, **13**, No. 1, 50 (1970).
47. J. Gill and J. Bokros, USAEC Rept. NAA-SR-6162 (May, 1960).
48. G. Ratz and K. Brickher, *React. Mater.*, **11**, No. 3, 167 (1968).
49. G. Ratz, *Nucl. Technol.*, **17**, No. 2, 153 (1973).
50. K. Natesan and T. Kassner, *J. Nucl. Mater.*, **57**, 223 (1970).
51. *React. Mater.*, **12**, No. 3, 181 (1969).
52. K. Kumerer et al., *Atomic Engineering Abroad*, No. 9 (1972), p. 26.
53. P. L. Kirillov et al., *Liquid Metals, Coll. of Articles*, Atomizdat, Moscow (1972).
54. E. Zobroski et al., see [3], p. 195.
55. J. Devan, see [3], p. 643.
56. G. Ilinchev, see [3], p. 131.

BOOK REVIEWS

B. I. Taratorin

STRESS SIMULATION IN NUCLEAR REACTOR DESIGNS

Reviewed by A. F. Gurov

Direct experimental methods of investigation are out of the question or are very difficult for solving problems of plasticity, creep, operating capability and reliability of nuclear reactor materials. Here, as nowhere else, methods for investigating stresses and the deformed state on models are essential. Because of this, the book by B. I. Taratorin which is being reviewed here, is timely and is of interest to a wide circle of specialists.

The book discusses problems of stress simulation and one of the means of effecting the simulation method – the polarization-optical method of stress investigation. A large number of problems is considered, arising from simulation of the stressed and deformed state of nuclear reactor components, problems of thermophotoelasticity, thermophotoplasticity and thermophotocreep.

The usual simulation relationships are presented in general form for polymers and metals, which makes it possible to select the optimum materials of the model for describing stresses in manufactured articles. Generalized relations are obtained – dimensionless characteristics, which permit processes of material creep and stress relief under thermal loading conditions to be described.

The present-day state of the optical method of stress investigation is discussed and recommendations are made for its application to the solution of practical problems.

The book contains the practical results of temperature stress investigations; interesting data are presented concerning the thermophysical properties of polymers and their methods of determination; recommendations for the choice of dimensions of the model, methods of preparation and processing of the data; recommendations for the optimum temperature of "freezing" of the model, and its rate of heating; inspection of "frozen" deformations and their interpretation.

But the book is not free from deficiencies. In many cases it would be interesting to compare the author's results with the data obtained in the reports by N. I. Prigorovskii, N. A. Shchlegolevskii, M. M. Frokhta, D. V. Monakhenko, and Alabushev in the field of simulation and photoelasticity. The author does not assess the effect of Poisson's coefficient in stress simulation, although this effect is large in the solution of three-dimensional problems and is widely discussed in the literature. Important problems of simulation of temperature fields under nonsteady thermal loadings and radiation are not represented.

Errors, mistakes and procedural inaccuracies are in evidence. For example, the temperatures of the model are given in absolute units and in degrees centigrade. The recommendations given in the example in §6 concerning the rate of cooling of polymers in the highly-elastic state (12.5 deg/h) are questionable; they differ from Prigorovskii's recommendations (2-2.5 deg/h). In §23, the method of "freezing" discussed as applicable to thin-walled cylindrical shells does not agree with the similar method in the paper by S. T. Kardash and E. V. Chemokhud. All this should be corrected in a repeat issue of the book.

On the whole, B. I. Taratorin's book contains up-to-date and valuable information in the field of simulation and the optical method of stress investigation. It will be a useful textbook for designers and specialists concerned with simulation and with the optical method of stress investigation.

Translated from Atomnaya Energiya, Vol. 36, No. 4, p. 300, April, 1974.

© 1974 Consultants Bureau, a division of Plenum Publishing Corporation, 227 West 17th Street, New York, N. Y. 10011. No part of this publication may be reproduced, stored in a retrieval system, or transmitted, in any form or by any means, electronic, mechanical, photocopying, microfilming, recording or otherwise, without written permission of the publisher. A copy of this article is available from the publisher for \$15.00.

ABSTRACTS

DOSE DISTRIBUTIONS IN BIOLOGICAL TISSUE FROM
SUPERHIGH-ENERGY NUCLEON BEAMSI. M. Dmitrievskii, E. L. Potemkin,
and V. V. Frolov

UDC 539.12.08

The present paper presents the methods and results of calculating dose distributions in small tissue phantoms from neutron beams having energies in the range 0.4-100 GeV.

Secondary-particle angular distributions were taken into account; according to Ranft's equations [1] for energies above 0.4 GeV, and using the analytical expressions in [2, 3] for energies up to 0.4 GeV.

The Ranft equations [1] hold for incident-particle energies up to 30 GeV. However, keeping in mind that the dose is determined mainly by the secondary-particle mean multiplicity, we assume it is possible to use Ranft's equations [1] for dose calculations up to 100 GeV energies, and for even higher energies for estimated calculations. The program for calculating dose distributions was written in FORTRAN.

Figure 1 shows the dependence of the maximum absorbed dose on incident-neutron energy for beams 1, 5, 10, and 25 cm in diameter and for a broad beam. Figure 2 gives absorbed-dose distributions for neutrons having energy 30 GeV, with respect to beam radius at depths 0, 10, 20, and 30 cm from the phantom frontal plane.

We propose to compare the theoretical results with experimental data on dose distributions obtained with a beam of neutrons having average energy ~ 30 GeV.

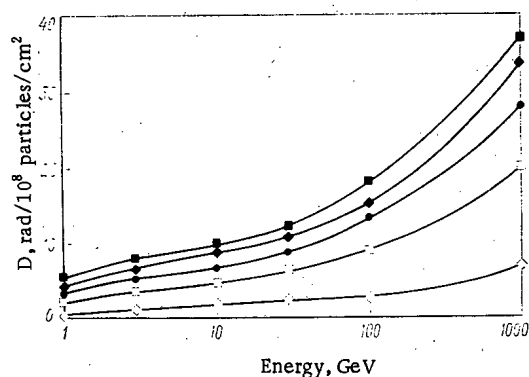


Fig. 1

Fig. 1. Energy dependence of maximal absorbed dose D for beams having various radii: \blacksquare) broad beam; \blacklozenge) $r = 25$ cm; \bullet) $r = 10$ cm; \square) $r = 5$ cm; \blacklozenge) $r = 1$ cm.

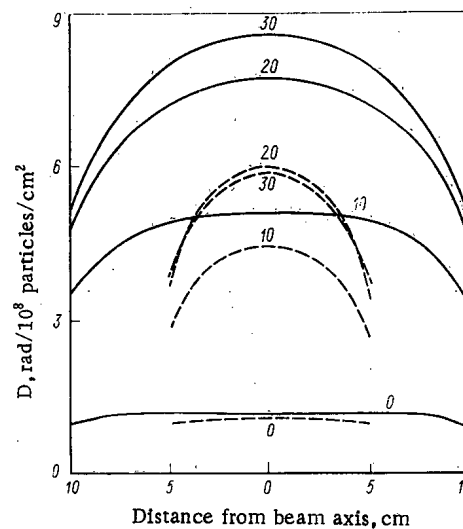


Fig. 2

Fig. 2. Absorbed-dose distribution in tissue phantom from beam of neutrons having energies 30 GeV and radii 5 (---) and 10 (—) cm at various distances from forward wall of phantom. (Uniform particle-flux distribution in beam.)

Translated from *Atomnaya Energiya*, Vol. 36, No. 4, pp. 301-304, April, 1974. Original article submitted February 9, 1973.

© 1974 Consultants Bureau, a division of Plenum Publishing Corporation, 227 West 17th Street, New York, N. Y. 10011. No part of this publication may be reproduced, stored in a retrieval system, or transmitted, in any form or by any means, electronic, mechanical, photocopying, microfilming, recording or otherwise, without written permission of the publisher. A copy of this article is available from the publisher for \$15.00.

LITERATURE CITED

1. Ranft, Nucl. Instrum. and Methods, 48, 133 (1967).
2. R. Alsmiller et al., ORNL-4046 (1967).
3. R. Alsmiller et al., ORNL-TM-2277 (1968).

ABSORBED-DOSE DEPTH DISTRIBUTION IN TISSUE-EQUIVALENT ABSORBER FOR QUASIISOTROPIC INCIDENCE OF 1 MeV ELECTRONS

R. Ya. Strakovskaya, G. N. P'yankov,
and I. R. Entinon

UDC 539.171.4

This paper studies the problem of absorbed-dose distribution with isotropic electron incidence on the absorber surface. Isotropic electron incidence on the surface is modeled by uniform rotation of an object having, for example, cylindrical shape in a broad, parallel electron beam produced by an electron accelerator. Such irradiation is called quasiisotropic.

It is shown that with quasiisotropic irradiation the absorbed-dose distribution over the object depth differs significantly from the distribution corresponding to normal electron incidence on the absorber, and may be obtained approximately from the expression

$$D_{is}(x) = 2 \int_0^{\alpha_k(x)} 0.5 D_{max} \cos \alpha \left[1 + \sin \left(\frac{4.5x}{R_e \cos \alpha} + 0.2 \right) \right] d\alpha,$$

where α_k is determined from the condition $4.5 x/R \cos \alpha_k + 0.2 = (3/2)\pi$.

Here, $D_{is}(x)$ is the dose distribution with quasiisotropic irradiation; x is the absorber thickness; D_{max} is the maximum of the distribution $D_{is}(x)$; α is the variable angle of rotation for the object under the beam when modeling isotropic radiation; R_e is the extrapolated electron path.

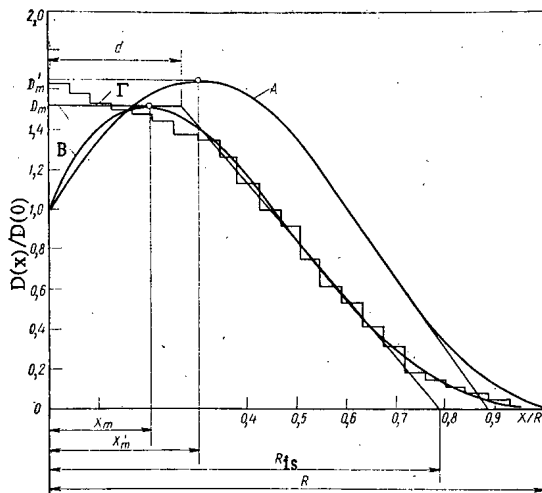


Fig. 1. Absorbed-dose distribution with respect to absorber depth: A) with normally incident electrons; B, Γ) quasiisotropic incidence (theory and experiment, respectively); Δ) approximating piecewise-linear distribution for quasiisotropic electron incidence.

Original article submitted May 29, 1973; revision submitted November 5, 1973.

Figure 1 shows the absorbed-dose distribution with quasiisotropic irradiation, found by computer analysis (curve B); also shown for comparison is the absorbed-dose distribution with normal electron incidence (curve A); the histogram shown (curve Γ) was obtained experimentally with quasiisotropic irradiation of a stack of dosimetric films.

Curves B and Γ practically coincide everywhere except for the initial portion at small absorber thicknesses. Much better agreement of experimental data is observed with the distribution for isotropically incident electrons calculated by V. V. Arutyunov using the Monte-Carlo method.

The curve for the absorbed-dose depth distribution in a tissue-equivalent absorber with isotropically incident 1 MeV electrons may be approximated by the piecewise-linear function $\varphi(x)$ such that in the interval $[0, d]$ the function $\varphi(x)$ is constant, while in the interval $[d, R_{is}]$ the function $\varphi(x) = a - bx$ is linear. The function $\varphi(x)$ is also shown in Fig. 1 (curve Δ).

The feasibility of simple approximation for the absorbed-dose distribution function for objects rotating under an electron beam has practical significance in the design of technology for radiation treatment of objects.

ELECTRON MICROSCOPIC STUDY OF OXIDE FILMS ON ZIRCONIUM ALLOYS

T. Kh. Margulova, T. I. Malova,
V. A. Dmitriev, and V. M. Ryabov

UDC 669.018.822

To study oxidation processes in zirconium alloys with 1 and 2.5% Nb we conducted an electron microscopic and electron diffraction analysis of oxide films 800-2200 Å thick separated from the substrate. Samples were oxidized in high-purity water and in an aqueous solution of Trilon B (Komplekson) with a concentration of 0.5 g/kg at a temperature of 300°C.

The studies showed that films obtained by oxidation of zirconium alloys in pure water and in the Komplekson solution are characterized by a granular structure that repeats the grains of the alloys. The grains consist of large numbers of fine crystallites (subgrains) with sizes of order 100-200 Å. The grains of the oxide film from the zirconium alloy with 1% Nb have regular contours and the average size of the section is 5-10 μ . The grains of the oxide film from the zirconium alloy with 2.5% Nb have an irregular contour, with sizes of 1.3 μ , and the boundaries between them are indistinct. Oxide films obtained in the Komplekson solution are finer than the grains obtained in pure water and are uniform throughout the thickness of the film and within the limits of a single grain.

Small light sections 0.05-0.20 μ in diameter were observed in the oxide films from both alloys. These sections have a thinner oxide film that is formed in sections rich in Nb. For the zirconium alloy with 2.5% Nb they are larger, finely dispersed, and concentrated in the boundaries of grains and subgrains.

The electron diffraction analysis of oxide films obtained in pure water and in the Komplekson solution showed that the film consists mainly of monoclinic zirconium oxide with a small amount of cubic (or tetragonal) phase, the amount of this phase decreasing with increasing oxidation times. The electron diffraction patterns indicate epitaxial conformity of the structures of the film and the alloy and reflect the existence of texture.

Original article submitted June 29, 1973; abstract submitted November 15, 1973.

EFFECT OF COHERENT SCATTERING ON THE SPATIAL DISTRIBUTION OF THE INTENSITY OF γ -RADIATION FROM A POINT MONODIRECTIONAL SOURCE

A. M. Kol'chuzhkin, A. I. Ksenofontov,
A. M. Panchenko, V. N. Potapov,
and V. V. Uchaikin

Theoretical studies of the penetration of γ -rays through matter generally neglect both coherent (Rayleigh) scattering and incoherent scattering from bound electrons. In some cases, however, these effects can be important, particularly in determining various characteristics of the γ -ray distribution close to collimated beams.

The role of coherent scattering is not easily traced by using a point monodirectional source. Since the radiation field of such a source for small angles θ_0 (Fig. 1) is determined mainly by single scattered γ -rays [1, 2] the contribution of coherent scattering was estimated by using the single scattering model. We used the Monte Carlo method to calculate the spatial distributions of the intensity of radiation $I'(R, \theta_0)$ from both coherent and Compton scattering for source energies $E_0 = 0.1$ MeV and $E_0 = 0.5$ MeV in iron and lead. In addition the distributions of the intensity of incoherent scattering by bound electrons in lead were determined.

The calculations showed in particular that for detection points at small angles ($\theta_0 \approx 1^\circ$) coherent scattering leads to an increase in intensity of 60-70% in aluminum, and practically completely determined the intensity in lead.

An analytic expression was obtained for calculating the spatial distribution of intensity in the single, Compton, and coherent scattering approximation. Figure 1 shows a comparison of the results calculated with this formula and these obtained by the Monte Carlo method.

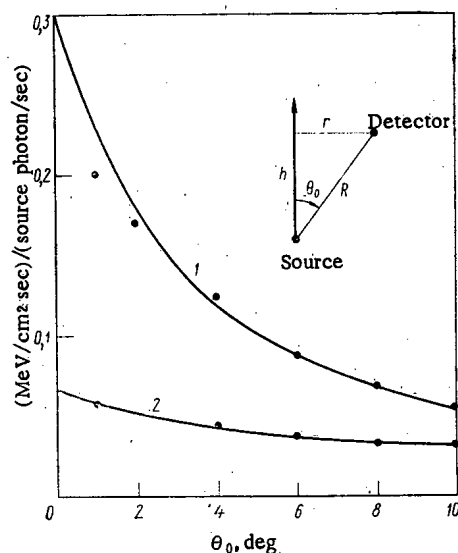


Fig. 1. Spatial distribution of intensity of scattered radiation from a point monodirectional source in lead for $\mu(E_0)R = 4$; $E_0 = 0.279$ MeV. 1) Taking account of coherent scattering; 2) without taking this into account; —) calculated by formula; ○) calculated by Monte Carlo method.

LITERATURE CITED

1. V. G. Zolotukhin et al., Proceedings of an SEV Symposium on the Problems of Shielding against Penetrating Reactor Radiations [in Russian], Vol. 4, NIAR, Melekess (1969), p. 5.
2. A. M. Kol'chushkin and V. V. Uchaikin, Izv. VUZ. Fiz., No. 1 (1971), p. 107.

LETTERS TO THE EDITOR

HEAT EXCHANGE IN THE INTERPIPE SPACE OF
THE INTERMEDIATE HEAT EXCHANGER OF A
BOR-60 INSTALLATIONV. I. Kondrat'ev, L. K. Krupkin,
and V. F. Masnyi

UDC 621.039.526

Countercurrent motion of the sodium coolant for the primary loop (in the interpipe space) and the sodium coolant for the secondary loop (inside of the pipes) takes place in the intermediate heat exchangers (IHE) of a BOR-60 installation.

The coefficient of heat transfer in an IHE was investigated for a constant flow rate, equal to $Q_2 = 300 \text{ m}^3/\text{h}$, of the coolant in the secondary loop and a flow rate which varied from 30 to 500 m^3/h , at 100, 150,

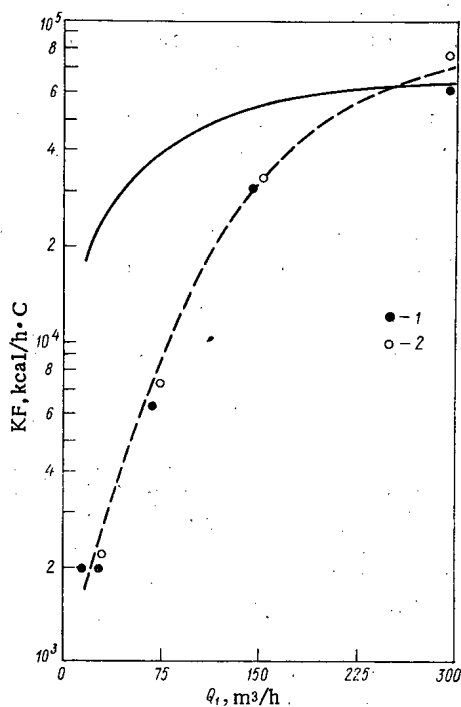


Fig. 1

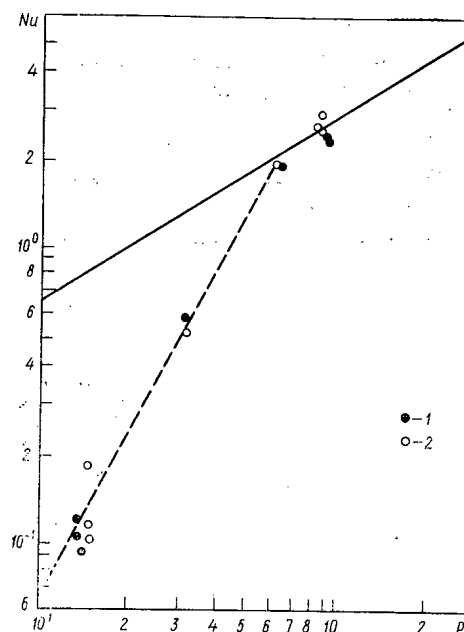


Fig. 2

Fig. 1. Variation in the coefficient of heat transfer in the intermediate heat exchanger of a BOP-60 installation (KF) with the coolant flow rate in the primary loop (Q_1): —) theoretical; ---) experiment; 1) primary loop IHE; 2) secondary loop IHE.

Fig. 2. Dependence of the coefficient of heat transfer in the interpipe space of the intermediate heat exchanger of a BOR-60 installation on the Peclet number (Pe): —) theory; ---) experiment; 1) primary-loop IHE; 2) secondary-loop IHE.

Translated from *Atomnaya Energiya*, Vol. 36, No. 4, pp. 305-306, April, 1974. Original article submitted May 10, 1973.

© 1974 Consultants Bureau, a division of Plenum Publishing Corporation, 227 West 17th Street, New York, N. Y. 10011. No part of this publication may be reproduced, stored in a retrieval system, or transmitted, in any form or by any means, electronic, mechanical, photocopying, microfilming, recording or otherwise, without written permission of the publisher. A copy of this article is available from the publisher for \$15.00.

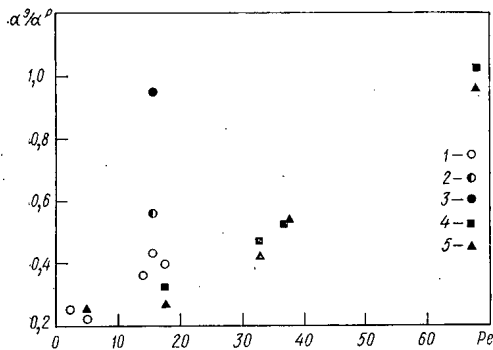


Fig. 3. Comparison of the experimental and theoretical values of the coefficient of heat exchange in the interpipe space of the intermediate heat exchanger of a BOR-60 installation:

$$\left. \begin{aligned} 1 - \Delta t_1 = 100^\circ \text{C} \\ 2 - \Delta t_1 = 150^\circ \text{C} \\ 3 - \Delta t_1 = 200^\circ \text{C} \end{aligned} \right\} Nu_1 = 61.2 Pe^{0.5} \left(\frac{\alpha_1}{\alpha_2} \right)^{1.2}, [2];$$

$$4 - Nu_1 = 8 \cdot Pe^{0.5} \cdot d_{r1}/l_1, [3];$$

$$5 - Nu_1 = 8[d_{r1}/l_1 + 0.027(x-1.1)^{0.46} \cdot Pe^{0.5}], [1] \quad \Delta t_1 = 100^\circ \text{C}.$$

and 200°C temperature drops in the primary loop. The procedure for the experimental investigation and the analysis of the results is similar to that discussed in [1].

The nature of the variation in the heat-transfer coefficient KF with the coolant flow rate in the primary loop is shown in Fig. 1. Here also, there is represented the theoretical curve, obtained from the equations:

$$KF = \frac{F}{\frac{1}{\alpha_1} + \frac{d_e}{2\lambda_{st}} \ln \left(\frac{d_e}{d_{in}} \right) + \frac{d_{in}}{d_e} \cdot \frac{1}{\alpha_2}};$$

$$\alpha_1 = (8\lambda_1/d_{r1}) Pe_1^{0.6} [d_{r1}/l_1 + 0.027(x-1.1)^{0.46}];$$

$$\alpha_2 = \frac{\lambda_2}{d_{r2}} \cdot (5 + 0.025 \cdot Pe_2^{0.8})$$

(subscript 1 refers to the primary and subscript 2 refers to the secondary loop).

As follows from the graph, the experimental points are found below the theoretical ones for coolant flow rates in the primary loop lower than 300 m³/h. An analysis of the same results, separating out the heat exchange in the interpipe space, was made in dimensionless form and is presented in Fig. 2. When the value of the dimensionless number $Pe_1 \approx 100$, the experimental and theoretical values of the Nusselt number are in better agreement.

Kirillov et al. [1], who formulated the equation mentioned above for calculating the coefficient of heat exchange in the interpipe space α_1 , recommend that one utilize it for values of $Pe > 200$. For the heat exchanger under consideration, the value of $Pe_1 = 200$ is a maximum; in practice, its operating range lies in the 60-100 interval. One can explain the lower values of the Nusselt number as compared to the calculated values for $Pe_1 < 60$ by the absence of thermal and hydrodynamic stabilization of the coolant flow with the given parameters. This was clearly shown by comparing the conditions when $Pe_1 = 16$ and the temperature drops between the entrance and exit of the interpipe bundle of the heat exchanger are equal to $\Delta t_1 = 100, 150$, and 200°C. From Fig. 3, it follows that a higher value of the heat-exchange coefficient occurs for large drops in the temperature between the entrance and the exit. This can explain the onset of a counter composite convection, leading to better balancing of the temperature over the cross section of the bundle for large values of Δt_1 . The results of processing the experimental data according to the equation for the heat-exchange coefficient in [1-3] are also presented in Fig. 3. The results of the analysis utilizing three equations virtually agree over the range of variation in the Peclet number under consideration.

Thus, better agreement of the experimental results with theory for the coefficient of heat exchange of the intermediate heat exchanger of a BOR-60 installation is obtained when coolant flow rates in the primary loop are higher than 300 m³/h (which corresponds to a value of $Pe_1 \geq 80$) and 300 m³/h in the second. For lower flow rates ($Pe_1 < 80$) in the primary loop (interpipe space), the value of the experimental heat-exchange coefficient is lower than the theoretical value.

LITERATURE CITED

1. P. L. Kirillov and M. Ya. Suvorov, in: Liquid Metals [in Russian], P. L. Kirillov, V. I. Subbotin, and P. A. Ushakov (editors), Atomizdat, Moscow (1967), p. 194.
2. V. M. Borishanskii et al., Liquid-Metal Coolants [in Russian], Second Edition, Atomizdat, Moscow (1967), p. 209.
3. V. I. Subbotin et al., III Geneva Conference on the Peaceful Uses of Atomic Energy, Report No. 328 (1964).

FORMING OF THE STRUCTURE OF VIBRATION-COMPACTED URANIUM DIOXIDE IN FUEL ELEMENTS DURING FULL-SCALE TESTS IN A FAST BOR-60 REACTOR

E. F. Davydov, V. N. Syuzev,
A. A. Petukhov, and M. M. Antipina

UDC 621.039.548

An experimental assembly of fuel elements, in which uranium dioxide, including that produced electrochemically, is compacted by a vibration process up to 8.0, 8.5, and 9.0 g/cm³, is irradiated in a BOR-60 reactor until ~2.3% of the heavy atoms are depleted.

The designs of the assembly, fuel elements, and materials utilized, except for the fuel, did not differ from the standard assemblies of a BOR-60 [1]. In order to eliminate possible movement in the fuel element, the vibration-compacted uranium dioxide was restrained on both sides by porous nickel plugs. The fuel elements were assembled in a 37-element bundle.

The power output of the reactor was built up gradually (Fig. 1, Table 1).

As a result of initial studies of the assembly and the fuel elements, their satisfactory conditions after irradiation is established. One did not observe changes in the form, or disruptions in the rectilinearity and airtightness of the fuel elements.

Metallographic analysis of the fuel at various densities enabled one to establish the following distinctive features: the usual, for uranium dioxide, central cavity and a three-zone structure were formed in all of the fuel elements; an axial cavity, ~1.5 mm in diameter, is uniform along the entire height of the active

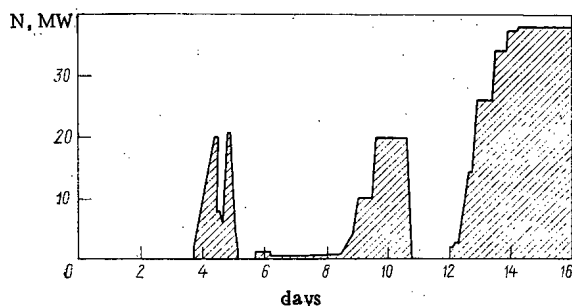


Fig. 1

Fig. 1. Graph of the output of a BOR-60 reactor at a power of 38 MW.

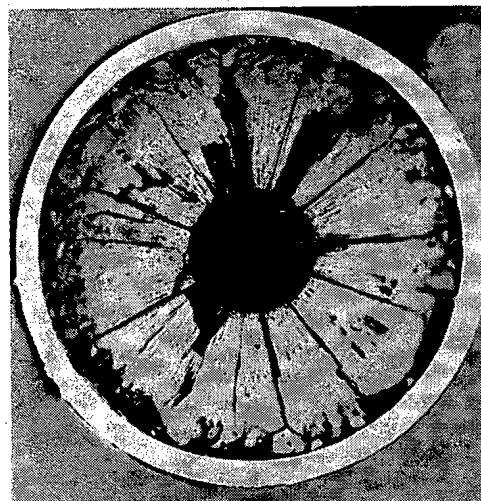


Fig. 2

Fig. 2. Macrostructure of center section of fuel element with vibration-compacted uranium dioxide at a density of 9.0 g/cm³.

Translated from *Atomnaya Energiya*, Vol. 36, No. 4, pp. 306-308, April, 1974. Original article submitted July 18, 1973; revision submitted October 12, 1973.

© 1974 Consultants Bureau, a division of Plenum Publishing Corporation, 227 West 17th Street, New York, N. Y. 10011. No part of this publication may be reproduced, stored in a retrieval system, or transmitted, in any form or by any means, electronic, mechanical, photocopying, microfilming, recording or otherwise, without written permission of the publisher. A copy of this article is available from the publisher for \$15.00.

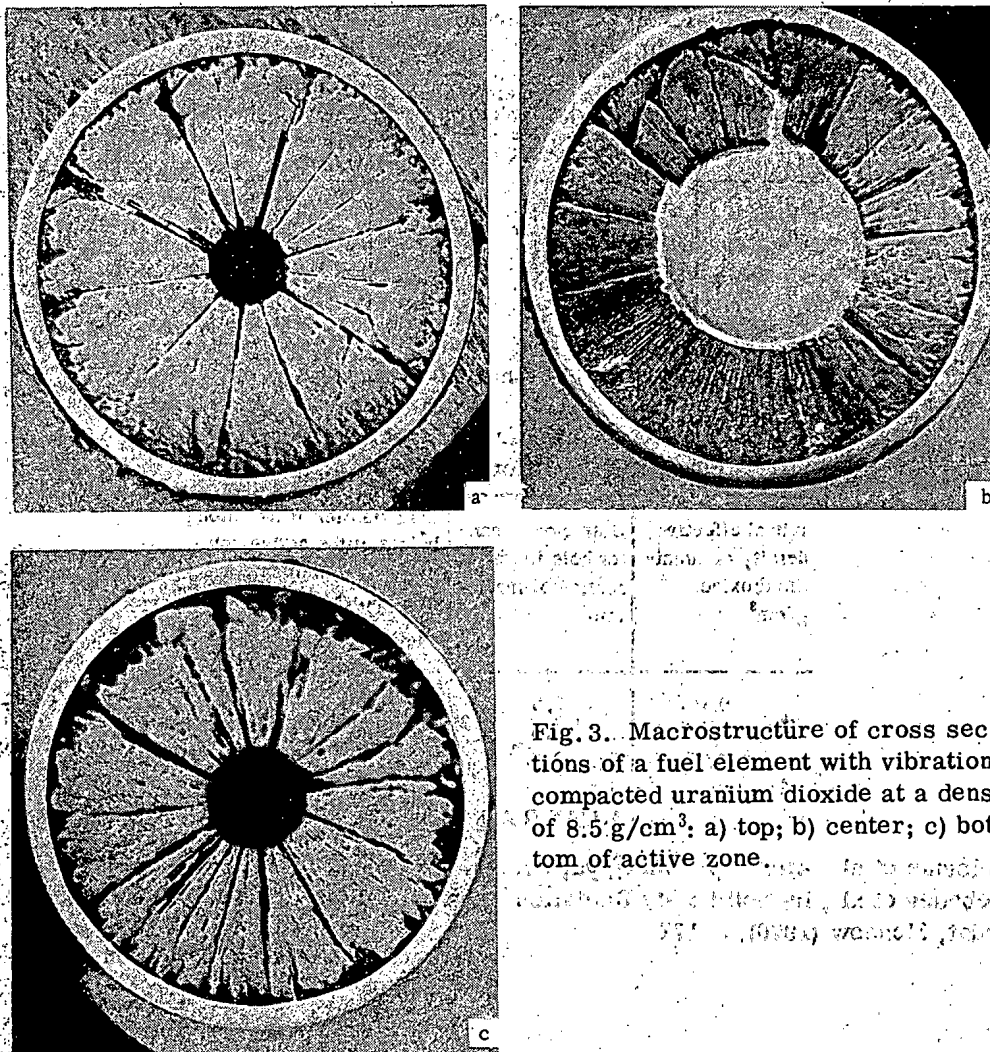


Fig. 3. Macrostructure of cross sections of a fuel element with vibration-compacted uranium dioxide at a density of 8.5 g/cm^3 : a) top; b) center; c) bottom of active zone.

zone in fuel elements with a uranium dioxide density of 9.0 g/cm^3 . The zone of columnar grains occupies $\sim 75\%$ of the diameter of the core, the remaining 25% represents the zones of equiaxial grains and the original structure; there is a central cavity, which is nonuniform along its height, whose diameter amounts to $\sim 2.6 \text{ mm}$ at the mid-section of the core, in fuel elements with a density of 8.5 and 8.0 g/cm^3 (both the baked and that obtained by electrochemical means). The zone of columnar grains extended over more than 90% of the area of the cross section of the core. Less than 10% occurs in the zone of equiaxial grains and the original structure.

The characteristic cross sections of these fuel elements are shown in Figs. 2 and 3. Similar structures of vibration-compacted uranium dioxide after irradiation are described in [2].

It is established by the methods of quantitative metallography and γ -transillumination that, in fuel elements with uranium dioxide of 8.0 and 8.5 g/cm^3 density, the nonuniformity of the central cavity is a consequence of axial mass transfer of fuel from the center to the ends of the active zone. The quantities which characterize the axial mass transfer in fuel elements with variable fuel density are shown in Table 2.

The character of the mass transfer in fuel elements with an effective density of 8.0 and 8.5 g/cm^3 (decrease at the center and an increase at the ends of the active zone) enables one to conclude that the redistribution of the uranium dioxide is connected with an initially high temperature level at the center of the fuel element and results in a vapor phase in the field of the axial temperature gradient. Axial mass transfer is absent in fuel elements with an effective density of 9.0 g/cm^3 for a prescribed range of the reactor's power output; such fuel elements can be recommended for further tests.

TABLE 1. Thermal Characteristics of an Assembly of Fuel Elements Containing Vibration-Compacted Uranium Dioxide

Reactor power, MW	Assembly power, kW	Temperature of sodium at assembly exit, °C*	Maximum specific load of fuel elements, W/cm	Maximum temperature of jackets, °C
10	136	381	140	413
20	273	433	209	460
30	409	485	313	525
40	545	538	418	584
42	573	550	449	600

*Temperature of sodium at reactor entrance is 330°C.

TABLE 2. Mass Transfer of Uranium Dioxide along the Height of the Fuel Core

Initial effective density of uranium dioxide, g/cm ³	Diameter of center hole in mid-section of fuel, mm	Mass transfer of fuel along height of the active zone of the fuel element (at selected cross sections), %		
		Top	Center	Bottom
9,0	1,5	0	0	0
8,5	2,5	+12	-16	+12
8,0	2,6	+10	-6	+10

LITERATURE CITED

1. I. S. Golovnin et al., *Atomnaya Energiya*, 30, No. 2, 216 (1971).
2. I. G. Lebedev et al., in: *Solid State Radiation Physics and the Reactor Study of Materials* [in Russian], Atomizdat, Moscow (1970), p. 171.

EFFECT OF THERMAL CONDUCTIVITY OF SURFACE LAYER ON CONTACT THERMAL RESISTANCE

V. V. Kharitonov, L. S. Kokorev,
and Yu. A. Tyurin

UDC 621.039.517

The contact thermal conductivity α_c W/m²·deg is one of the important characteristics of heat exchange in fuel elements and anode packets of thermionic converters. The quantity α_c may decrease appreciably during the formation of oxide films on adjacent metal surfaces [1] and may increase considerably if layers of metals with high thermal conductivity are deposited on the surfaces in contact [2]. That part of α_c which depends on the surface properties of the materials is determined by the density of the contact spots n (m⁻²) and the resistances R_1 and R_2 (deg/W) of constriction of the lines of heat flux to these spots in both bodies [1-3]:

$$\alpha_c = n / (R_1 + R_2). \quad (1)$$

In the present work a most complete calculation of R is done with the purpose of obtaining valid recommendations for the choice of the optimum thickness of the coatings and for estimates of α_c in the presence of oxides and other surface layers.

In one of the contacting bodies we separate out an equivalent cell in the form of a cylinder of height equal to the thickness of the body L and diameter equal to the mean distance between the contact spots $2b$ determined from the density of the spots from the formula $n\pi b^2 = 1$. The upper surface is cooled by the heat-transfer agent with heat-transfer coefficient α . Heat is supplied to the cell from below through a contact spot of radius a uniform density $Q/\pi a^2$. The surface layer of thickness δ has thermal conductivity λ_0 different from the thermal conductivity of the main material λ .

By definition the thermal resistance of constriction is

$$R = \Delta T / Q,$$

where ΔT is the desired increase of temperature thrust in the cell due to the discrete nature of the spots; Q is the flow rate of heat across the cell in W. The formulated problem (Neumann boundary-value problem) is solved by the method separation of variables as in [3]. The temperature fields in the layer and the basic material are "joined" at their boundaries by equating the temperatures and the fluxes. The final solution is of the form

$$R = \frac{\psi}{4a\lambda}; \quad \psi = \frac{16}{\pi\eta} \sum_{k=1}^{\infty} \frac{J_1^2(\mu_k \eta)}{\mu_k^3 J_0^2(\mu_k)} \omega_k; \quad \omega_k = \frac{\frac{\lambda}{\lambda_0} \left(\varepsilon_k \operatorname{th} \mu_k \frac{\delta}{b} - 1 \right) \operatorname{th} \mu_k \frac{\delta}{b} + \left(\operatorname{th} \mu_k \frac{\delta}{b} - \varepsilon_k \right)}{\frac{\lambda_0}{\lambda} \left(\operatorname{th} \mu_k \frac{\delta}{b} - \varepsilon_k \right) \operatorname{th} \mu_k \frac{\delta}{b} + \left(\varepsilon_k \operatorname{th} \mu_k \frac{\delta}{b} - 1 \right)}; \quad (2)$$

$$\varepsilon_k = \frac{\operatorname{Bi} \operatorname{th} \mu_k \frac{L}{b} + \mu_k \frac{L}{b}}{\operatorname{Bi} + \mu_k \frac{L}{b} \operatorname{th} \mu_k \frac{L}{b}}; \quad \operatorname{Bi} = \frac{\alpha L}{\lambda}; \quad \eta = \frac{a}{b}.$$

Here μ_k are the roots of the Bessel function $J_1(\mu_k) = 0$.

In the absence of the layer ($\delta = 0$ or $\lambda_0 = \lambda$) $\omega_k = \varepsilon_k$; then (2) coincides with the solution given in [3]. For appreciable thickness of the body ($L > b$) $\varepsilon_k = 1$. In this case even in the absence of the layer $\alpha_k = 1$ and resistance (2) can be approximately expressed by the formula:

$$R = \frac{c(1-a/b)^{3/2}}{4a\lambda}; \quad c = \frac{8}{\pi} \int_0^{\infty} \frac{J_1^2(x)}{x^2} dx = \frac{32}{3\pi^2}. \quad (3)$$

Translated from *Atomnaya Energiya*, Vol. 36, No. 4, pp. 308-310, April, 1974. Original article submitted June 25, 1973.

© 1974 Consultants Bureau, a division of Plenum Publishing Corporation, 227 West 17th Street, New York, N. Y. 10011. No part of this publication may be reproduced, stored in a retrieval system, or transmitted, in any form or by any means, electronic, mechanical, photocopying, microfilming, recording or otherwise, without written permission of the publisher. A copy of this article is available from the publisher for \$15.00.

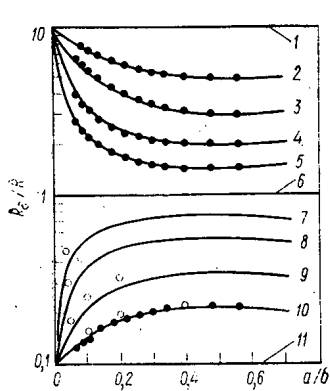


Fig. 1

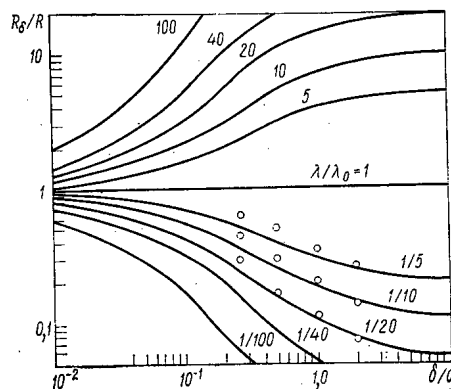


Fig. 2

Fig. 1. Dependence of R_δ/R on a/b for $b = \text{const}$ and $L = \infty$ obtained from Eq. (2): (●) experiment on USM-1; (○) approximate computation from [2]: 1-5) for $\lambda/\lambda_0 = 10$; 7-11) for $\lambda/\lambda_0 = 0.1$; 1, 11) $\delta/b = \infty$; 2, 10) $\delta/b = 0.1$; 3, 9) $\delta/b = 0.05$; 4, 8) $\delta/b = 0.1$; 5, 7) $\delta/b = 0.01$; 6) $\delta/b = 0$.

Fig. 2. Dependence of R_δ/R on δ/a for $b = \infty$, $L = \infty$ (4): (○) approximate computation from [2] for $a/b = 0.05$.

with a good accuracy. Under the condition of constancy of the temperature in the spot $c = 1$. It can be shown that for $a = \text{const}$ the constriction function ψ [see (2)] has a weak dependence on the relative area of the actual contact $\eta^2 = (a/b)^2$, when this area is small. In the range $\eta < 0.1$, which is of practical interest, this makes it possible to express the ratio of the resistance R_δ (in the presence of the layer) to the resistance R (without the layer) [see (3)] for $b \gg a$ in the form

$$\frac{R_\delta}{R} = \frac{3\pi}{4} \int_{\pi\eta}^{\infty} \frac{J_1^2(x)}{x^2} \omega(x) dx. \quad (4)$$

Here we have made use of the asymptotic properties of Bessel functions: $J_0(\mu_k) \rightarrow \sqrt{2/\pi\mu_k}$, $\mu_k \rightarrow k\pi$; $x = k\pi\eta$.

In the limit $\eta = 0$ ($b = \infty$) integral (4) is the exact solution. Similarly, for $b = \text{const}$ and $a \rightarrow 0$ the ratio R_δ/R can be expressed in terms of an integral over k . In the range $0.3 < \eta < 0.7$ the series in (2) is mainly determined by the first term; therefore here $R_\delta/R = \omega_1$. The complete range of R_δ/R is from 1 to λ/λ_0 .

The results of a numerical computation* of R_δ/R and simulation on a USM-1 analog computer are given in Figs. 1 and 2. The results in Fig. 2 (computation from formula (4)) are approximately described by the formulas:

$$\frac{R_\delta}{R} = \frac{1 + (\lambda/\lambda_0) \text{th}(\delta/ma)}{1 + (\lambda_0/\lambda) \text{th}(\delta/ma)}; \quad m = \begin{cases} 1, & \lambda_0 < \lambda; \\ 1.5, & \lambda_0 > \lambda, \end{cases} \quad (5)$$

which can be recommended for engineering estimates; the error does not exceed 30%.

As seen from the figures the constriction resistance is completely determined by the surface layer, when its thickness is greater than the radius of the contact spot a . In the contact of rough surfaces $a \approx 30 \mu$ [1, 4, 5]; therefore a coating of a few tens of microns thickness will noticeably change R , which has been repeatedly observed in experiments [6, 7]. However, for a real contact (for example, of the fuel with the casing of the fuel element) R is mainly determined by the large-scale roughnesses (for example, the waviness [1, 4]). Here a reaches a value of a few fractions of a millimeter and larger, so that coatings of the thicknesses mentioned above are ineffective.

Oxide layers on the surface of metals have a thickness of not more than 1μ . Their thermal conductivity is smaller than that of metals by a factor of 3-30. Therefore the contact resistance has a weak dependence on the thermal conductivity of the oxide layer for the contact of wavy or even rough surfaces.

The mechanical properties of the surface layers can have a large effect on α_c , since they determine the density of the contact spots (see (1)). For example, in conditions of plastic deformations of rough surfaces n is related to the pressure p and the hardness H of the more plastic surface through the well-known

*Kummer rule of improvement of convergence of series and integrals was used in the computations.

formula [5]

$$n = p/\pi a^2 H,$$

which together with (1) permits to estimate the effect of the surface layer on the thermal conductivity of the contact from experimentally measured values of H .

LITERATURE CITED

1. K. Sanokawa, Bull. ISME, 11, 253 (1968).
2. B. Mikich and D. Karnaskiali, Teploperedacha (Heat transfer), No. 3, 168 (1970).
3. V. V. Kharitonov, L. S. Kokorev, and V. K. Yurenkov, Atomnaya Energiya, 32, 471 (1972).
4. A. Klauzing and B. Chao, Teploperedacha (Heat transfer), No. 3, 38 (1965).
5. N. B. Demkin, Contact of Rough Surfaces, Nauka, Moscow (1970).
6. B. A. Mal'kov and P. A. Dobashin, Inzh. Fiz. Zh., 17, 871 (1969).
7. V. K. Koshkin, Yu. I. Danilov, et al., Izv. VUZ. Aviatekhnika, No. 3, 3 (1971).

EFFECT OF DEGREE OF PERFECTION OF STRUCTURE OF GRAPHITE ON THE CHANGES OF ITS DIMENSIONS DURING NEUTRON IRRADIATION

Yu. S. Virgil'ev, I. P. Kalyagina,
and V. G. Makarchenko

UDC 66.017:620.1

The changes of the dimensions of carbonic materials during neutron irradiation have been investigated in many studies. One of the most important factors determining the dimensional stability is the temperature of processing of the carbonic material, since it determines the degree of perfection of the crystal-line structure.

It has been established that an increase of the temperature of processing lowers the level of radiation compression of the dimensions of graphite samples during high-temperature irradiation. Data on irradiation of model materials, i.e., pyrocarbon differing in the degree of perfection of the lattice, and also of anisotropic reactor materials [1, 2] show that the effect of dimensional changes (increase along the c-axis and compression in the plane of the base) gets weaker as the degree of perfection of the crystal increases. However, a quantitative theory of this process has not yet been developed. The qualitative model suggested for carbonic materials on the assumption that during the irradiation processes similar to graphitization processes occur, has not been experimentally verified. The existing quantitative methods determine the dimensional changes of only highly perfect materials.

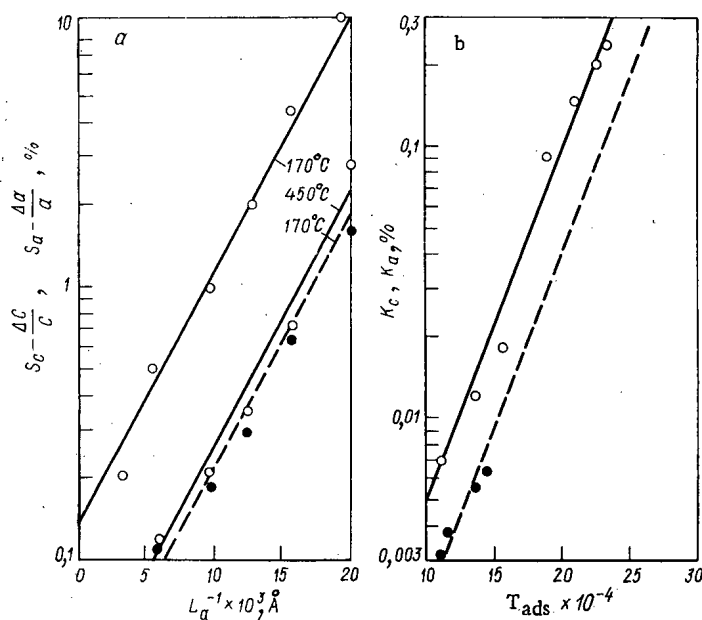


Fig. 1. Dependence of function F on the diameter of crystals (a) and temperature of irradiation (b) for a neutron flux of $1 \cdot 10^{20}$ neutron/cm²: —) direction of c-axis; ---) direction of a-axis.

Translated from *Atomnaya Energiya*, Vol. 36, No. 4, pp. 310-312, April, 1974. Original article submitted June 28, 1973.

© 1974 Consultants Bureau, a division of Plenum Publishing Corporation, 227 West 17th Street, New York, N. Y. 10011. No part of this publication may be reproduced, stored in a retrieval system, or transmitted, in any form or by any means, electronic, mechanical, photocopying, microfilming, recording or otherwise, without written permission of the publisher. A copy of this article is available from the publisher for \$15.00.

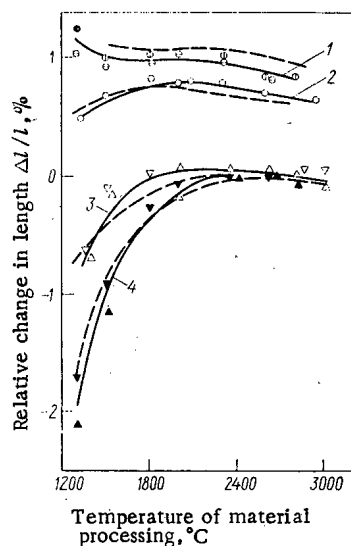


Fig. 2. Dependence of relative change of dimensions of samples of carbonic materials of mark GMZ on temperature of processing for different temperatures and neutron doses ($E \geq 0.18$ MeV) of irradiation: 1) 140°C, $3 \cdot 10^{20}$ neutron/cm²; 2) 200°C, $4 \cdot 10^{20}$ neutron/cm²; 3) 450°C, 4.5 neutron/cm²; 4) 600-650°C, $13 \cdot 10^{20}$ neutron/cm²; ---) computation; —) experiment.

TABLE 1. Change in the Characteristics of the Samples in the Process of Thermal Processing

Temperature of processing, °C	Coefficient of thermal expansion, 1/deg*	Dimensions of the regions of x ray coherent scattering, A		Degree of graphitization $\gamma = \frac{I_{(112)}}{I_{(110)}}$
		along c axis	along a axis	
1300	—	40	70	—
1500	—/5,9	75	90	—
1800	6,6/6,2	80	130	—
2000	6,5/6,2	120	285	—
2100	—	150	450	—
2300	6,1/5,8	190	660	0,20
2600	5,3/4,9	215	> 1000	0,35
2800	5,8/5,3	215	> 1000	0,40
3000	5,4/5,1	240	> 1000	0,54

* Measured at temperature of 20-500°C.

In view of this the method of determining a quantitative relation of the dimensional changes of carbonic materials with the characteristics of their crystalline structure acquires large significance. This method is based on the assumption that in imperfect carbonic materials characterized by the existence of packets of graphite-like layers a large number of defects with smaller dimensions of the clusters are observed as a result of irradiation; this is explained by the presence of imperfections containing irradiation defects in the structure. Such a model is very useful for an estimate of the dimensional changes of insufficiently graphited carbonic materials, since it permits to use the well-known quantitative methods which are valid for highly crystalline materials close to single-phase materials [3].

It is known that the change of the form of graphite samples is determined from the change of the dimensions of individual crystallographic regions in the directions of c and a axes (S_c , S_a respectively). The quantities S_c and

S_a are commensurate with the rate of change of the dimensions of a monocrystal; the relative changes of the dimensions of a polycrystal $y_{||}$, y_{\perp} and monocrystal S_c , S_a are linearly related to each other with coefficients of proportionality k_1 , k_2 , k_3 , k_4 called the accommodation coefficients which take account of the specific characteristics of the given material (porosity, texture, etc.):

$$\begin{aligned} y_{||} &= k_1 S_c + k_2 S_a, \\ y_{\perp} &= k_3 S_c + k_4 S_a. \end{aligned} \quad (1)$$

For carbonic materials in the presence of not very high doses, and for highly perfected pyrographite a large levels of irradiation an equality of the relative change of the parameters and the dimensions of the crystallographic regions is observed. However, in the general case [2]

$$S_c > \Delta c/c, \quad S_a > \Delta a/a,$$

therefore we can write

$$S_c = \Delta c/c + F_1, \quad S_a = \Delta a/a + F_2,$$

where F_1 , F_2 are functions of the dose and the temperature of irradiation, describing the deformations of the crystals as a result of appearance of the clusters.

In the computation of the quantities S_c and S_a from the change of the form of samples differing in the degree of perfection a certain divergence of the results is obtained. It becomes especially noticeable if

low-perfection carbonic materials are used instead of graphite. In this case S_c and S_a decrease sharply as the degree of perfection of the material irradiated in identical conditions is reduced.

Figure 1 shows the dependence of function F on the temperature of irradiation and the diameter of the region of coherent scattering (RCS), obtained from an analysis of published data. By plotting the dependence of $S_c - \Delta c/c$ and $S_a - \Delta a/a$ on the integral flux of neutrons for fixed temperature and dimension of RCS we find that the function F is proportional to the dose raised to power 1.6.

The dependences shown in Fig. 1 permit to approximate the function F by the expression

$$F = Kx^{1.6} \exp\left(\frac{E}{RT}\right) \exp\left(\frac{B}{L_a}\right), \quad (2)$$

where L_a is the dimension of the region of coherent scattering determined by x-ray method and K , B are constants.

The parameters of Eq. (2) can be estimated from the graphs of Fig. 1. For the direction parallel to the c -axis parameter K is equal to $4 \cdot 10^{-6}$ and $1.6 \cdot 10^{-6}$ for the axis perpendicular to it. The constant $B = 220$; therefore for $L_a > 220 \text{ \AA}$ the exponent does not decrease very appreciably, while for $L_a < 220 \text{ \AA}$ it increases significantly.

Equations (1) and (2) make it possible to estimate the dependence of the dimensional changes of carbonic materials characterized by a certain value of the diameter of the crystals on the conditions of irradiation, i.e., the dose and the temperature. A comparison of the computational results and experimental data was carried out on the basis of the investigations of radiational dimensional stability; of samples of mark GMZ material obtained by processing at temperatures of 1300-3000°C.

The coefficient of thermal expansion of the samples changed in the range of about 15-20% (the accuracy of determination $\pm 0.3 \cdot 10^{-6} \text{ 1/deg}$); the degree of perfection was changed appreciably (see Table 1).

The tests were conducted at temperatures of 140-650°C and neutron doses of irradiation up to $1.3 \cdot 10^{21}$ neutron/cm ($E \geq 0.18 \text{ MeV}$). At low temperatures, when there is a homogeneous nucleation of the defects (in artificial graphites up to 300°C), the changes of the dimensions are essentially independent of the degree of perfection of the material if the temperature of its processing exceeds 1500°C; all the samples increase almost equally (Fig. 2). A distinguishing feature of the samples after processing at 1300°C is a somewhat larger value of the growth at an irradiation temperature of 140°C; at an irradiation temperature of 200-250°C this growth already becomes smaller than the average change of dimensions of samples processed at 1500-3000°C. With further increase of the irradiation temperature a shrinkage of the samples processed at lower temperatures is observed.

If the temperature of irradiation exceeds 300°C, the changes of the dimensions depends substantially on the degree of perfection of the material. At 600-650°C materials with three-dimensional ordering of the crystal lattice, i.e., materials graphitized at temperatures higher than 2300°C, were found to be stable.

The obtained experimental results agree satisfactorily with the results of the computations done with the equations presented in this article.

LITERATURE CITED

1. J. Price, Influence of Microstructure on Irradiation-Induced Dimensional Changes in Annealed Oriented Pyrocarbons, Rept. NG-2, Gatlinburg, Tennessee (1973).
2. J. Simmons et al., Third International Conference on Peaceful Uses of Atomic Energy, Geneva (1964), p. 163.
3. J. Simmons, Proc. Third Conference on Carbon, Oxford, Pergamon Press (1959), p. 559.

ABSORPTION SPECTRA FOR THIN FILMS OF ZIRCONIUM DIOXIDE

Kh. V. Shalimova, T. Kh. Margulova,
T. I. Malova, M. M. Malov,
and S. M. Klimova

UDC 669.296:669.018.8

Zirconium-niobium alloys are the main structural material for water-cooled-reactor cores. Therefore, it is important to devise methods for increasing these alloys' corrosion resistance. Such methods include processing the alloys with water solutions of complexons during their thermal or radiation-thermal decomposition.

To establish the effect of the complexon on oxide-film growth we studied absorption spectra for layers obtained by oxidizing in water and complexon solution Zr alloys containing 1% Ni which had been annealed at 580°C for 24 h. The samples were oxidized in stainless-steel autoclaves in oxygenless, demineralized water and in water solution of the complexon (Trilon B = 0.5 g/kg) at 120°C (pressure 3 kg/cm²) for 1.5 h and then the temperature was raised to 300°C (pressure 87 kg/cm²) and oxidation continued for 2, 5, and 10 h. The oxide films were separated from the metallic backing by dissolving the metal in 10% bromine solution in amyl acetate at room temperature [2] and then were bonded to a quartz plate. The films' optical absorption was studied at room temperature on a spectrometer SF-8 in the wavelength interval 0.2-2.5 μ [2].

The oxide-film thickness on the Zr alloy was calculated from the interference diagram occurring in the reflection. The refraction coefficient was taken as 2; the phase shift at the boundary was disregarded, since the beam incidence angle on the sample was close to normal [3, 4]. The calculation showed that on samples oxidized in water solution of complexon and in water at 300°C for 2 and 5 h there form films 0.08-0.12 and 0.17-0.21 μ thick, respectively.

Figure 1 shows the absorption spectra for the Zr oxide films. As it turned out, the absorption spectra for zirconium-oxide films, obtained in water and in complexon solution, with treatment duration 5 h, were

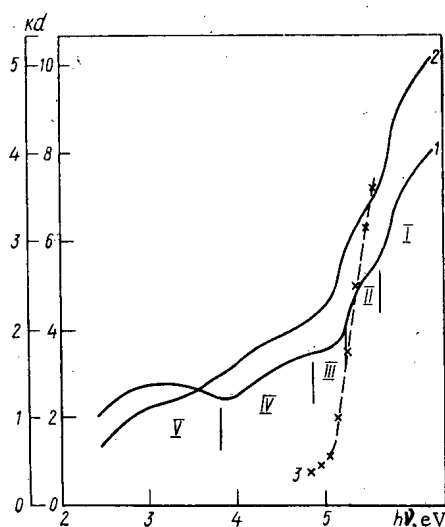


Fig. 1. Absorption spectra for films obtained by oxidizing Zr alloy containing 1% Ni in water and in complex solution, with oxidation duration 5 and 10 h, and also for films coated by the ion-plasma method (right-hand scale for curve 3).

Translated from *Atomnaya Energiya*, Vol. 36, No. 4, pp. 312-313, April, 1974. Original article submitted June 29, 1973; revision submitted January 3, 1974.

© 1974 Consultants Bureau, a division of Plenum Publishing Corporation, 227 West 17th Street, New York, N. Y. 10011. No part of this publication may be reproduced, stored in a retrieval system, or transmitted, in any form or by any means, electronic, mechanical, photocopying, microfilming, recording or otherwise, without written permission of the publisher. A copy of this article is available from the publisher for \$15.00.

identical (curve 1). Curve 2 corresponds to the absorption spectrum for films obtained after 10 h treatment in water solution of the complexon. Figure 1 also shows the absorption spectrum for an oxide film deposited on a quartz backing by ion-plasma vaporization of zirconium in an oxygen-argon atmosphere (curve 3); this spectrum agrees completely with the absorption spectrum for monoclinic ZrO_2 [2]. The forbidden-band width, determined from the intersection of the x-axis with a straight line tangent to the absorption curve [5], is 4.99 eV.

Five regions are observed in the absorption spectrum for zirconium-oxide films obtained in water and in complexon solution (see Fig. 1, curves 1 and 2): I) 200-225 nm; II) 225-235 nm; III) 235-255 nm; IV) 255-325 nm; V) 325-500 nm. Each region contains an inflection point as follows: I) 5.82 eV (213 nm); II) 5.41 eV (229 nm); III) 4.99 eV (248.4 nm); IV) 4.46 eV (278 nm); V) 3.1 eV (400 nm).

The absorption region 200-225 nm for zirconium-oxide film produced in water and in complexon solution agrees with the absorption for monoclinic HfO_2 [5]. This fact, and also the presence of hafnium (0.03-0.04%) in the Zr alloy used, gives us a basis for assuming that this absorption region for Zr oxide films is determined by the presence of HfO_2 , possibly a solid solution of Hf and Zr oxides.

A clear maximum appears at 229 nm on the absorption curves for Zr oxide films produced in water and in complexon solution. Such an absorption band is characteristic for thin (300 Å) ZnO_2 films produced by oxidizing Zr in vapor at 500°C and pressure 1 kg/cm² [3]. Wilkins affirms that this absorption region is determined by a nonstoichiometric oxide present in the ZrO_2 film. However, it is more correct to ascribe this absorption to cubic ZrO_2 , which [6] arises in a zirconium alloy at the first stages of its oxidation.

The absorption region 235-255 nm for Zr oxide films produced in water and in complexon solution corresponds to the long-wave absorption region for a layer deposited by the ion-plasma method (see Fig. 1); this gives one a basis for considering this region to be related to absorption by monoclinic ZrO_2 .

Thin niobium-oxide films produced by anodizing are characterized by absorption in the wavelength region below 350 nm [7]. Our Zr-alloy samples contained 1% Ni. Therefore, the absorption region 255-325 nm for thin ZrO_2 films produced in water and in complexon solution can be ascribed to NiO absorption, possibly to a solid solution of Ni and Zr oxides with forbidden-band width 4.46 eV.

The absorption region 325-500 nm for Zr oxide films produced in water and in complexon solution should be ascribed to absorption by chromium oxide, since the presence of chromium in these films was established when they were studied on an MAR-1; this is due to using the stainless-steel autoclave.

LITERATURE CITED

1. T. Kh. Margulova, L. V. Ryabova, and T. I. Malova, *Teploenergetika*, No. 7, 83 (1973).
2. R. Salomon et al., *J. Chem. Phys.*, **32**, 310 (1960).
3. N. Wilkins, *Corr. Sci.*, **5**, 3 (1965).
4. N. Wilkins, *Corr. Sci.*, **4**, 17 (1964).
5. J. Bendoraitis and R. Salomon, *J. Phys. Chem.*, **69**, 3666 (1965).
6. E. S. Sarkisov et al., *Atomnaya Energiya*, **5**, 550 (1958).
7. W. Graven et al., *J. Chem. Phys.*, **33**, 954 (1961).

THE PROSPECTS OF RESEARCH ON γ -FIELDS OF
ROCKS AND SOILS ON THE EARTH'S SURFACE
WITH THE AID OF SEMICONDUCTOR DETECTORS

V. A. Ionov, Yu. E. Kazakov,
I. M. Nazarov, S. I. Patrakeev,
V. N. Sorokin, and Sh. D. Fridman

UDC 550.835

The present article discusses the possibility of γ -spectrometry with semiconductors. In this spectrometry, the results of both model measurements, in which volume and film sources are simulated, and measurements of the radioactivity of soils under natural conditions were analyzed [1]. The measurements were made with a coaxial Ge(Li) detector which had a volume of 56 cm³ and was inserted in a radiation shield having a half-angle of 70°. The pulses were registered with a 800-channel amplitude analyzer. The energy resolution of the detector was 4.8 keV at the 1.33 MeV ⁶⁰Co line, when measurements were made with a point source which was located close to the detector housing at a distance of 100 mm from the same. The ratio of the photopeak to the Compton peak was 12.

In measurements of the γ -field of three-dimensional sources, the scattered radiation slightly reduces the "apparent" resolution of the detector [1].

Airborn measurements of γ -spectra were simulated by covering both the volume sources and film sources with 3.8 and 7.3 g/cm² aluminum sheets, which corresponds to heights H = 30 and 57 m of the air-plane [2].

TABLE 1. Counting Rate of Semiconductor Detectors in the Photopeaks of the Uranium and Thorium Series, of K⁴⁰, and of Cs¹³⁷; Data on the Background Counting Rate

E ₀ , MeV	Pulses/min					E ₀ , MeV	Pulses/min				
	n _U ^U	n _{st} ^U U	n _{st} ^U Th	n _{st} ^U K	n _{st} ^U Cs		n _{Th} Th	n _{st} Th Th	n _{st} Th U	n _{st} Th K	n _{st} Th Cs
0,184	0,980	10,61	6,50	15,2	10,8	0,239	1,59	4,56	8,20	12,7	9,82
0,242	0,795	7,75	3,20	10,1	7,7	0,398	0,23	1,39	2,24	4,40	3,30
0,295	1,63	6,95	3,33	9,80	7,50	0,458	0,07	0,70	2,05	2,78	4,45
0,352	2,40	4,65	2,45	8,40	6,0	0,511	0,24	0,86	1,42	3,15	2,22
0,609	2,26	1,78	0,90	3,82	1,57	0,583	0,82	0,78	1,42	3,05	0,63
0,666	0,08	0,77	0,48	1,76	—	0,727	0,10	0,54	0,70	2,02	—
0,769	0,203	0,93	0,44	1,89	—	0,790	0,05	0,29	0,94	1,52	—
0,935	0,12	0,67	0,22	1,73	—	0,860	0,07	0,25	0,58	1,74	—
1,120	0,480	0,61	0,17	2,42	—	0,908	0,26	0,34	0,70	2,08	—
1,238	0,13	0,32	0,18	2,08	—	0,960	0,31	0,27	0,66	2,27	—
1,378	0,15	0,38	0,13	0,42	—	1,580	0,10	0,11	0,16	—	—
1,509	0,06	0,18	0,06	—	—	2,620	0,24	0,008	—	—	—
1,728	0,07	0,07	0,07	—	—						
1,764	0,44	0,13	0,11	—	—						
2,117	0,04	0,03	0,08	—	—						
2,204	0,14	0,03	0,14	—	—						
2,446	0,03	0,007	0,04	—	—						
E ₀ ^K	n ₀ ^K	n _{st} ^K K	n _{st} ^K U	n _{st} ^K Th	n _{st} ^K Cs	E ₀ ^{Cs}	n ₀ ^{Cs}	n _{st} ^{Cs} Cs	n _{st} ^{Cs} U	n _{st} ^{Cs} Th	n _{st} ^{Cs} K
1,46	7,10	4,40	0,25	0,09	—	0,662	42,5	3,9	1,33	0,96	4,40

Translated from Atomnaya Energiya, Vol. 36, No. 4, pp. 313-315, April, 1974. Original article submitted April 25, 1973.

© 1974 Consultants Bureau, a division of Plenum Publishing Corporation, 227 West 17th Street, New York, N. Y. 10011. No part of this publication may be reproduced, stored in a retrieval system, or transmitted, in any form or by any means, electronic, mechanical, photocopying, microfilming, recording or otherwise, without written permission of the publisher. A copy of this article is available from the publisher for \$15.00.

TABLE 2. Radiation Efficiency of the Semiconductor and Scintillation Detectors Used for an Emitting-Absorbing Half-Space

E_0 (MeV)	radiation efficiency		E_0 (MeV)	radiation efficiency	
	Ge(Li) $V = 56$	NaI(Tl) $V = 50$		Ge(Li) $V = 56$	NaI(Tl) $V = 50$
0,3	0,180	0,250	1,5	0,034	0,047
0,5	0,105	0,150	2,0	0,025	0,035
0,7	0,075	0,105	2,5	0,020	0,028
1,0	0,052	0,072	3,0	0,017	0,028

TABLE 3. Relative Mean-Square Errors of the Determination of Concentrations of Natural Radioactive Elements in Soils (10 min measurements)

Detector	H , (g/cm ²)	error ε_q (%)		
		U	Th	K
Ge(Li); $V = 56$ cm ³	0 7,3	30 54	17 25	11 15
NaI(Tl); $V = 50$ cm ³	0 7,3	51 92	32 47	18 25
NaI(Tl); $V = 1800$ cm ³	0 7,3	7,6 12	2,8 4,1	0,8 0,6

The resulting values of the radiation efficiency of our Ge(Li) detector are listed in Table 2 in comparison with the radiation efficiency of a 40 × 40 mm NaI(Tl) crystal.

The mean-square errors σ_{q_j} of the mean weighted concentration \bar{q}_j of an element was determined from measurements of all photopeaks n_{0ij} of the instrument-induced spectrum and can be stated as follows:

$$\sigma_{q_j} = \frac{1}{\sqrt{\sum_{i=1}^h 1/\sigma_{q_{ij}}^2}} \quad (1)$$

The magnitude of the mean-square errors $\sigma_{q_{ij}}$ determined from the i -th photopeak originating from the j -th element which is present in a certain concentration in a mixture with radioactive elements can be calculated with Eq. (1)

$$\sigma_{q_{ij}} = \frac{1}{n_{0ij}} \sqrt{\left(q_i n_{0ij} + 2 \sum_{j=1}^m q_i n_{st, ij} \right) / t} \quad (2)$$

where $n_{st, ij}$ denotes the counting rate of background radiation resulting from the j -th element in the region of the photopeaks n_{0ij} .

Table 3 lists the ε_{q_j} values which were determined in determinations of uranium, thorium, and potassium with the data of Table 1 and with Eqs. (1) and (2). The elements were present in the following average concentrations in the soils [3]: $q_U = 1.8 \cdot 10^{-4}\%$; $q_{Th} = 6.0 \cdot 10^{-4}\%$; and $q_K = 1.4\%$. Table 3 includes for comparison the values ε_{q_j} obtained in measurements with NaI(Tl) scintillation counters having the dimensions 40 × 40 mm or 150 × 100 mm.

It follows from Table 3 by interpolation that, as far as the accuracy of measurements of the concentration of natural radioactive elements is concerned, the semiconductor detector used is equivalent to an

Table 1 lists the counting rates n_0^U in the photopeaks for a large group of monochromatic components of the uranium family ($H = 0$), because the monochromatic components appear clearly in the spectra of the instrument proper. Table 1 includes the counting rates n_{stU}^U of the uranium family, n_{stTh}^U of the thorium family, n_{stCs}^U of a Cs¹³⁷ film source of background radiation (stand) in the region of the photopeaks which result from the scattered γ -radiation of the radioisotopes. All values were obtained for a time $t = 1$ min and with identical uranium concentrations q_U and thorium concentrations q_{Th} amounting to $1 \cdot 10^{-4}\%$, potassium concentrations $q_K = 1.0\%$, and Cs¹³⁷ surface densities $\sigma = 0.1 \mu\text{C}/\text{km}^2$.

Table 1 includes data referring to the thorium family, potassium, and Cs¹³⁷.

The data of Table 1 characterizes the metrological possibilities of using our Ge(Li) detector with its volume of 56 cm³ for measurements of the concentrations of uranium, thorium, and potassium in their natural beds in rocks and soils, and for determining the contamination of locations by artificial radio-isotopes. In particular, the data is the basis for calculating the radiation efficiency and the statistical accuracy of the determinations of the concentrations of radioactive elements.

The following activities were used in the models: $q_U = 3.5 \cdot 10^{-3}\%$; $q_{Th} = 7.6 \cdot 10^{-3}\%$; $q_K = 13.2\%$; and $\eta_{Cs} = 3.5 \text{ C}/\text{km}^2$.

NaI(Tl) crystal scintillation detector with a volume of 150-200 cm³ (70 × 50 mm). Satisfactory accuracy in the determination of uranium concentrations (<15%) with the aid of the Ge(Li) detector can be obtained for t = 50 or 100 min and for H = 0 and 7.3 g/cm², respectively. When the concentration of the radioactive element increases, the accuracy of the measurements increases substantially. Contrary to scintillation spectrometry, when radium is determined in its natural bedding with the aid of semiconductor detectors, the radium determinations can be made directly from the 0.184 MeV radium photopeak [4].

The equipment was used to measure the radioactivity of forest soil in its natural position. Apart from photopeaks which result from the γ -radiation of the natural radioactive elements, photopeaks, which are related to the long-lived fragments of nuclear explosions, appear on the spectrogram measured during 390 min. These fragments are present in the global fallout and are as follows: 0.427, 0.464 MeV (Sb¹²⁵); 0.662 MeV (Cs¹³⁷); 0.724 MeV (Zr⁹⁵); 0.757 + 0.768 MeV (Zr⁹⁵ + Nb⁹⁵); and 0.512 MeV (Ru¹⁰⁶). The radioactivity of this type of soil is low. According to our calculations, $1.6 \cdot 10^{-4}\%$ of equilibrium uranium, $5.3 \cdot 10^{-4}\%$ of equilibrium thorium, and 1.2% of equilibrium potassium are present in the soil. There are 140, 35, and 10 $\mu\text{C}/\text{km}^2$ of Cs¹³⁷, Sb¹²⁵, and Zr⁹⁵ + Nb⁹⁵, respectively, stored in the soil.

LITERATURE CITED

1. R. M. Kogan, I. M. Nazarov, and Sh. D. Fridman, Principles of γ -Spectrometry of Natural Media [in Russian], Atomizdat, Moscow (1960).
2. V. A. Ionov, Atomnaya Energiya, **19**, No. 4, 397 (1965).
3. A. P. Vinogradov, Geochemistry of Rare and Scattered Chemical Elements in Soils [in Russian], Izd. AN SSSR, Moscow (1957).
4. V. A. Ionov et al., in: Spectrometric Methods of Analyzing the Radioactive Contamination of Soils and Aerosols [in Russian], A. N. Silant'ev (editor), Gidrometeoizdat, Moscow (1974).

USING THERMOLUMINESCENCE OF RUBY FOR THE DOSIMETRY OF γ -RADIATION

M. S. Yunusov, A. N. Tsoi,
K. M. Muminkhodzhaev, and V. Ya. Khaimov-Mal'kov

UDC 535.37:548.736.53.07
/98+53.001.5

Investigations of the luminescence properties of synthetic ruby which was irradiated with ionizing radiation [1, 2] have shown that it is possible to use ruby for the dosimetry of pulsed high-energy radiation and for the dosimetry of emergency conditions [3, 4]. A previous communication reported on several dosimetric characteristics of γ -irradiated ruby [5].

The present article provides additional information on dosimetry on the basis of thermoluminescence of ruby.

Thermoluminescence was studied in samples of ruby with various concentrations of admixed chromium. The samples were cut in the form of plates with a diameter of about 10 mm and a thickness of 0.5–4 mm. The dose rate of the γ -radiation from a Co^{60} isotope source was varied within wide limits ($0.1\text{--}3 \cdot 10^3$ rad/sec). The thermal deexcitation of the crystals was recorded with an photoelectric attachment using an FEU-18 photomultiplier; the heating rate was constant and amounted to 0.16 deg/sec.

We studied the dependence of the intensity of ruby thermoluminescence upon the γ -radiation dose and the chromium concentration under various irradiation and measurement conditions. Figure 1 displays the dependence of the relative intensity of thermoluminescence upon the dose in log scale. The dependence is almost linear in the dose interval of $1\text{--}10^4$ rad. When the chromium concentration in the sample varies, a corresponding change in the thermoluminescence intensity is observed, but the ratio of the height of the thermoluminescence peak to the height of the maximum at the saturation dose $D_s \approx 10^6$ rad changes only insignificantly. It follows from Fig. 2 that this ratio is independent of the admixture concentration in the

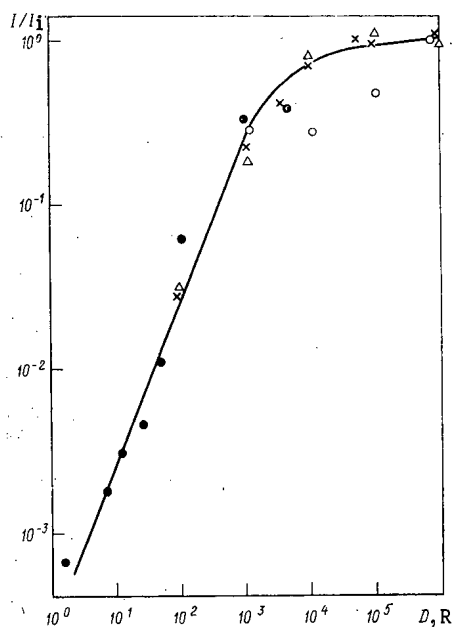


Fig. 1. Dependence of the relative intensity of thermal deexcitation upon the dose in the case of ruby:
●) 0.025% Cr; Δ) 0.05% Cr; \times) 0.1% Cr; \circ) 2% Cr.

Translated from *Atomnaya Energiya*, Vol. 36, No. 4, pp. 315–317, April, 1974. Original article submitted March 6, 1973.

© 1974 Consultants Bureau, a division of Plenum Publishing Corporation, 227 West 17th Street, New York, N. Y. 10011. No part of this publication may be reproduced, stored in a retrieval system, or transmitted, in any form or by any means, electronic, mechanical, photocopying, microfilming, recording or otherwise, without written permission of the publisher. A copy of this article is available from the publisher for \$15.00.

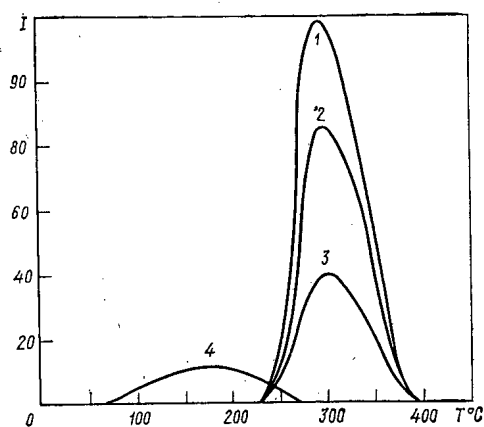


Fig. 2

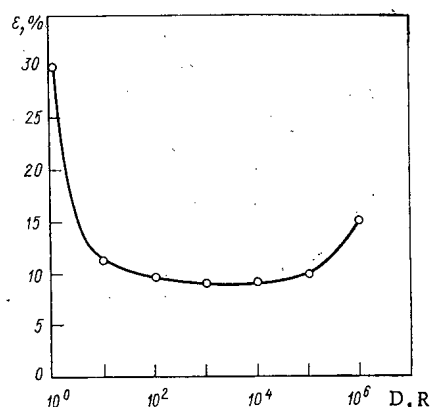


Fig. 3

Fig. 2. Thermal deexcitation curves of ruby containing various admixture concentration; dose 1000 rad: 1) 0.1% Cr; 2) 0.025% Cr; 3) 0.05% Cr; 4) 2% Cr.

Fig. 3. Dependence of the errors upon the dose.

interval 0.025-2%. In the case of a sample with an admixture concentration of 2%, a slight reduction of the relative intensity of thermoluminescence is observed for $D > 10^4$ rad. Figure 2 includes the thermoluminescence curves obtained for various concentrations of admixed chromium at the dose 10^3 rad. The thermoluminescence curves for sample concentrations of 0.025-0.1% form a single, broad band with a deexcitation maximum $T_{\max} \approx 300^\circ\text{C}$. The maximum of the thermoluminescence intensity is observed at a chromium concentration of about 0.1%. The thermoluminescence curve of a ruby which contains 2% chromium and is characterized by the characteristic concentration-dependent attenuation is sharply bent in the low-temperature range with $T_{\max} \approx 175^\circ\text{C}$. Figure 3 shows the curve of standard errors of the dose measurements. The minimum error is characteristic of the region of the linear dependence of the thermoluminescence intensity of ruby upon the dose. For $D < 10$ rad, the error can be reduced by increasing the sensitivity of the recording equipment. In this case, the minimum dose which can be reliably recorded can be reduced to 0.1 rad. The optimal thickness of the sample was selected on the basis of investigations in which the dependence of the thermoluminescence intensity of ruby on the dose, the degree of coloration, the heating conditions, etc., was investigated. The best results were obtained with samples having an admixture concentration of 0.025-0.5% and a thickness of 1-2 mm. When the sample thickness was increased, a decrease in the specific intensity of the thermoluminescence (intensity per unit volume) was observed. This decrease may be related to reabsorption at color centers.

The reduced dependence of the sensitivity upon the radiation energy ($Z_{\text{eff}} \approx 11$) is the great advantage of ruby over other thermoluminescent dosimeters. A long-lasting storage of dosimetric information is guaranteed by the satisfactory depth of the traps in ruby (activation energy ~ 1.5 eV). Thus, when irradiated ruby having an admixture concentration of about 0.1% was stored at room temperature in the dark for 2 months, the dosimetric information did not noticeably change (the reduction of the intensity of the peak amounted to about 4%).

In addition, we investigated the radiation processes in corundum samples containing Co, Mn, Cu, V, and Fe impurities. Compared with these crystals, ruby is characterized by a higher light output and by a position of the peak in the high-temperature range in which thermoluminescence of secondary admixtures does not occur.

Dosimeters on the basis of ruby have a higher light output and neither worse stability nor higher cost than LiF dosimeters [6]. Apart from this, ruby is characterized by high mechanical and chemical resistance and stability of the dosimetric information obtained in repeated use of the dosimeter. These qualities suggest that the thermoluminescent properties of ruby be extensively used in the dosimetry of γ -radiation.

The authors use this opportunity to thank A. G. Sokolova for fruitful discussions of the present work.

LITERATURE CITED

1. C. Philbrick, W. Buckman, and N. Underwood, *Health Phys.*, **13**, No. 7, 798 (1967).
2. M. S. Yunusov, Effect of Penetrating Radiation upon some Physical Properties of Synthetic Ruby [in Russian], Ph. D. Dissertation, Tashkent (1966).

3. J. Halpin and R. Wenzel, *Rev. Scient. Instrum.*, 39, No.8, 1117 (1968).
4. G. Portal et al., in: *Handb. Radiat. Accidents, Proc. Symp.*, Vienna (1969), pp.299-314.
5. M. S. Yunusov et al., in: *Dosimetry and Radiative Processes in Dosimetric Systems* [in Russian], FAN, Tashkent (1972), p.138.
6. R. MacDougall and S. Rudin, *Health Phys.*, 19, No.2, 281 (1970).

INFLUENCE OF NEUTRON IRRADIATION UPON THE CHARACTERISTICS OF FULLY DEPLETED SILICON SURFACE BARRIER DETECTORS

M. É. Kaganskaya, O. P. Fedoseeva,
and B. I. Sinitsyn

UDC 621.382.2

When fully depleted (dE/dx) surface barrier semiconductor detectors are used in fields of neutron irradiation, defects which influence the basic parameters of the detector (inverse current, signal amplitude, energy resolution, etc.) are generated in the structure of the crystal. The overall changes in the electrical and physical parameters of semiconductor surface detectors and drift-diffusion detectors have been rather thoroughly investigated [1-5]. But there exist no publications on investigations of the radiation stability of surface barrier detectors having a geometrical thickness equal to the extension of the sensitive region of the detector.

dE/dx detectors are characterized by the absence of a base layer so that only effects resulting from processes which occur inside the junction and are masked in other detectors by changes in the properties of the base material affect the electrical and physical parameters of the detectors.

We investigated industrially produced fully depleted (dE/dx) silicon surface barrier detectors. The detectors had been made from n-type silicon of the KEM brand with the specific resistivity $\rho = 10,000$ ohm \cdot cm and the lifetime $\tau = 500$ - 1000 μ sec. We investigated ten detectors having a width of 90 - 120 μ of the sensitive region and a sensitive surface area of 0.5 cm^2 . The detectors were irradiated with the neutrons of the beam of the RIZ reactor. The ratio of the flux densities of fast neutrons and γ -radiation at the point of irradiation amounted to ~ 100 , and the density of the neutron flux in the beam as 10^3 neutrons/ $\text{cm}^2 \cdot \text{sec}$. The integral neutron flux was determined with a special sensing instrument of the reactor. The sample temperature did not exceed 30°C during irradiation.

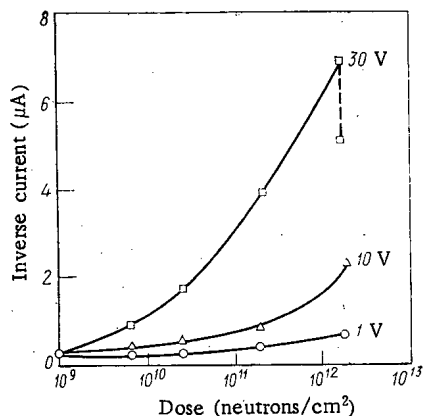


Fig. 1

Fig. 1. Dependence of the inverse current of the detectors upon the dose of the incident neutrons at various voltages.

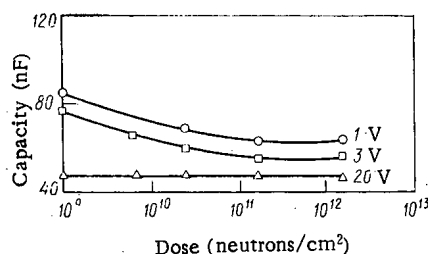


Fig. 2. Dependence of the detector capacitance upon the incident neutron dose at various bias voltages.

Translated from *Atomnaya Energiya*, Vol. 36, No. 4, pp. 317-318, April, 1974. Original article submitted June 25, 1973.

© 1974 Consultants Bureau, a division of Plenum Publishing Corporation, 227 West 17th Street, New York, N. Y. 10011. No part of this publication may be reproduced, stored in a retrieval system, or transmitted, in any form or by any means, electronic, mechanical, photocopying, microfilming, recording or otherwise, without written permission of the publisher. A copy of this article is available from the publisher for \$15.00.

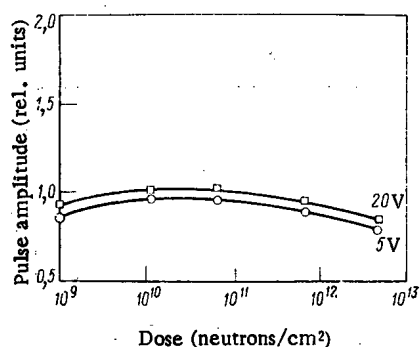


Fig. 3

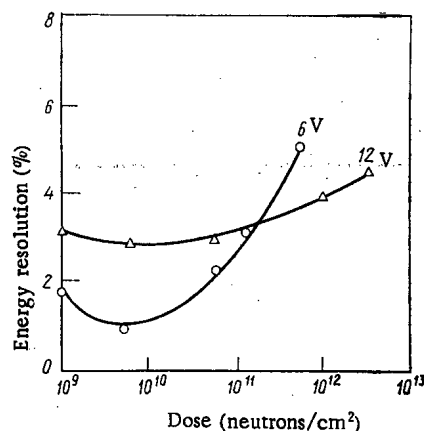


Fig. 4

Fig. 3. Dependence of the amplitude of the detector pulse upon the incident neutron dose at various bias voltages.

Fig. 4. Dependence of the energy resolution upon the incident neutron dose at various bias voltages.

The detectors were irradiated in succession with neutron fluxes of 10^{10} – 10^{13} neutrons/cm². Before and after each irradiation stage, we measured the following detector characteristics: signal amplitude, energy resolution for α particles (Am^{241}), capacity of the p–n junction, and inverse currents. The spread of the parameters did not exceed 20% before irradiation.

It was found as a result of our work that the inverse current of the detectors increases with increasing integral neutron flux (Fig. 1). We observed a slight increase in the inverse current up to $4.5 \cdot 10^{11}$ neutrons/cm². Beginning from $(1.2\text{--}7.5) \cdot 10^{12}$ neutrons/cm², the inverse current increased sharply. Figure 2 depicts the change in the capacity of the detectors. Up to $7 \cdot 10^{11}$ – 10^{13} neutrons/cm², a decrease in capacity was observed at low inverse voltages.

The capacity of the detector is independent of the irradiation at voltages which result in complete depletion. When the detectors are irradiated with high integral fluxes, total depletion sets in at reduced inverse voltages, because the resistivity of the irradiated semiconductor material has been increased.

Figure 3 depicts the changes in the amplitude of the detector pulses produced by α particles in dependence of the dose of the incident neutrons. After irradiation with a flux of $8.4 \cdot 10^{10}$ neutrons/cm², a certain increase in the pulse amplitude and an improved resolution were observed (Fig. 4). When the irradiation is further increased (more than $4.2 \cdot 10^{11}$ neutrons/cm²), the amplitude of the detector pulses and the energy resolution begin to drop sharply.

Our investigations dealt also with the restoration of the dE/dx silicon detectors during some time after the last irradiation cycle. The inverse current decreased by 15% in the first hours, but pulse amplitude and energy resolution were constant. After storing the detectors at room temperature (20°C) for 20 days, the inverse current was restored to 40%, but the amplitude of the detector pulses and the energy resolution were practically unchanged.

During the irradiation of the detectors with a neutron flux, the elastic and inelastic interactions of the incident particles with the silicon nuclei result in radiation damage to the semiconductor crystal lattice. When a nucleus receives energy exceeding the energy of defect formation, the nucleus can produce a new series of dislocations before the nucleus is slowed down and stopped in the lattice. The principal radiation defects, on which the capture of charge carriers and the recombination in silicon with n-type conductivity depend, are A and E centers, i.e., associations of a single vacancy with an impurity atom. The rate of formation of these centers is necessarily proportional to the intensity with which single vacancies are introduced, independent of the detailed mechanism of vacancy formation.

The inverse current of the detectors increases as a consequence of the reduced lifetime of the charge carriers. The amplitude of the detector pulses depends upon the charge carrier collection process. In or-

der to obtain full collection of the charge in detectors, the relation $\tau \gg T$ must be satisfied, where τ denotes the lifetime of the charge carriers, and T , the collection time.

The width of the sensitive region coincides with the geometrical thickness of the detector in the case of fully depleted surface barrier detectors. Let us consider the charge carrier-collection process in the sensitive region of the detector.

The deep levels, which are formed in the forbidden gap during the irradiation of the detectors with a neutron flux, are effective traps and recombination centers of the charge carriers. These levels substantially reduce the lifetime of the charge carriers.

The energy resolution of the detectors is strongly affected by an inhomogeneity of the trap distribution and recombination center distribution, because these distributions result in a spread of the lifetime of the charge carriers in various parts of the sensitive region of the detector and in a nonuniform charge collection. According to the results of [6], the resistivity of an irradiated semiconductor material increases, which, in turn, leads to an increase in the width of the sensitive region of detectors and, hence, to a "full depletion" of the detectors at reduced bias voltages.

Radiation damage, which reduces the lifetime of the charge carriers in a semiconductor, causes irreversible deterioration of the electrical and physical parameters of fully depleted surface barrier detectors.

Our investigations of the radiation stability of fully depleted (dE/dx) surface barrier detectors have shown that these detectors have a much greater radiation stability than detectors with full absorption, because the influence of the base layer, which leads to a deterioration of electrical and physical parameters of the detector (such as series resistance, energy resolution, etc.), is immaterial in fully depleted (dE/dx) surface barrier detectors.

LITERATURE CITED

1. A. E. Antropov, P. A. Vaganov, and L. S. Gatsenko, *Kosmicheskie Issledovaniya*, 5, No. 4, 622 (1967).
2. L. S. Brykina et al., *Kosmicheskie Issledovaniya*, 3, 499 (1965).
3. I. A. Baranov, *Pribory i Tekh. Eksperim.*, No. 2, 181 (1964).
4. J. Colmman et al., *IEEE Trans. Nucl. Sci.*, 15, 363 (1968).
5. I. I. Lazutkin et al., *Atomnaya Energiya*, 31, 636 (1971).
6. C. V. Lark-Horovitz, in: *Semiconductor Materials* [Russian translation], V. M. Guchkevich (editor), *Izd. Inostr. Lit.*, Moscow (1954), p. 62.

HALF-LIFE OF Am^{241}

V. G. Polyukhov, G. A. Timofeev,
P. A. Privalova, and P. F. Baklanova

UDC 539.163:546.799.5

The most accurate value for the half-life (T_α) of Am^{241} before 1967 was considered to be 458 yr [1]: the average of the values $T_\alpha = 458.1 \pm 0.5$ [2] and 457.7 ± 1.8 yr [3]. In 1967, Etting and Hann, using a metallic Am^{241} sample, measured T_α by the calorimetric method and obtained the value 432 ± 0.7 yr [4]. After them, other authors obtained reported values $T_\alpha = 436.6 \pm 3$ [5] and 433 ± 7 [6] yr.

In many cases, one must have an accurate value for T_α for Am^{241} ; therefore, another determination of the constant was made by $4\pi\alpha$ measurements of the aliquot of a solution having known Am^{241} concentration.

We used Am^{241} which accumulated during Pu^{241} decay. The dioxide of Am^{241} , containing about 2% Np^{234} , 0.16% Pu^{239} , and no more than 2% inert impurities, after dissolving underwent painstaking purification including three-stage precipitation of trivalent americium chloride for freeing it from Pu and Np, which had previously been oxidized in 1 mole of nitric acid by ammonium persulfate at 80°C, and by three-stage precipitation of the rare-earth-element fluorides. Americium before sedimentation was oxidized to valence 6 in 0.1 mole nitric acid by ammonium persulfate in the presence of silver nitrate at 80°C. Then took place repeated extraction by a 0.5-mole solution of di-diethylhexylphosphoric acid in decane for additional purification from Np, Pu, and inert impurities.

Radiochemical purification of Am^{241} from curium isotopes was monitored by an α spectrometer with semiconductor Si(Au) detector. The Pu^{238} content was evaluated by the radiochemical method. The total α activity for Pu^{238} and the isotopes Cm^{242} , Cm^{243} , and Cm^{244} in the sample did not exceed $10^{-3}\%$.

Trivalent americium oxalate was precipitated from the solution obtained and, after recrystallization and careful washing, it was fired to produce the dioxide. X-ray analysis showed that the oxide obtained has fluorite structure with crystal-lattice parameter $5.3771 \pm 0.0005 \text{ \AA}$, which according to the literature, corresponds to stoichiometric AmO_2 ($5.3772 \pm 0.0004 \text{ \AA}$ [7]). Spectral-analysis data show that the AmO_2 contained 0.3% impurities.

TABLE 1. Results of Determining Unit α Activity for Am^{241}

Series number	Number of samples in series	$\bar{Q}_\alpha \times 10^{-11}$ decay $\cdot \text{sec}^{-1} \cdot \text{g}^{-1}$	Rms error $S\bar{Q}_\alpha \times 10^{-11}$
1	6	1,2533	0,0253
2	6	1,2537	0,0132
3	5	1,2898	0,0225
4	5	1,3218	0,0251
5	5	1,2376	0,0415
6	6	1,2570	0,0207
7	7	1,2663	0,0239
8	9	1,2640	0,0356
Average		1,2679	0,0080

A weighed sample of freshly prepared oxide, 65.8 mg, was quantitatively dissolved in 8 moles of nitric acid. Correcting for impurities, the Am concentration in the initial solution was 0.4066 ± 0.0014 mg/g solution. Moreover, the Am concentration in this solution was established by an independent method: multiple complexonometric titration by a solution of diethylenetriaminepentaacetic acid in acetate buffer with pH = 4.2 using xylene orange as a metallic indicator. The value obtained is 0.4055 ± 0.0028 mg/g solution and is close to that established by the gravimetric method. For all subsequent calculations we used the value of the Am concentration determined by the gravimetric method.

Translated from *Atomnaya Energiya*, Vol. 36, No. 4, pp. 319-320, April, 1974. Original article submitted August 15, 1973.

© 1974 Consultants Bureau, a division of Plenum Publishing Corporation, 227 West 17th Street, New York, N. Y. 10011. No part of this publication may be reproduced, stored in a retrieval system, or transmitted, in any form or by any means, electronic, mechanical, photocopying, microfilming, recording or otherwise, without written permission of the publisher. A copy of this article is available from the publisher for \$15.00.

Further dilution and deposition of the solution aliquot on a backing was conducted by the gravimetric method. The dilution factor was usually $2 \cdot 10^4$.

The method for preparing samples and constructing a proportional $4\pi\alpha$ counter is similar to that described in [8]. In determining the weight of aliquot deposited on the backing, an experimentally determined correction for solution evaporation during weighing was introduced each time. A 10% solution of insulin in distilled water [9] was used on the film for more even distribution of the substance over the active-spot surface. The samples were measured at three potentials on the α plateau (five times for each potential) with statistical accuracy no worse than $\pm 0.7\%$. The averaged data were corrected for the effect of film thickness and for the recording-apparatus discrimination. Eight series of $4\pi\alpha$ samples were prepared from eight dilutions of the initial Am^{241} solution. Table 1 shows results of determining the unit α activity Q_α for Am^{241} .

The dispersion-analysis method [10] showed no significant differences between the average values of \bar{Q}_α for individual series and their dispersions. The average value of \bar{Q}_α calculated from the data in Table 1 is $(1.2679 \pm 0.0080) \cdot 10^{11} \text{ decays} \cdot \text{sec}^{-1} \cdot \text{g}^{-1}$. Excepting the following values for constants [4]: $N_0 = 6.02252 \cdot 10^{23} \text{ mole}^{-1}$; $A = 241.057$ on the C^{14} scale; $\ln 2 = 0.693947$; $1 \text{ yr} = 365.24 \text{ days}$, we obtain for Am^{241} $T = 432.8 \pm 3.1 \text{ yr}$ ($\bar{P} = 0.95$). The error in determining T_α consists of errors in preparing and measuring the $4\pi\alpha$ samples (0.62%) and in determining the Am concentration in the initial solution (0.34%). The magnitude of T_α obtained agrees well with the results of [4, 6] and is somewhat lower than that obtained in [5].

LITERATURE CITED

1. C. Ledere, J. Hollander, and J. Perlman, *Tables of Isotopes*, Sixth Edition, Wiley (1967).
2. J. Hall and T. Markin, *J. Inorg. and Nucl. Chem.*, **4**, 137 (1957).
3. J. Wallman, P. Graf, and L. Goda, *J. Inorg. and Nucl. Chem.*, **7**, 199 (1958).
4. F. Octting and S. Grum, *J. Inorg. and Nucl. Chem.*, **29**, 2659 (1967).
5. R. Stone and E. Hulet, *J. Inorg. and Nucl. Chem.*, **30**, 2591 (1968).
6. L. Brown and R. Propst, *J. Inorg. and Nucl. Chem.*, **30**, 2591 (1968).
7. T. Chikalla and L. Eyring, *J. Inorg. and Nucl. Chem.*, **30**, 133 (1968).
8. S. A. Baranov and R. M. Polevoi, *Pribory i Tekh. Eksperim.*, **3**, 32 (1967).
9. B. D. Peit, in: K. K. Aglintsev and G. A. Dorofeev (editors), *Metrology of Ionizing Radiation (Problems of Radiometry)* [in Russian], Gosatomizdat, Moscow (1962).
10. K. Doerfel, *Statistics in Analytical Chemistry* [Russian translation], Mir, Moscow (1969).

EFFECTIVE CHARGE OF FISSION FRAGMENTS

A. M. Miterov and E. A. Borisov

UDC 539.173.8

Besides "pure" ionization processes and elastic collisions with atoms of the medium, the passage of fission fragments through a medium is accompanied by exchange processes involving electrons and atoms of the medium. Thus, the effective charge, which at the start of the path equals the nuclear charge, decreases continuously. Lassen [1] and Fulmer and Cohen [2] made detailed measurements of fragment effective charges in various media; Nikolaev [3] analyzed theoretical viewpoints on this problem.

The effective charge is usually determined from the expression

$$z_{\text{eff}} = z^{\alpha} \frac{v}{v_0}, \quad (1)$$

where z and v are, respectively, the nuclear charge and the fragment velocity; v_0 is the electron velocity in the first Bohr orbital; the coefficient α is equal to $1/3$. Bohr [4] obtained such a relationship for electron charge based on his criterion that at each point of its path the fragment retains those electrons whose velocities are equal to or greater than its own. Here it is assumed that the electron velocity distribution in the atom is similar to Eq. (1) with $\alpha = 1/3$.

Analysis of experimental data has shown [3] that Eq. (1) with $\alpha = 1/3$ gives elevated values for effective charge, although it correctly describes its dependence on the fission-fragment velocity of motion.

Using for the ionization energies Q_n (where the Q_n are the energies needed to transform a neutral atom into n -fold ions) the values calculated from the approximate Sommerfeld equation [5]

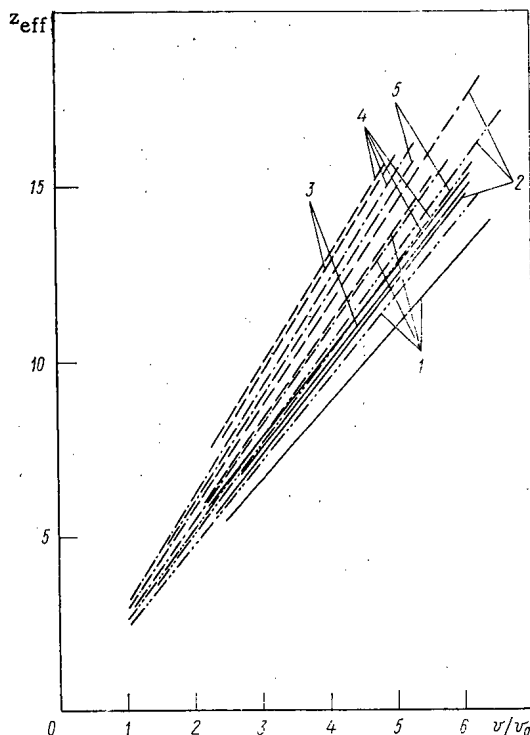


Fig. 1. Effective charges of fission fragments in various gases: 1) hydrogen; 2) helium; 3) air; 4) argon; 5) nitrogen; ---, —) experimental data from [2] for heavy and light fragments, respectively; -·-·-, -·-·-) data obtained in the present work for heavy and light fragments, respectively.

Translated from *Atomnaya Energiya*, Vol. 36, No. 4, pp. 320-321, April, 1974. Original article submitted September 14, 1973.

© 1974 Consultants Bureau, a division of Plenum Publishing Corporation, 227 West 17th Street, New York, N. Y. 10011. No part of this publication may be reproduced, stored in a retrieval system, or transmitted, in any form or by any means, electronic, mechanical, photocopying, microfilming, recording or otherwise, without written permission of the publisher. A copy of this article is available from the publisher for \$15.00.

$$Q_n = 1.27 \frac{n^{7/3}}{1 - 0.903 \left(\frac{n}{z} \right)^{1/4}}, \quad (2)$$

which holds for $n \ll z$, determining the energy needed to remove the n -th electron from the atom:

$$J_n = Q_n - Q_{n-1} = mu_n^2/2,$$

and, finally, assuming the Bohr criterion valid, the present authors obtained for effective charge an expression similar to Eq. (1), but with $\alpha = 1/4$.

The effective-charge values in hydrogen in Eq. (1) with $\alpha = 1/4$ correspond better to the experimental results in [2, 3], and they coincide for the case of a heavy fragment. This agreement shows that Bohr's criterion holds for fragment deceleration in hydrogen, but for more complex media, in which there are electrons having various velocities of motion, this criterion is insufficient. Taking into account that there is no good theory for explaining the medium's effect and that z_{eff} depends weakly on the medium's nuclear charge z_i (except for light media, $2 < z_i < 12$), the medium's effect on z_{eff} may, with good approximation, be taken into account by introducing into Eq. (1) the factor

$$\eta = \left(\frac{1 + z_i^{2/3}}{z_i^{2/3} + z^{2/3}} \right)^{3/4} \left(\frac{z_i I_H}{I_i} \right)^{1/2}, \quad (3)$$

where I_H and I_i are the average ionization potentials for hydrogen and the i -th medium having atomic number z_i , respectively.

Such a dependence of z_{eff} and z_i and I_i follows from comparing the dependences of I_i/z_i on z_i [6] and z_{eff} on z_i [1, 2], and also from comparing the equations for stopping power according to Bohr and the LSS theory with the value of ξ given in [7].

Figure 1 compares the experimental results in [2] to the results of calculating z_{eff} according to Eq. (1) with introduction of the multiplier η and the exponent $\alpha = 1/4$. The theoretical values obtained in [8] were used as average ionization potentials.

LITERATURE CITED

1. N. Lassen, Dan. Math.-Fys. Medd., 25, No. 11 (1949).
2. C. Fulmer and B. Cohen, Phys. Rev., 109, 94 (1958).
3. V. S. Nikolaev, Usp. Fiz. Nauk, 85, 679 (1965).
4. N. Bohr, Phys. Rev., 58, 654 (1940); 59, 270 (1941).
5. P. Gombasch, Statistical Theory of the Atom and Its Application [Russian translation], IL, Moscow (1951).
6. S. Allison and S. Warshaw, Rev. Mod. Phys., 25, 779 (1953).
7. V. P. Lutsenko et al., Atomnaya Energiya, 32, 411 (1972).
8. V. K. Ermilova et al., Zh. Eksperim. Teor. Fiz., 56, No. 5, 1608 (1969).

ENERGY DEPENDENCE OF AVERAGE NUMBER OF PROMPT NEUTRONS IN Pu^{241} FISSION

N. P. D'yachenko, N. P. Kolosov,
B. D. Kuz'minov, A. I. Sergachev,
and V. M. Surin

UDC 539.173

In the development of nuclear power, an important role is assigned to fast breeder reactors. In such installations, the buildup of the basic fuel – Pu^{239} – is accompanied by the formation of heavier isotopes of plutonium, the effects of which on reactor operation depend on their nuclear-physics properties. As of the

TABLE 1. Dependence of Average Kinetic Energy and of Average Number of Prompt Neutrons on Energy of Neutrons Producing Fission

E_n , MeV	\bar{E}_K , MeV	$\bar{\nu}$ *	$\Delta\bar{\nu}$	E_n , MeV	\bar{E}_K , MeV	$\bar{\nu}$ *	$\Delta\bar{\nu}$
0,28	179,273	2,975	0,015	1,74	179,101	3,139	0,040
0,40	179,421	2,974	0,015	1,94	178,781	3,195	0,048
0,55	179,243	3,008	0,017	2,15	178,992	3,201	0,050
0,70	179,119	3,031	0,022	2,36	178,872	3,250	0,056
0,85	179,290	3,031	0,022	2,56	178,825	3,250	0,056
1,00	179,236	3,047	0,026	2,74	178,642	3,305	0,065
1,33	179,181	3,092	0,032	5,00	178,394	3,660	0,115
1,54	179,052	3,126	0,038				

* $\bar{\nu} = 2,921$ for thermal-neutron fission of Pu^{241} ; $\Delta\bar{E}_K = 0,1$ MeV (everywhere).

present time, however, there is still no sufficiently complete set of experimental data characterizing the interactions of neutrons of various energies with these nuclei. In particular, detailed information is lacking for the energy dependence of $\bar{\nu}$ for Pu^{241} in the neutron energy region $E_n < 2$ MeV. There is only a single value of $\bar{\nu}$ which was measured in [1] at the neutron energy $E_n = 0.52$ MeV. In the main, this situation is related to the difficulties in direct measurements of $\bar{\nu}$ during fission of Pu^{241} by fast monoenergetic neutrons. It is quite useful to use another method for filling the gap in the experimental data on the energy dependence of $\bar{\nu}$ for Pu^{241} .

In the present work, the energy dependence of $\bar{\nu}$ for Pu^{241} was determined on the basis of fission energy balance

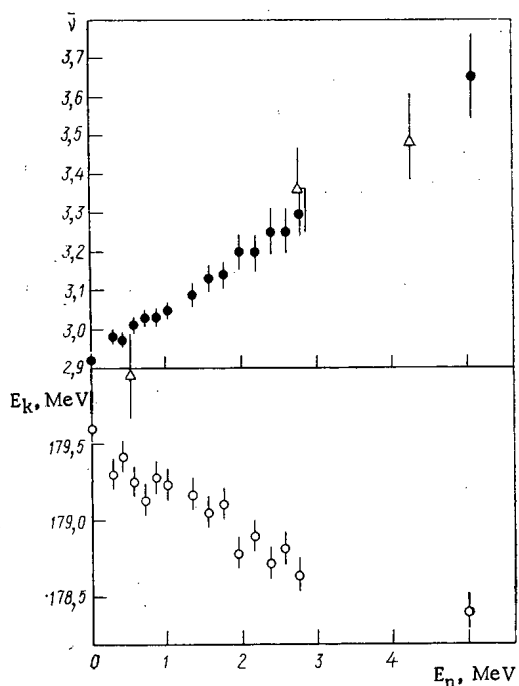


Fig. 1. Dependence of average number of neutrons $\bar{\nu}$ [O] this work, Δ) data from [1] and of average kinetic energy of fission fragments, E_K (O), on E_n .

Translated from *Atomnaya Energiya*, Vol. 36, No. 4, pp. 321-322, April, 1974. Original article submitted September 24, 1973.

© 1974 Consultants Bureau, a division of Plenum Publishing Corporation, 227 West 17th Street, New York, N. Y. 10011. No part of this publication may be reproduced, stored in a retrieval system, or transmitted, in any form or by any means, electronic, mechanical, photocopying, microfilming, recording or otherwise, without written permission of the publisher. A copy of this article is available from the publisher for \$15.00.

drawing on experimental measurements of fission-fragment mass and kinetic energy distributions. The method for measurement of yield and kinetic energy of fission fragments and also the physical basis of the method for determining the energy dependence of $\bar{\nu}$ are described in detail in [2-4].

In this work, we measured the mass and kinetic energy distributions of the fragments from Pu^{241} fission by monoenergetic neutrons in the energy range 0-2.8 MeV in steps of 150-200 keV and for $E_n = 5$ MeV. The relative accuracy in the measurement of average fragment kinetic energy was ± 100 keV. For calibration of the energy scale and analysis of the results, we used the recommendations in [5] for Pu^{241} fission by thermal neutrons ($\bar{E}_k = 179.6$ MeV).

The energy dependence of $\bar{\nu}$ can be expressed in the following way [3],

$$\bar{\nu}(E_n) = \bar{\nu}_0 + \alpha(E_n - \Delta\bar{E}_k) + \Delta\bar{\nu}_j,$$

where E_n is the energy of the neutrons causing fission; $\bar{\nu}_0$ is the average number of prompt neutrons for thermal-neutron fission of Pu^{241} [6]; $\Delta\bar{E}_k$ is strictly the change in fragment kinetic energy not associated with a change in fragment yields; $\Delta\bar{\nu}_j$ is the change in the number of prompt neutrons resulting only from the difference in fragment yields for neutrons of energy E_n and for thermal neutrons. The quantities $\Delta\bar{E}_k$ and $\Delta\bar{\nu}_j$ were determined experimentally from measurements of fragment kinetic energies and yields. The main difficulty lies in the determination of the quantity α .

We consider two possibilities.

1. Experimental values for the average number of prompt neutrons from spontaneous fission of Pu^{242} and from thermal-neutron fission of Pu^{241} are given in [6]. The mass and kinetic energy distributions of the fragments for these same cases of fission of the compound nucleus Pu^{242} were measured in [7]. Using this set of data, a value $\alpha = 0.094 \text{ MeV}^{-1}$ which is typical of neutron energies close to thermal energies can be obtained on the basis of fission energy balance.
2. In the neutron energy range $2.5 < E_n < 5.0$ MeV, there are two direct measurements of $\bar{\nu}$ for Pu^{241} fission by neutrons with energies of 2.71 and 4.19 MeV [1]. The accuracy of the measurements is about 3%. Using the results obtained in this work for fragment yields and kinetic energies at $E_n = 2.74$ and 5 MeV, a value of α can be selected such that the value of $\bar{\nu}(E_n)$ calculated from Eq. (1) agrees best with the results of the direct measurement of $\bar{\nu}$ at $E_n = 2.71$ and 4.19 MeV.

In this way, a value $\alpha = 0.12 \text{ MeV}^{-1}$ was obtained which is more typical of the upper region of the neutron energy range being considered. The two values of α differ by approximately 20%. The same error in the determination of α follows from the error of the direct measurement of $\bar{\nu}$ at $E_n = 4.19$ MeV.

It should be emphasized that an error $\approx 20\%$ in the determination of α corresponds to an error of 0-1.5% in the determination of $\bar{\nu}$ for a variation in neutron energy from 0 to 2 MeV. Such an error in the determination of $\bar{\nu}$ is at least 2-3 times less than the error of direct measurements of $\bar{\nu}$ at $E_n \approx 0.52$ MeV made in [1].

For the determination of the energy dependence of $\bar{\nu}$, it was assumed in this work that α increases linearly from 0.094 for thermal-neutron fission of Pu^{241} to 0.120 MeV^{-1} for fission by 5 MeV neutrons. The results are given in Fig. 1 and Table 1. The errors indicated include the error in the measurements of fragment kinetic energy (± 100 keV) and the error in the determination of the quantity α (20%).

It was shown [4] that the method used for the determination of $\bar{\nu}$ quantitatively describes local variations in the energy dependence of $\bar{\nu}$ for all nuclei studied. There is no basis for assuming the fissile nucleus Pu^{242} is an exception.

The authors thank V. F. Mitrofanov for helping with the measurements and the operating staffs of the KG-2.5 and EG-1 accelerators for providing favorable conditions for the measurements.

LITERATURE CITED

1. H. Connde, J. Hansen, and M. Holmberg, Nucl. Energy, 22, 53 (1968).
2. N. I. Akimov et al., Yad. Fiz., 3, 434 (1971).
3. V. G. Vorob'eva et al., Nuclear Data for Reactors, Vol. 11, IAEA, Vienna (1970), p. 177.
4. V. G. Vorob'eva et al., Preprint FEI-367, Obninsk (1972).
5. J. Neiler, F. Woller, and H. Schmitt, Phys. Rev., 149, No. 3, 894 (1966).
6. F. Manero and V. Konshin, Atomic Energy Rev., 10, 637 (1972).
7. N. P. D'yachenko et al., Preprint FEI-366, Obninsk (1972).

INVESTIGATION AND TEST OF THE MAGNETIC SYSTEM OF THE JUPITER-1M ELECTROMAGNETIC TRAP

A. V. Georgievskii, V. E. Ziser,
O. A. Lavrent'ev, M. G. Nozdrachev,
and D. P. Pogochev

UDC 621.039.624:537.212

The Jupiter-1M experimental assembly, designed for the production and study of a plasma with thermonuclear parameters (density to 10^{14} cm³ and average ion energy more than 15 keV), is a cusped geometry device whose magnetic gaps are plugged by negative electrostatic potentials [1]. The main parameters and dimensions (Fig. 1) are the following:

1. The radius of the confinement region from the horizontal axis to the center of the annular slot $R = 10$ cm.
2. The length of the confinement region between the axial magnetic mirrors $2L = 41$ cm.
3. The width of the annular slot $2a = 0.1$ cm.
4. The radius of the axial opening in the region of the center of the edge of the coil $r_0 = 0.5$ cm.
5. The magnetic system is fed from a 0.025 F capacitor bank charged to a p.d. of 4.5 kV. The calculated value of the magnetic field in the mirrors $H_m = 130$ kOe, and in the slot $H_s = 40$ kOe. The half-period of the current in the windings is 25 msec.

The magnetic system of the assembly (Fig. 2) was chosen in such a way that all the magnetic flux passing through the annular slot emerges through the axial openings [2]. The magnetic field in the central region of such a system is described by the equations

$$A_\phi = \frac{H_s}{R} rz; H_r = -\frac{H_s}{R} r; H_z = \frac{2H_s}{R} z,$$

where A_ϕ is the magnetic potential; H_r is the component of the magnetic field in the plane of symmetry; H_z is the axial component of the magnetic field; and r and z are coordinates.

The generating surface boundary the plasma volume is described by the equation

$$r^2 z = \text{const} = R^2 a.$$

The graphs of the distribution of magnetic field intensity along the axis and along the radius in the plane of symmetry of the assembly and the trace of the lines of force lying on the surface bounding the plasma volume are shown in Fig. 3.

The magnetic field distribution pattern along the axis and along the radius in the plane of symmetry measured under steady conditions by using a Hall-effect probe agreed with the calculations to within $\pm 2.5\%$. Rather stringent accuracy requirements are imposed on such magnetic systems: the right and left-hand parts must not be off axis by more than 0.05 cm; the misalignment must not exceed $30'$; the planes of geometric and magnetic symmetry must coincide along the average radius of the slot to within 0.01 cm. Therefore the traces of the lines of force forming the surface bounding the plasma volume were determined experimentally.

A schematic diagram of the experimental arrangement is shown in Fig. 2. Point guns which can inject 30 eV electrons into the trap from any point of a region of 1 cm radius are located in regions I and II ± 24 cm from the center of the assembly. The radial position can be measured to 0.5 mm.

Translated from *Atomnaya Energiya*, Vol. 36, No. 4, pp. 323-324, April, 1974. Original article submitted August 24, 1973.

© 1974 Consultants Bureau, a division of Plenum Publishing Corporation, 227 West 17th Street, New York, N. Y. 10011. No part of this publication may be reproduced, stored in a retrieval system, or transmitted, in any form or by any means, electronic, mechanical, photocopying, microfilming, recording or otherwise, without written permission of the publisher. A copy of this article is available from the publisher for \$15.00.

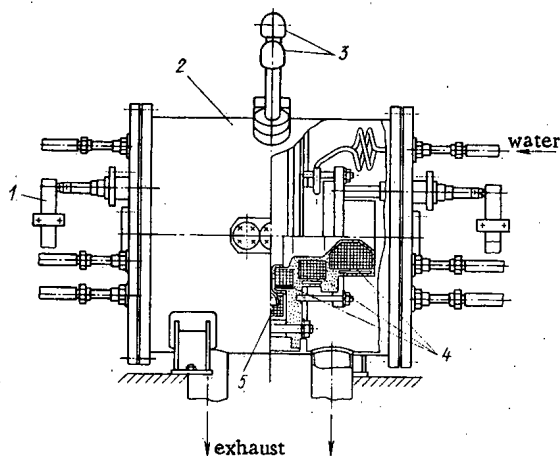


Fig. 1

Fig. 1. Jupiter-1M assembly: 1) coil terminals; 2) chamber; 3) electrode terminals; 4) magnetic system coils; 5) insulator.

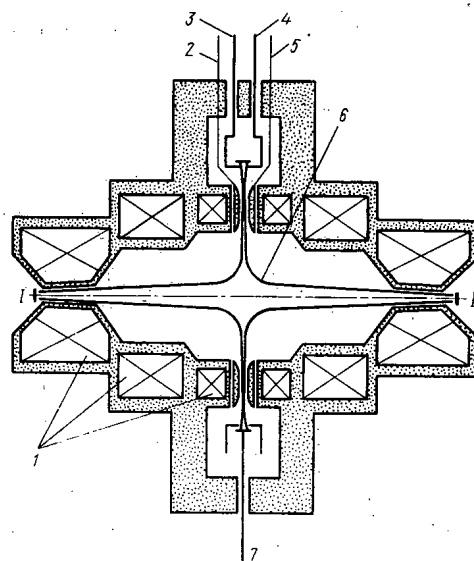


Fig. 2

Fig. 2. Magnetic system of Jupiter-1M assembly and schematic diagram of the experiment: 1) coils; 2, 3) terminals of electrodes bounding the slot; 3, 4) terminals of lateral annular electrodes; 6) generating surface bounding the plasma volume; 7) central electrode; I and II) are locations of electron guns.

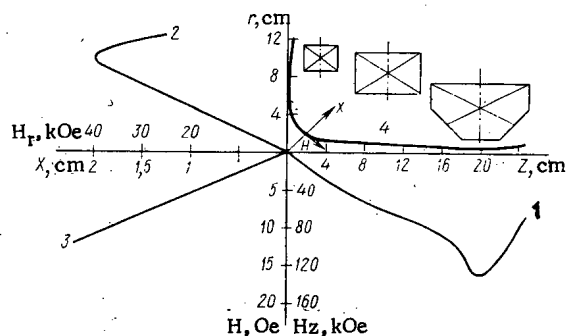


Fig. 3. Distribution of magnetic field intensity 1) along the axis; 2) in the plane of symmetry of the Jupiter-1M assembly; 3) in the x direction; 4) trace of magnetic lines of force bounding the plasma volume.

The coincidence of the geometric and magnetic axes and the geometric and magnetic planes of symmetry for various positions of the electron sources can be judged from the currents to electrodes 2, 3, 4, 5, and 7. The experiments were performed under steady conditions with mirror fields of 3 kOe. It was shown that all the magnetic flux through a circle of 0.5 cm radius in the central axial openings passes through the 1 mm slot and falls on the central electrode 7; when the radius is increased to 0.6 cm part of the flux falls on electrodes 3 and 4, and a further increase in radius causes the magnetic flux to begin to "stick" to electrodes 2 and 5 limiting the size of the slot. When the point sources are rotated about the geometric axis of the magnetic system the current distribution to the electrodes is unchanged for the right- and left-hand sides of the assembly, confirming the coincidence of the geometric and magnetic axes and also the geometric and magnetic planes of symmetry. It is estimated that the inaccuracy of the magnetic system does not exceed the permissible limits.

The experiments showed that with the type of coils and cooling system selected a magnetic field of the required intensity can be obtained in pulses of up to 25-30 msec duration repeated after intervals of 2-3 min. At the present time the mirror fields in the Jupiter-1M device reach 100 kOe for a magnetic field of 31 kOe in the slot.

LITERATURE CITED

1. O. A. Lavrent'ev, in: Plasma Physics and Problems of Controlled Thermonuclear Fusion [in Russian], No. 3, Naukova Dumka, Kiev (1968), p. 77.

2. L. A. Artsimovich, Controlled Thermonuclear Reactions [in Russian], Fizmatgiz, Moscow (1961).

INFORMATION

TWENTY-FIVE YEARS OF THE ENGINEERING PHYSICOCHEMICAL FACULTY

B. V. Gromov and Ya. D. Zel'venskii

In February this year the engineering physicochemical faculty of D. I. Mendeleev Moscow Chemico-technological Institute completed 25 years of its existence. The work on the creation of the faculty was stated as early as in the end of 1948. The idea of organizing such a faculty within D. I. Mendeleev MCTI, advanced by the rector of the institute Academician N. M. Zhavoronkov, was ardently supported by I. V. Kurchatov, the minister for higher education S. V. Kaftanov, and prominent directors of a number of branches of the industry who took active part in defining the profile of the faculty and discussing the bases of the scientific plan and programs and directly assisted in its organization.

The creation of the engineering physicochemical faculty coincided with an extensive development of research in nuclear energetics in our country and demanded much force and work from its organizers and first group of teachers among which were Academicians G. K. Boreskov, I. V. Petryanov, N. P. Sazhin, Corresponding Members of the Academy of Sciences of the USSR A. P. Zefimov, M. G. Slin'ko, V. V. Fomin, Professors P. A. Zagortsa, O. E. Zvyagintsev, Ya. D. Zel'venskii, V. B. Shevchenko, Assistant Professor A. V. Gordievskii and others.

In the first few years of its existence the faculty had two principal departments, chemistry and technology of radioactive elements and separation and use of isotopes. Somewhat later the department of electrovacuum devices and materials was started and from 1957 the preparation of specialists in radiation chemistry was organized. In 1960 the department of cybernetics of chemicotechnological processes headed by corresponding member of the Academy of Sciences of the USSR Professor V. V. Kafarov was created, which was the first of its kind in the country.

Under the direction of its founders and the first group of teachers of the faculty cadres of young scientists emerged from the graduating classes, who now form the main structure of the teaching staff of the faculty. A large amount of the scientific-organizational work was done by Assistant Professor A. B. Gordievskii, Professors P. A. Zagorets, G. A. Yagodin, P. V. Kovtunencko, and others.

At present the faculty has five departments: the department of radiation chemistry and radiochemistry (chairman, Professor Ya. D. Zel'venskii), department of technology of radioactive and rare elements (chairman, Professor B. V. Gromov), department of chemical technology of electrovacuum materials and devices (chairman, Professor A. A. Bundel'), department of cybernetics of chemicotechnological processes (chairman, corresponding member of the Academy of Sciences of the USSR Professor V. V. Kafarov).

Among the prominent group of teachers at the faculty there are now one academician, one corresponding member of the Academy of Sciences of the USSR, 12 professors, doctors of science, and 45 assistant professors and candidates of science.

The numerous laboratories of the special departments are equipped with modern equipment. An All-Union procedural-consultative center for methods of cybernetics in chemistry and chemical technology has been created and is operating successfully.

In the 25 years of its existence the faculty has produced more than 3550 young specialists for the industry and scientific research organizations of the country. Among these more than 700 have defended candidate dissertations and 35 have defended doctoral dissertations. Among the graduates of the faculty many are directors of large scientific groups and recipients of Lenin and State premiums.

Translated from Atomnaya Energiya, Vol. 36, No. 4, p. 125, April, 1974.

© 1974 Consultants Bureau, a division of Plenum Publishing Corporation, 227 West 17th Street, New York, N. Y. 10011. No part of this publication may be reproduced, stored in a retrieval system, or transmitted, in any form or by any means, electronic, mechanical, photocopying, microfilming, recording or otherwise, without written permission of the publisher. A copy of this article is available from the publisher for \$15.00.

The engineering physicochemical faculty made a significant contribution to the preparation of engineering personnel for socialist and developing countries.

The staff of the faculty has published over 60 monographs, textbooks and student aids, and more than 1300 articles and scientific reports. Over 160 works are covered by inventors' certificates of the USSR. A considerable part of the technological developments has been introduced into more than 25 industrial undertakings in the country. The annual sum of contract work of the faculty is more than half a million rubles. There are two problem laboratories functioning at the faculty.

At present the construction of a new educational complex of D. I. Mendeleev MCTI has started. The construction of a special teaching-laboratory building for the engineering physicochemical faculty has the first priority. A considerable extension of the area, technological refitting of the laboratories and auditoriums with latest equipment will undoubtedly benefit the faculty and would permit to raise its work to a still higher standard.

CONFERENCES AND MEETINGS

INTERNATIONAL CONFERENCE ON OPEN TRAPS

V. A. Chuyanov

A conference on open traps, organized by Livermore Lawrence Radiation Laboratory (LRL), was held in Berkley (USA) from December 3 to 7, 1973. About 50 physicists from various laboratories and universities of the USA, and also from Great Britain, USSR, and France participated in the conference. The Soviet scientists presented reports on the research on the stability of plasma in open traps PR-6, PR-7, and "Orga-2T," the development of methods of stabilization of plasma instabilities by feedbacks, and the development of high-power fast atom injectors. These papers generated great interest.*

At present the research work on open traps in the USA is entirely concentrated at the Livermore laboratory and is being carried out on two main equipment, 2XII and "Baseball-II." We should discuss the new results of the experiments on the corkscrew trap 2XII, where the decay of a dense plasma ($n \geq 10^{13} \text{ cm}^{-3}$), produced by the injection from a titanium gun and subsequent adiabatic compression, is investigated.

1. With the injection of a beam of hydrogen atoms with 16 keV energy and 5 eqv. A intensity it was possible to measure the density of the plasma during the compression and in the early stage of the decay. (The microwave interferometry used earlier did not permit to measure the density higher than $4 \cdot 10^{13} \text{ cm}^{-3}$.) It was found that at the early instants of compression, when the magnetic field is still not very large, the plasma density is close to 10^{14} cm^{-3} , while β (the ratio of the plasma pressure to magnetic pressure) reaches 0.4-0.6. Although values of $\beta \approx 1$ had been observed earlier in experiments with fast electrons, such high values of β with hot ions have been reported for the first time. Furthermore it was detected that β is bounded from above and this limiting threshold depends on the magnetic field and corkscrew ratio. The obtained dependence agrees with the limitation imposed on β by "mirror" instability with good accuracy.

2. A relation between the vacuum conditions and the rate of decay of the plasma was also detected. The vacuum conditions were regulated by a change of the area of the surface of the wall covered by titanium. The transition from complete covering to covering of only the corkscrew regions at ion energies of 1.5-2 keV (at this energy in any condition the decay occurs smoothly without fast surges) increases n by a factor of two (from $0.8 \cdot 10^{10}$ to $1.6 \cdot 10^{10} \text{ cm}^{-3} \cdot \text{sec}$), which almost coincides with Fokker-Planck calculations of Coulomb decay. At an ion energy of 3 keV this transition increased $n\tau$ from $0.6 \cdot 10^{10}$ to $2.6-4.2 \cdot 10^{10} \text{ cm}^{-3} \cdot \text{sec}$ and eliminated the fast surges. An improvement of the confinement was observed with the increase of the density of the corkscrewed plasma up to 4% of the plasma density at the center of the trap. For complete coverage the density of the corkscrewed plasma is of the order of 1% of the density at the center of the trap; however, even this is significantly higher than the value expected in the case if the density beyond the plugs were completely determined by the plasma flux exiting through them. We note that in previous works this group had asserted complete absence of correlation between the density of the corkscrewed plasma and the rate of decay of the plasma.

3. Attempts to confirm the theory of quasiclassical scattering of Baldwin-Kollen from the measurements of the dependence of confinement on the average energy of the ions w_i , the electron temperature T_e , and their ratio were not successful.

4. Laser scattering experiments showed that the electron temperature changes from pulse to pulse in the range 30-200 eV. In most cases it is close to 70-100 eV, which is 0.05 of the energy of the ions for an average energy of ions equal to 1.5-2 keV, whereas in Coulomb decay $T_e/w_i = 0.1$. With the increase of the ion energy T_e does not increase and the difference from Coulomb value increases. The observed disagreement can be partially explained by the fact that the decay time is smaller than Coulomb decay time and the electrons are not able to get heated from the ions.

*The papers by the Soviet scientists and scientists from European countries were discussed at the VI European conference on controlled nuclear fusion and plasma physics (see "Atomnaya Energiya," 1973, Vol. 35, p. 447).

Translated from Atomnaya Energiya, Vol. 36, No. 4, pp. 326-328, April, 1974.

© 1974 Consultants Bureau, a division of Plenum Publishing Corporation, 227 West 17th Street, New York, N. Y. 10011. No part of this publication may be reproduced, stored in a retrieval system, or transmitted, in any form or by any means, electronic, mechanical, photocopying, microfilming, recording or otherwise, without written permission of the publisher. A copy of this article is available from the publisher for \$15.00.

5. In zones with accelerated decay (w_i higher than 2 keV) probe measurements indicated the presence of oscillations with frequencies close to the ion-cyclotron frequency and with characteristic wave numbers $k_{\perp} \approx 4/a_i$, where a_i is the Larmor radius for an ion with energy w_i .

The experiments on 2XII equipment have been now discontinued; the installation has been dismantled and the new 2XIIB equipment is being installed at a fast pace (about 4 million dollars has been released for the work). It will be distinguished by a longer duration of the existence of the magnetic field (up to 20 m sec) and the possibility of installation of an injector of fast atoms consisting of 12 modules and with a total equivalent current of 600 A. An injector module with 50 A current an injection energy of 20 keV and the duration of the pulse up to 10 m sec has been developed at LRL. This module is an ion source without magnetic field, in which a large ion current is obtained on account of the large emission area. The ion stream is led out from 105 slits of 7 cm length and 2 mm diameter each. For the "illumination" of the emission surface by the plasma an arc discharge is ignited in the source with a heated cathode without magnetic field (arc current 4000 A, voltage up to 70 V). The gaseous efficiency of the source reaches 38%. Charge exchange of the ions occurs in the immediate vicinity of the source in the gas flowing out from it. The absence of the magnetic field makes it possible to easily assemble the modules into a high-power injector. At present a still larger module with 200 A is being developed, in which the emission area is of the order of 1000 cm² and the arc current is of the order of 20 kA. These successes in the development of high-current injectors permits to approach the experiments on open traps in a new way. At an injection current of 600 A in the volume of 2XII trap it is possible to confine a plasma with density $2 \cdot 10^{13}$ cm⁻³ even for a lifetime of $\tau \approx 200$ μ sec (this is worse by a factor of two than that obtained at present at ion energy of 2 keV). Due to the charge exchange of the fast atoms to the ions of the plasma the energy of the ions will rapidly grow to the injection energy. Thus the developed technology permits to obtain and investigate plasma with parameters very close to those of thermonuclear plasma: $n \geq 10^{13}$ cm⁻³, $w_i \geq 10$ keV. Investigations of the stability of such a plasma will undoubtedly give more important and decisive results than any model experiments.

On "Baseball-II," a trap with injection of fast atoms, experiments on the program of plasma buildup with the stable Coulomb distribution held constant were carried out. For this purpose the injection was done in good vacuum conditions (τ of charge exchange comprised a few seconds) and at low injection energy ($w_i \approx 1$ keV), so that even at a plasma density of $n \approx 10^8$ cm⁻³ the charge exchange time was larger than the Coulomb scattering time. In these experiments a completely stable plasma with Coulomb velocity distribution of ions at densities up to a few units of 10^9 cm⁻³ was actually obtained. At such densities the charge exchange losses were smaller by a factor of six than the losses due to the drift into the cone in the presence of paired collisions and all the parameters of the plasma were in good agreement with Fokker-Planck calculations. However, during attempts to increase the density an instability was detected lowering the lifetime to 0.1 sec destroying the Coulomb form of the ion distribution function and hindering further buildup. The investigations showed that the instability threshold is determined not by the density itself but by its ratio to the square of the magnetic field and can be written in the following form

$$\varepsilon = \frac{\omega_{oi}^2}{\omega_{Bi}^2} = 0.1.$$

The instability leads to a preferential ejection of ions beyond the plug and is accompanied by oscillations at the ion cyclotron frequency ω_{Bi} , the frequency of precession of ions with the injection energy in an inhomogeneous magnetic field ω^* , and by an increase of the plasma potential. With further increase of the density the region of the losses covers the entire plasma. At present it is not clear which oscillations, the high-frequency (ω_{Bi}) or the low-frequency (ω^*), cause the losses. An attempt to influence the low-frequency oscillations with the use of an electrostatic feedback system led to an increase of the density by 30%. This and other facts force the experimentalists working on "Baseball-II" to favor the hypothesis about the dominating role of the low-frequency oscillations. From the theoretical point of view the assumption of the primary role of the cyclotron oscillations is more plausible. It is not ruled out that the limit on ε is determined by the cyclotron instability localized at first in the surface layer of the plasma, where the density is too small for the establishment of collisional stable distribution. However, irrespective of the nature of the instability it is clear that the original program, i.e., to go through the lowest to the maximum densities in the presence of complete stability of the plasma, in its initial stage is unattainable without taking recourse to some new ideas. In the presence of instability the life times observed on "Baseball-II" are still sufficiently large in order that for more powerful injection it is possible to move to higher densities. However, at an injection energy of 1-3 keV it is difficult to hope to obtain injection currents of more than 20-30 mA. Therefore a new injector with the energy of ions equal to 20 keV and current up to 0.5 A is now being

installed in "Baseball-II." An attempt will be made to increase the density of the plasma with the use of "brute force."

High-power injectors developed at Berkley have changed the idea of the experiments on "Baseball-II." At present a variant of replacement of the injection into vacuum by injection into a precreated target is being considered. The possibility of such injection had been investigated earlier, but at small injection currents for a successful buildup it was necessary that the temperature of the electrons of the plasma-target be not less than a few kiloelectronvolts. At an injection current of 50 A the electron temperature may be a few tens of electron volts, since in this case the time of accumulation of hot ions is small and a strong cooling of the ions at the electrons of the target is possible. Two variants are being considered: injection into a hydrogen arc and injection into a plasma formed by the evaporation of a solid target by laser light. At present laser plasma targets are being successfully developed in the laboratory of United Aircraft (Boston). Here under the direction of A. Hot a trap "Light" is being developed with a baseball field, injection of neutrals, and laser target. The laser target is formed by the irradiation of a 20 micron sphere of lithium deuteride by a pulse from a neodymium laser having a power of 500 MW and duration of 8 nsec. The temperature of the ions of the target is ~ 100 eV, their lifetime in the trap ~ 150 μ sec, and the nature of the decay is Coulomb ($\tau \sim w_i^{3/2}$). A beam of hydrogen atoms with 10 keV energy and current up to 0.5 A will be injected into this target (its parameters must be somewhat improved). A. Hot presented calculation of the build up, according to which for the displacement of the ions of the target by the fast ions of the beam and for obtaining a density $\sim 10^{13}$ cm^{-3} a density of the fast atoms injected into the target higher than 5 mA/cm² is sufficient, which appears quite realistic. The actual launching of "Light" is planned for the spring of 1974.

Computers are extensively used in the investigations of corkscrew confinement at LRL. A review of the studies made in this direction was given by J. Killin. They can be divided into four groups: Fokker - Planck calculations of Coulomb confinement, calculations of MHD equilibrium for large β and real magnetic configurations, solution of dispersion equations and nonlinear problems in collisionless approximation, and calculations of build up in the presence of injection with collisions in the real geometry taken into consideration. The available Fokker - Planck programs permit (assuming separation of variables) to investigate any number of components (ions of different types, electrons, α -particles and so forth). A two-dimensional code without assuming the separation of variables has been developed for taking into consideration real characteristics of the injection and the magnetic fields. Computations of Coulomb scattering, made recently by F. Verkoff in Grenoble (France) without the assumption of spherical symmetry of Rosenbluth - Trubnikov potential, showed approximately satisfactory values of the confinement time compared to the previous results. A similar program was developed at LRL for a verification of this result. Results of computation with this program did not give any significant improvement of the confinement. During the conference F. Verkoff and J. Killin compared their programs, but the reasons for the divergence of the results were not ascertained.

Calculations of the equilibrium for finite β made it possible to find maximum values of β and obtain the field distribution in the presence of the plasma for such real traps as 2XII and "Baseball-II." The following important conclusion was arrived at from the results of the solution of nonlinear problems: the cyclotron frequency and its harmonics dominate in the spectrum of the oscillations at the nonlinear stage of development of the oscillations irrespective of the real frequency at the linear stage of the oscillations. Therefore the frequency spectrum observed at the nonlinear stage of development of the instability can be used for its identification only with great precaution.

Recently the staff of LRL have proposed a variant of corkscrew reactor with the injection of fast atoms of deuterium into a cold titanium target. In the paper presented by R. Post on this subject only the problems requiring further investigation were indicated and no solutions were presented. An intensive computational work is being carried out at LRL in this direction. In particular, a special program for the computation of the outflow of plasma along a diverging magnetic field has been developed with the effect on the metallic boundary and the ionization of the gas taken into consideration.

At present the main attention in the program at LRL on open traps is being devoted to the injection of very high-power beams of neutrals into targets capable of ensuring a capture of these beams. All the experiments are being developed and further theoretical searches are being carried out in this direction.

In conclusion mention should be made of the good working atmosphere of the conference and valuable exchange of ideas and experience among the physicists of different laboratories of the world working in the field of research on corkscrew confinement of plasma.

RESULTS OF THE FIRST INTERNATIONAL SYMPOSIUM ON PLASMA CHEMISTRY

Yu. N. Tumanov

The first international symposium on plasma chemistry was held in Kiel (FRG) from September 6 to 10, 1973 for discussing the prospective directions and problems of technological (low-temperature) plasma. About 200 representatives from the USSR, USA, FRG, Canada, Great Britain, France, Japan, Switzerland, Italy, GDR, Yugoslavia, and Belgium took part in the symposium.

Six sections worked in which about 70 papers were presented and discussed.

1. Elementary Chemical Reactions in Plasma (13 papers). The topics discussed in this section were the mechanism and kinetics of elementary chemical reactions in a nonequilibrium plasma, the parameters of a low-pressure plasma from the point of view of plasma chemistry, chemical reactions in the field of an electrical discharge, chemical-ionization reactions, chemical conversions in different zones of electric discharges, processes of adhesion of electrons in electrically negative gases, and mass-spectroscopic analysis of chemically reacting plasma.

2. Chemistry of Gas-Phase and Heterophase Processes in Plasma (15 papers). In this section the following topics were discussed: thermodynamic and kinetic aspects of homogeneous and heterogeneous chemical reactions in a nonisothermal plasma, conversion of solid particles into plasma heat-carriers, interaction of the plasma with the condensed materials, synthesis and analysis of hydrocarbons, restoration of iron, copper, and aluminum from ores, separation of different components of ores.

3. Plasma-Chemical Diagnostics (10 papers). The applicability of different methods of diagnostics of chemical flames and plasma in the case of chemically reacting plasma was discussed (mass-spectrometry, and also emission and absorption spectroscopy, method of electrostatic probes etc.). The problems of diagnostics of plasma of electrical discharges in polyatomic gases containing heavy elements were discussed.

4. Engineering Applications of Plasma (14 papers). The main topics in this section were: technique of obtaining high-temperature gases for engineering and chemical applications, production of metals by reduction of oxides by carbon, of halides by hydrogen or thermal decomposition of unstable compounds (sulfides), synthesis of micron and submicron powders, fusion of high-melting substances, separation and enrichment of different ores and concentrates, obtaining high-temperature coatings and semiconductor integrated circuits for microelectronics.

5. Organic and Inorganic Synthesis (7 papers). The papers in this section were devoted to the mechanisms of energy transport in plasma-chemical synthesis, possibilities and limitations of this synthesis, synthesis of high-melting carbides and nitrides, organic and metallic-organic compounds, and to the problems of optimization of plasma-chemical process and reactor.

In the sixth, which was the concluding section, the results of the symposium were summarized and the prospective developments and problems of plasma chemistry were discussed.

The following directions of the use of plasma in chemistry and technology may be mentioned.

1. Plasma as a chemically active or neutral heat-transfer agent for the solution of specific problems (restoration of metals, conversion of chemical substances, enriching, pulverizing, analysis). The specific properties of the plasma are not significant, since the temperature falls rapidly due to endothermic effects in heated objects in the presence of a preliminary interaction with the plasma.

Translated from *Atomnaya Energiya*, Vol. 36, No. 4, pp. 328-329, April, 1974.

© 1974 Consultants Bureau, a division of Plenum Publishing Corporation, 227 West 17th Street, New York, N. Y. 10011. No part of this publication may be reproduced, stored in a retrieval system, or transmitted, in any form or by any means, electronic, mechanical, photocopying, microfilming, recording or otherwise, without written permission of the publisher. A copy of this article is available from the publisher for \$15.00.

In the subsequent interaction the temperatures of the gas and the heated material are equalized and then the temperature of the system falls due to both endothermic reactions and heat transfer along different channels (thermal conductivity, convection, radiation).

2. Thermodynamically nonequilibrium electric discharge plasma as a zone of chemical reaction. In a majority of cases the topic of discussion was the low-pressure plasma in which the temperature of heavy particles is considerably lower than the temperature of the electrons. The term "plasma chemistry" refers primarily to just such a plasma. The potential possibilities of nonequilibrium plasma are large; even now there are different applied works.

The problems related to generators, plasmatrons, and diagnostics are restraining the progress in plasma technology. As a science plasma chemistry, lying at the boundaries of chemistry, physics, technology, and electroenergetics, requires the development of a common point of view and terminology, and also of a proper theory for the investigation and prognosis of plasma-chemical reactions.

The use of plasma in chemical technology permit to replace the process "in the tank" by the process "in the stream" and to use intensive thermal processing of materials without large capital expenditures; it also permits rapid and homogeneous heating of materials and tempering of products of reaction and makes it possible to conduct high-temperature reactions in a reactor with cold walls and to lower the temperature of a gas in the zone of reaction as a result of the development of instability which may solve the problem of reducing corrosion of chemical reactor and so forth. At present applied research is being carried out with 20-1000 kW equipment.

The next symposium on plasma chemistry will be held in 1975.

FOURTH INTERNATIONAL SYMPOSIUM ON DISTILLATION OF SALINE WATER

O. I. Martynova, V. G. Shatsillo,
and V. B. Chernozubov

The symposium was held in Heidelberg (FRG) during the period September 9-14, 1973. 550 delegates from 36 countries took part in the symposium; 122 papers were presented (from the Soviet Union there were 8 persons and 19 papers were presented).

The main problems discussed at the symposium were:

1. Fundamental Investigations in the Field of Physical and Physicochemical Properties of Sea Water (one paper from the USSR), Heat- and Mass-Transfer (problems of intensification of heat exchange, contact heat exchange and mechanisms of particular cases of heat- and mass-exchange in evaporatory and other distillation equipment).

2. Problems of Deposition of Crust, Its Prevention, and Predistillation of Water in Large Thermal and Membrane-Type Distillers. Studies on the use of new polymer anticrust agents (polyacrylates) appeared; a number of papers were devoted to the search of methods of coping with high-temperature sulfate incrustation ($t = 110-150^{\circ}\text{C}$), in particular, the methods of seed crystals (France) and injection of low-molecular polyelectrolytes (Great Britain). Papers on the engineering-technological aspects of removal of crust from heat-exchanging surfaces were presented.

Thus a new information has been obtained about the methods of prevention of high-temperature encrustation and about the attempts of complex solution of the problem of coping with corrosion and encrustation.

3. Processes of Distillation. The topics discussed here were the experience in the operation of new industrial installations, modernization of the existing equipment, investigation of the processes of encrustation of water, tests of pilot equipment, constructional layout of new thermal distillators, investigation of dynamical properties of distillation-type desalinators as applied to the problem of their control etc.

4. Experience in Operation of New Installations. The most interesting papers were on the starting of a large equipment for instantaneous boiling (Italy), on a reconstructed equipment in Freeport (USA), and on the starting and operation of four instantaneous boiling distillators (Netherlands).

5. Investigation of Mechanism and Regularities of the Processes in Distillation Equipment. The most serious studies were presented from Great Britain and the USA; a good scientific base of stable successes, achieved in these countries in the field of thermal distillation, was demonstrated.

6. Construction of Equipment. The idea of vertical cascade of evaporation stages in multiframe evaporating equipment with horizontal bunches of tubes sprinkled from outside by falling sea water (concept of vertical tower) is noteworthy; a tendency toward the development of high thermal distillators occupying small area is observed.

7. Economic Investigation on the Use of Water Resources and Purification of Sewage Water. The economic feasibility of distillation of sea water in different geographical regions completely or partially devoid of natural sources of fresh water (for instance, the coast of Adriatic sea, Yugoslavia, river Colorado at the boundary between USA and Mexico, etc.) was analyzed.

Translated from Atomnaya Energiya, Vol. 36, No. 4, pp. 329-330, April, 1974.

© 1974 Consultants Bureau, a division of Plenum Publishing Corporation, 227 West 17th Street, New York, N. Y. 10011. No part of this publication may be reproduced, stored in a retrieval system, or transmitted, in any form or by any means, electronic, mechanical, photocopying, microfilming, recording or otherwise, without written permission of the publisher. A copy of this article is available from the publisher for \$15.00.

8. Technical-Economical Comparison of Methods of Distillation of Sea Water and Different Constructions of Distillation Desalinator Equipment. (France, USA, Israel). The feasibility of construction of distillation desalinator equipment with vertical long-tube equipment with dropping film was established. A tendency toward a changeover to multiframe evaporating equipment fitted with vertical or horizontal equipment with falling film of water is clearly marked. These equipment have an advantage over the instantaneous boiling ones in the intensity of heat transfer and specific capital investments. The tendency toward a combination of evaporators with falling film and evaporators with instantaneous boiling should also be noted.

A trend of the use of profiled surfaces for the purpose of intensifying the heat exchange is clearly seen in the symposium as common for all the firms and countries developing thermal distillers.

As an example of one of the possible methods of reducing the cost of distilled water a construction of an energetics complex based on nuclear reactors with the use of different combinations of distillations desalinators was discussed. In particular, the project and the technical-economical investigations of the construction of a complex for the distillation of saline water of Colorado river at the boundary of USA (California) and Mexico with an output of more than 300,000 m³/day and proposed cost of 0.2 dollar/m³ were discussed. Thermal distillation equipment are considered as well controlled terminal coolers for the external circuits of the nuclear reactors.

9. Investigations of Corrosion Resistance of Carbon and Low-Alloy Steels in Distillation Conditions (France, Italy). Practical results on corrosion of metals in different equipment (Israel, Mexico), use of corrosion inhibitors (India) and aluminum alloys in the technology of distillation (France), and also other problems of corrosion protection of nonmetallic materials (polymer coatings for steel, concrete, sheet concrete, etc.). Neoprene coatings, plating by sheet alloy - cupronickel, etc., are mentioned among the anti-corrosion coatings.

10. Distillation of Water by the Method of Electrodialysis. Twenty papers were devoted to this topic (four from USSR) including eight on the preparation and test of membranes and 12 on the optimization of the technological and constructional parameters of electrodialytic distillation equipment which have found widespread use in the whole world due to their reliability, long life and simplicity of servicing, and further improvements of ionoselective membranes (USSR, Netherlands, USA).

In the paper from the firm Ionics (USA) the results of the investigations of high-temperature electrodialysis as applied to distillation of sea water were presented; an increase of the temperature of the water being distilled to 80°C made it possible to reduce the energy expenditure in the process considerably.

11. Distillation of Saline, Salty, and Sewage Waters by the Method of Inverse Osmosis (42 papers). Such an increase of the interest is accounted for by the great prospects of the process which has already crossed the walls of research laboratories. The constructed distillation equipment have confirmed the high efficiency of the inverse osmosis equipment. At present the main problems and technological difficulties in the realization of the process have been overcome and its efficiency and reliability largely depend on the prior preparation of the water before its separation from salt.

The papers on the synthesis of a new type of membrane and the development of a new type of modules of inverse osmosis are of great interest. For instance, the special feature of the hollow fibers obtained from boron-silicate-sodium glass is the complete absence of hydrolytic disintegration of the material and, hence, reliability and durability of the filtering elements. Complex membranes of very thin films distinguished by high durability and operating at pressures up to 102 atm have been developed (USA). The work on the development of the theory of osmosis and optimization of modular systems is being continued (USA, Great Britain, Belgium, Israel, etc.).

Thus from an analysis of the papers presented at the symposium the following conclusions can be drawn:

the main type of prospective thermal distillers are vertical evaporating equipment of film type;

a tendency to combine vertical film-type equipment with those of instantaneous boiling type is observed;

the heat-transfer surfaces are made of profiled tubes both in demonstration installations and completed projects;

research and construction work in the field of thermal distillation is concentrated mainly on the development of extremely large equipment;

along with the traditional copper-nickel alloys stainless steel, titanium, and aluminum alloys are recommended as prospective constructional materials for the heat-transfer surfaces; the problem of use of thin-walled plastic tubes is also considered;

considerable attention is being devoted to the purification of sewage water and natural reservoir water with the use of membrane processes, mainly by inverse osmosis; in particular, the program of distillation in the USA is concentrating the main attention on these problems;

the economic efficiency of equipment with hydrophobic heat-transfer agent is placed in doubt;

the methods of freezing for distillation of water did not justify the hope placed in them;

a preliminary purification of the original water is of large significance for all membrane processes; with good purification the period of service of membranes is increased by several times;

a large significance is being attached to the studies of the membrane processes especially to high-temperature electrodialysis and inverse osmosis; at present there is a real technical possibility of constructing industrial equipment of inverse osmosis with productivity up to several hundred thousand cubic meters per day (USA).

REGULAR SESSION OF TECHNICAL COMMITTEE FORTY-FIVE OF MEC

V. V. Matveev and V. S. Zhernov

The regular sessions of the Technical committee 45 of MEC (International Electrotechnical Commission), its subcommittees (SC), and the working groups (WG) were held in Hague (Netherlands) from 18 to 27 October, 1973. Seventy-eight experts from 11 countries and representatives of other international organizations took part in the sessions. The delegation from the USSR was composed of the experts V. V. Matveev (head of the delegation), V. S. Zhernov, and L. G. Kiselev. The representative from Japan participated in the work of TC-45 for the first time.

We discuss the main results of the work and the plans of the future activities of TC-45, subcommittees 45A and 45B, and the working groups.

In the sessions of WG-1 (classification and terminology) two documents were discussed on terminologies and definitions used in the recommendations on multichannel analyzer and the terms included in chapter 9 of the third edition of International Electrotechnical Dictionary (MED). The remarks of national committees of a number of countries were discussed and changes in the definition and the names of the terms themselves were incorporated.

In the sessions of WG-3 (interchangeability) a large attention was given to the discussion of documents connected with standardization of the sizes of glass and plastic test tubes and test bottles for liquid scintillators. The national committees of England, France, and the USA manifested large interest in this problem. At present Technical committee 85 of the International Standards organization (ISO) is considering these problems. A document on the interface of the devices constructed on the module principle was discussed; two documents on the translation of the documents of the European Standards Committee for nuclear electronics (ESCNE) into documents of the secretariat of TC-45 according to KAMAK system were also discussed. A resolution was adopted that in the near future the main attention of WG-3 should be concentrated on the preparation of documents of MEC according to KAMAK system.

In the sessions of WG-6 (radio-isotope devices) two documents on radio-isotope thickness gauge and general recommendation on electrical measuring instruments, in which radioactive sources are used, were discussed. It is proposed to publish the second document in the form of a MEC publication. The preparation of a document on the terminology and methods of tests for radiation densimeters was planned.

In the sessions of WG-9 (detectors) the largest time was occupied by the discussion of a document on the methods of tests of PM for scintillation counters. The document is prepared for publication as MEC recommendations. The projects of publication 412 on the standard sizes of scintillators, publication 430 on the methods of tests of germanium detectors, and publication 340A on standard methods of tests of amplifiers and preamplifiers for semiconductor detectors were examined and recommended.

A document on the characteristics and methods of tests of detectors for reactor equipment was also discussed.

WG-10 (multichannel analyzer) examined the remarks of the national committees of England, USSR, USA, France, FRG, and Japan on the document "multichannel amplitude analyzers. Types, basic parameters, and technical requirements" were examined. This document was prepared by Soviet experts. The definitions included in it were discussed in the sessions of WG-1 and were essentially approved. The remarks of the national committees on the document "multichannel amplitude analyzers. Methods of tests"

Translated from Atomnaya Energiya, Vol. 36, No. 4, pp. 330-332, April, 1974.

© 1974 Consultants Bureau, a division of Plenum Publishing Corporation, 227 West 17th Street, New York, N. Y. 10011. No part of this publication may be reproduced, stored in a retrieval system, or transmitted, in any form or by any means, electronic, mechanical, photocopying, microfilming, recording or otherwise, without written permission of the publisher. A copy of this article is available from the publisher for \$15.00.

prepared on the basis of the proposals of the Soviet delegation, were also examined. It was decided to issue a new edition of the document which must include the description of the accelerated method of measurement of the differential nonlinearity of the analyzer with the number of quantization levels more than 4000 as a subsection. This subsection, prepared by the French delegation, was also discussed in the session of WG-10.

The document "amplifiers for multichannel amplitude analysis. Types, parameters, technical requirements, test conditions," prepared by the expert from FRG, was examined. This very complete document contains almost all the parameters that may characterize spectrometric amplifiers.

The document "equipment used with multichannel amplitude analyzers in the presence of high loading. Types, basic parameters, and methods of tests," prepared by the expert from the USA, was also discussed.

In the session of WG-11 (dc amplifiers) the remarks of the national committees on the document concerning dc amplifiers were examined. It was recommended that this be published as a MEC publication.

SC-45A (reactor instrument manufacture) heard reports on the activities of its working groups. It was recommended that the document "reactors with gaseous heat-transfer agent" be published as a MEC publication. It was decided that six documents of the secretariat be distributed to national committees after formation of the new editorial board for voting according to the six month rule. Among these documents are: "principles of construction of instruments for reactors with pressurized water" - Appendix to publication 231 of MEC; "principles of construction of instruments for channel-type nuclear reactors with heavy-water retarder cooled by water and vapor" - Appendix to publications 231 and 231A of MEC; "radiation detectors for instruments and systems of protection of nuclear reactors"; "use of systems of protection for other purposes not connected with safety"; "general recommendations on collection and evaluation of data for the determination of the characteristics of operation reliability of instrumentation of reactor protection systems."

It was decided to distribute two documents (high-temperature reactors with gaseous heat-transfer agent" and "liquid metal fast neutron reactors") to the national committees as the documents of the secretariat. A resolution was also adopted to send the recommendations of the French specialist on cable connections for reducing external pick up to the national committees as a secretariat document.

In the meetings of SC-45B (dosimetric instruments and radiation safety devices) and its working groups documents prepared by the secretariat and experts were discussed. In the open session the chairman of the SC informed about all the materials sent out as MEC publications, documents of the central bureau and the secretariat, prepared by the SC, and also mentioned the problems under consideration in a review of the activities of SC-45B from the time of its formation.

WG-B3 (meters and monitors of absorbed dose of β - and γ -radiations) discussed the goals and principles of measurement of the intensity of absorbed dose taking the requirements of publication 12 (§1) MCRH into consideration. The need for the measurement of two components of the radiation dose was agreed upon: the surface component acting on the skin and the penetrating component acting on the inner organs.

Although the group decided to concentrate its attention on instruments for the usual measurements, the need to examine the requirements on the calibration of these instruments was also recognized. In the first stage of development it was decided to examine only the terminology, the principles of measurement, and the methods of tests in respect of the radiation parameters. The electrical and mechanical characteristics, and the characteristics associated with the effect of the external medium are proposed to be discussed at the next stage of preparation of the recommendations.

The question of using the International System of units for the measurement of the absorbed dose and its intensity generated a discussion.

According to the resolution of WG-B4 (meters and monitors of radioactive gases) one of its tasks is essentially connected with the recommendation for meters and monitors of gases with the purpose of radiation protection of the workers. Projects of two documents on the control of tritium (oxide), radon and toron will be prepared.

It was also decided to prepare a plan of general recommendations on the determination of radioactive fallouts. These recommendations will be supplemented by the requirements connected with the control of noble gases.

The document "portable meters and monitors of intensity of low-energy x-ray or γ -ray radiations used in radiological protection," distributed to the national committees for voting in accordance with the six month rule, was approved and will be published as a MEC publication in the coming months.

Also the document "monitors and signaling devices of contamination of hands or feet" was distributed to the national committees for voting in accordance with the six month rule. The document "stationary meters, signal devices and monitors of intensity of radiation (x-ray or γ -ray radiation)" will be distributed for voting in accordance with the six month rule.

SC-45B examined the remarks on the document "meters and monitors of contamination by radioactive aerosols."

In the open plenary session of TC-45 a change of the secretary of TC-45 was announced. I. Treger (FRG) worked in this capacity for a long time and did much for strengthening international collaboration within the framework of MEC. The representative from FRG, M. Gandhi was nominated as the next secretary of TC-45.

The report of the secretariat of the committee on the results of voting in accordance with the six month rule, conducted by the national committees of the countries participating in the work of TC-45 MEC, and on 13 documents of the central bureau was presented and approved. These documents will be published shortly as MEC recommendations on different problems of standardization of the products of nuclear instrument manufacturing. The remarks of the national committees on a plan of 11 recommendations, sent out as secretariat documents, were also examined.

The detailed reports of the chairman of the subcommittees and working groups on their activities were also presented and approved. During the discussion of the reports of SC-45A and SC-45B a further enlargement of their activities and an increase in the interest in their work in many countries of the world was noted. Thus, in the sessions of SC-45A 24 experts from 9 countries participated; 22 experts from 10 countries participated in the sessions of SC-45B. Besides, representative from a number of international organizations also took part.

In the discussion of the report of WG-1 the termination of the work on the preparation of the third publication of MEC was mentioned, which marks an important phase in the field of systematization of concepts and international standardization of terminologies and definitions.

The chairman of the committee A. Riss (France) made a special mention of the fruitful activity of WG-9.

A further extension of the range of problems, with which WG-10 was concerned, caused considerable discussion. As an exception the committee decided that WG-10 start the preparation of two new documents related to the use of pulsed amplifiers used for spectrometry and to precision oscillators.

It was noted that the task of preparation of the document on dc amplifiers assigned to WG-11 was successfully completed. In view of this group finished its work and was dissolved.

The chairman of TC-45 proposed the creation of a new working group for the preparation of a document on logarithmic and linear intensity meters. The national committees were asked to express their opinion on the subject.

Information was given on the session held by the operating committee of MEC jointly with the chairmen of the technical committees on working out standards for designs of electronic equipment and on the attitude of MEC toward KAMAK system. It was mentioned that the problems of designs are being considered by several technical committees of MEC and there is a lack of the necessary coordination of their activities. Therefore all the work is evenly distributed by the operating committee of MEC among the respective committees and subcommittees. The designs of all form of equipment will be under the jurisdiction of the newly formed TC-48 of MEC. TC-45 is assigned the work of translation of the documents of ESCNE committee into MEC documents in accordance with KAMAK system. WG-3 will be concerned with further examination of these problems.

Problems of interaction of TC-45 of MEC with ISO, MCRE, and other international organizations were also discussed.

INTERNATIONAL SYMPOSIUM ON NUCLEAR ELECTRONICS

A. N. Sinaev

The VII international symposium on nuclear electronics, organized by the Joint Institute of Nuclear Research jointly with the Central Institute of Physical Research (CIPR) of the Academy of Sciences of the Hungarian National Republic, was held in Budapest in September 1973. It was devoted to the automatization of physical experiment with the use of small computers operating in real time. About 100 specialists from the countries participating in the JINR took part in the symposium and about 60 papers were presented.

A number of papers reported the development of electronic blocks in KAMAK standard proposed by the European Standards Committee (ESCNE) on nuclear electronics. The activities of this committee were narrated by its member R. Trekhchinskii (Poland). At present the committee is working on the development of a standard for nuclear research and its extension to other branches of science and technology. A large attention is being devoted to the development of a series system which would permit to connect a large number of frames, and also to the development of special programming languages. During the last two years significant advances in the use of KAMAK standard have been made in the institutes of a number of countries participating in the JINR. A large set of counters, registers, converters of amplitude into a code, nanosecond blocks, controllers for coupling with computer of different types etc., have been developed in the laboratories of the JINR. Several papers on the development of blocks in KAMAK standard were presented by the Institutes from Hungary and Poland.

In some countries participating in the JINR industrial production of equipment in KAMAK standard individual elements of this standard has started. In Hungary a number of blocks (counters, input and output registers, converters, distributors, controllers, etc.) have been developed and are ready for serial production. In Poland frames with supply sources are being produced and in Czechoslovakia 86-contact and coaxial joints are being prepared.

The equipment and methods of presentation of data directly during the experiment occupied a significant place in the symposium. Different types of displays on electron-beam tubes were communicated in the papers. Sufficiently universal displays have been developed at the Institute of Nuclear Physics at Rzhesh (Czechoslovakia) and at the Neutron Physics Laboratory of the JINR. These displays have a tube with magnetic deflection; along the axes of the tube 1024 points are arranged. They contain vectors and sign generators and are equipped with light pencil and other interaction devices. Simpler and cheaper specialized displays were presented by the Technical University of GDR (Dresden) and the laboratory of nuclear reactions of the JINR. These displays are made on the basis of oscillographic tubes and are equipped with movable markers. At the CIPR of Hungary television type displays have been developed.

A large attention was devoted to the instrumentation of measuring-computational centers which would permit to conduct several experiments simultaneously. V. Zakharov (England), who was present as a guest, talked about a system including about 10 small computers of different types which can be used in the experiments simultaneously. These computers are connected to a central computer (IBM-370/165) through a medium class buffer computer (IBM-1802); the central computer has a fast operating memory of 2 M bits and abundant peripheral equipment. The smaller computers are terminals of the central computer and are freed from the function of analysis of the arriving information. Through an interactive display each experimenter can carry out direct dialogue with the central computer and can make use of all its abundant mathematical facilities. The use of KAMAK standard imparts a large flexibility to the entire system.

The laboratory of nuclear problems of the JINR presented a paper about the experience in operation of a system using a HP-2116C computer with sufficiently large peripheral equipment connected with six

Translated from *Atomnaya Energiya*, Vol. 36, No. 4, pp. 332-333, April, 1974.

© 1974 Consultants Bureau, a division of Plenum Publishing Corporation, 227 West 17th Street, New York, N. Y. 10011. No part of this publication may be reproduced, stored in a retrieval system, or transmitted, in any form or by any means, electronic, mechanical, photocopying, microfilming, recording or otherwise, without written permission of the publisher. A copy of this article is available from the publisher for \$15.00.

measuring-accumulating devices, used in the experiments. The center created in Rossendorf (GDR) is based on two type TRA computers connected to a large computer. An original system for simultaneous conduction of experiments based on a memory device has been developed at the Institute of Atomic Physics in Bucharest.

Among the experimental equipment made in KAMAK standard and directly connected to a computer, mention should be made of a system consisting of four frames and instruments for measuring of the parameters of synchrotron pulses (High Energy Laboratory of the JINR), a system of counters (Laboratory of Nuclear Problems of the JINR), a device for the investigation of the behavior of a beam in the adhesion of the collective accelerator (Division of New Methods of Acceleration, JINR), a system of control by neutron spectrometer (Sverk, Poland), and a system for the selection of scattering events (Institute of Nuclear Physics, Leningrad). Of considerable interest are also equipment connected with a computer such as the system of multiparametric analysis with digital windows (Laboratory of Nuclear Reactions of the JINR), equipment for the study of proton-proton scattering at the extracted synchrotron beam (Laboratory of Computational Technology and Automatization, JINR), a system for the study of annihilation of electrons in an accelerator with counter beams (Institute of Nuclear Physics, Novosibirsk), etc.

A small-size 1024-channel analyzer based on integrated circuits ICA-70 has been developed at the CIPR in Hungary for industrial production; it is intended for extensive use.

The proceedings of the symposium will be published by the publications division of the JINR.

V FORATOM CONGRESS

M. Matushek and P. Strugar

The V Foratom congress was held in Florence from 15 to 19 October, 1973. The theme of the congress was "atomic power stations in West Europe, yesterday, today, and tomorrow." Besides the representatives from the 15 West European countries, who are members of Foratom (Austria, Belgium, Great Britain, Netherlands, Denmark, Spain, Italy, Luxemburg, Norway, Portugal, Finland, France, FRG, Sweden, Switzerland) delegates from the USA, Canada, and Japan, and observers from Australia, Brazil, Hungary, GDR, Greece, Israel, Poland, Turkey, and Yugoslavia were present at the congress. Representatives from IAEA, European economic commission of the UNO and other organizations, in all 850 persons from 27 countries were present.

A special feature of this congress, unlike the preceding congresses which were devoted to a more narrow range of problems, was the discussion of the entire complex of problems of nuclear energetics in West Europe. Thus, for example, fast reactors were discussed in the congress in London 6 years ago and fuel cycles were discussed in the congress in Stockholm 3 years ago.

Each session started with one review article prepared by the organizers of the congress, the representatives from Italy. Afterwards, in the discussion opened on the paper, the delegates from three non-European countries (USA, Canada, and Japan) were invited to take part.

We shall dwell on the main problems discussed at the congress.

1. Experience Gathered in the Field of Design and Construction of APS. The most important factors in construction of APS are: a trend toward the decrease of the dependence on classical energy sources, the requirement and possibility of development of intrinsic industry and for acquiring experience in utilization of new technologies, advantages in respect of protection of the environment, and only in the last place the hope that nuclear power will become more economical than the conventional forms and sources of energy.

During the discussion on the types of agreements on the construction of APS the dominant opinion was that the responsibility of the construction must rest with a single organ. Most of the countries were in favor of the so-called turn-key agreement about completely manned APS. Nevertheless, for the time being all the countries are unanimous only in this respect that the nuclear part of a power station should be constructed on the basis of the turn-key agreement. An interesting example is the treaty signed by Finland with the USSR for the construction of a nuclear reactor, in which she imports the equipment from FRG and herself takes an active part in the construction. The advantages of such a construction are larger adaptability to local conditions and smaller cost; the disadvantages are the larger risk in respect of reliability of the installations and meeting the schedule of construction.

It is typical that in the construction of APS the predicted periods are generally passed. The main reasons for the delay of the construction are limited experience in the use of the new technology, introduction of technological novelties during the construction, absence of norms on safety or their nonconformity in local conditions, and the use of new materials and criteria for checking the quality. In order to avoid these problems it is proposed to have maximum possible standardization of the objects. According to the participants experience has shown that changes should not be introduced in the course of the construction because the problems appearing in this case can cancel out all the positive effects of such changes.

It was pointed out that the capital investment in the mechanical base of nuclear energetics is too high and the industrial potential of each European country individually is too low to justify the existence of specialized plants. Therefore it is advantageous to rely on the industry specialized in the field of design and construction of classical power stations.

Translated from Atomnaya Energiya, Vol. 36, No. 4, pp. 333-335, April, 1974.

© 1974 Consultants Bureau, a division of Plenum Publishing Corporation, 227 West 17th Street, New York, N. Y. 10011. No part of this publication may be reproduced, stored in a retrieval system, or transmitted, in any form or by any means, electronic, mechanical, photocopying, microfilming, recording or otherwise, without written permission of the publisher. A copy of this article is available from the publisher for \$15.00.

2. Progress in the Field of Design and Construction of APS. It is accompanied by a constant complication of the design technology, the output, and first of all the verification that the new standards and requirements set forth by social organizations are satisfied. As a result APS get complicated, the period of construction gets prolonged, and in the final analysis their cost increases.

The present time is characterized by a large increase of the unit power of reactors (from a thermal power of 500 MW for APS of the first generation to 3800 MW) and a sharp increase of the number of atomic power stations. This requires an analysis of possible breakdowns, no longer of a single isolated APS, but of a complex of APS.

The time that passes from the moment of taking decision on the construction of an APS to its putting into operation is increasing in most West European countries and is 8-10 years on the average. Of this 3-4 years are spent in the choice of the area, in obtaining permission for the construction, and in other heuristic measures. The construction work begins after 4 years on the average and the installation 6 years after the decision on construction has been taken. It is obvious that a correct estimate of the future energy requirements as well as timely decision on the construction of APS is of decisive importance.

In recent years the specific cost of APS has not increased primarily because of the increase in the power of their blocks. In FRG, for example, the specific cost varies from 1050-1100 mark/kW (el) for blocks with 950-100 MW (el) and from 900 to 950 marks for blocks with 1250-1320 MW (el). Nevertheless, it should be noted that with a further increase of the unit power the specific cost will not decrease; on the contrary it will increase. The ratio of the specific cost of APS to the specific cost of TPS is used as a rough criterion for the economic index of APS. For USA this ratio is 1.6, for France it is 1.4, and for Spain 1.55.

The role of APS in resolving the problem of conservation of the environment was noted. From the very beginning of the development of nuclear energetics there was the requirement for the fulfillment of very strict measures of conservation of environment and safety, which resulted in an increase of the cost of atomic energy and a certain lag of its competitive capacity in comparison to other forms of energy. Nevertheless, these unfavorable circumstances have subsequently become indisputable advantage especially in thickly populated countries where the problem of contamination of the environment is very acute.

3. Hopes for Further Development of Nuclear Energetics. The experience in commercial operation of APS in ten countries, which are members of Foratom, has been gained over ten years (1962-1972) and refers to 32 APS (216 reactor years) with total rated power of 12,040 MW (el). Among these 64.4% (158 reactor years) are graphite-gas reactors, 35% (53 reactor years) are light-water reactors, and 0.6% (4.5 reactor years) are heavy-water gas-cooled reactors. The collected data permit reliable conclusions about the operation of APS, their safety, and the problems of protection of the environments. At the same time these data are a very reliable index in planning further development of nuclear energetics.

It is expected that by 1980 the power of APS in West Europe will be over 70,000 and by 1985 ~160,000 MW (el). This will equal 10-20% of the total electrical power in 1980 and 20-30% in 1985. Since APS will always operate with large average load, the specific weight of APS in the generation of electric power will be still larger. In Sweden and Spain, for example, it will be about 50% by 1985. Long-range prognosis shows that toward the end of the century in industrially developed countries about 60% of the power potential will be ensured by APS.

In the next two years the demands on the construction of APS will be 12,000 MW (el)/yr, and from 1976 to 1980 it will be 17,000 MW (el)/yr. The power of the blocks will vary in the range 900-1300 MW (ten latest norms of safety stipulate a limit of power at 1300 MW (el)). It is assumed that in the member countries of Foratom have sufficient capacity for the design and construction of APS and production of all the necessary components. They can satisfy their own requirements and ensure an export of 3-4 complexes of APS per year.

In the foreseeable future there is no reason to fear scarcity of nuclear fuel and no appreciable increase in its cost is predicted. It is assumed that the present capacity for the reprocessing of irradiated fuel is sufficient. What is considered insufficient is the technology of the process and the capability of uranium enrichment. This problem has become specially acute due to almost complete reorientation to light-water reactors.

Taking an overall view, in the coming years less attention will be paid to further improvement of the technical data of reactors. All the same improvements with the purpose of reducing the construction cost

and increasing the safety of APS will be carried out. The basic problem of industrial development of APS is striving toward standardization of components and increase of reliability of operation.

In resolving the problems of safety and environment protection special significance is attached to the selection of the site for the APS. Up till now the idea has prevailed that the APS should be constructed as far from populated points as possible. The greatest attention has been given to such effects as heating of water used for cooling the condensers. Less attention has been given to the problems of storage of radioactive wastes, which will apparently be successfully resolved by consolidation of highly active liquid wastes and their burial in geological formations suitable for this purpose.

It is useful to cite some of the results communicated by the representatives from USA, Japan, and Canada. In USA 39 APS have been operated up to October, 1973; 55 are being constructed and 90 have received order; decision has been taken on the construction of 16 more APS. The most important reasons for the construction of such a large number of APS are given as the constant growth of demand on all forms of energy, in particular, of electrical energy, and the tendency toward further increase; depletion of intrinsic resources of organic fuel which at the present rate of consumption will last till 2012-2050; expectations that the expenditure in the production of energy from APS will be lower than from TPS in spite of the large cost of APS.

In Japan there are five APS in operation; their power is 1823 MW (el); 17 APS at 13,633 MW are being constructed. The construction of APS is justified on the following considerations: the need to have more reliable energy source; hope that even in the near future nuclear energy can compete with the energy from traditional sources in respect of its cost; advantages of APS from the point of view of ecology. All the reactors in Japan are light-water reactors excepting one which has gas-cooled graphite reactor.

In Canada even in future preference will be given to its own heavy-water reactor of type CANDU. Such of its advantages as low fuel component of energy, high level of utilization of natural uranium, excellent technology of production of fuel elements ensuring high reliability of operation; continuous replacement of the fuel during the operation of the reactor; the presence of a series of power reactors of different powers with standardized components and similar technology are also cited.

4. Economic Aspects and Role of Thermal and Fast Reactors. Of the types of reactors checked, light-water reactors (boiling and with water under pressure) have undoubtedly an advantage from technical and economical point of view. In West Europe all the APS being constructed or planned for construction will be equipped with light-water reactors with the exception of the APS in Great Britain and prototype and experimental reactors. It is thought that they satisfy the maximum fraction of the need of atomic energy in the near and foreseeable future. However, a certain significance of other types of reactors is also not excluded.

Of the improved reactors (converters) apparently the most promising are reactors using natural uranium with heavy water as retarder and heat-transfer agent. Such reactors have excellent characteristics also as plutonium producer; they can play a significant role in the introduction of fast reactors and repeated use of possible excess of plutonium. It is also thought that heavy-water reactors cooled by ordinary boiling water deserves further development, since it has all the positive qualities of heavy-water reactors and permits a sharp reduction of the losses of heavy water. High-temperature gas reactors also draw special attention; they are being developed mainly in two directions: for operation with gas turbine directly and for use of high temperatures in certain industrial processes.

A large part of the basic and applied research in the countries of West Europe is devoted to fast breeder reactors. Mainly one type, i.e., a reactor cooled by liquid sodium and having fuel in the form of a mixture of uranium and plutonium oxides is being developed. Other types of fast breeder reactors, for example, high-temperature gas reactors are still at the stage of preliminary investigation.

BRIEF COMMUNICATIONS

Fourth Regular Session of All-Union School of Theoretical Nuclear Physics at Moscow Engineering Physics Institute was held from 6 to 20 June, 1973 on the country grounds of MEPI. Forty young scientific workers and teachers representing almost all institutes and universities, where work on the physics of the nucleus is being carried out, participated in the session. This session was devoted to certain promising directions in the investigation of the structure of the nucleus.

The lecture formulated the urgent tasks and problems which can serve as the topics for theoretical research in nuclear physics.

Detailed abstracts of all the lecture courses were published at MEPI toward the start of the session. Besides the participants of the session the scientific libraries of the corresponding institutes and universities also have these abstracts.

It was the unanimous opinion of the participants that the session was a success, which was contributed by the high scientific level of the lectures, a clear organization of the school, and the excellent conditions created for work by the participants.

A Meeting of Experts of IAEA on Evaluation of Radiation Doses in Population was held from October 29 to November 2, 1973 in Warsaw. Twenty-three experts from 12 countries took part in the meeting along with three representatives of international and regional organizations. The object of the meeting was to discuss the contents of a report prepared under the aegis of the IAEA and containing methods and examples of estimates of individual, collective, and population doses from the fall outs of radioactive substances into the outer medium and from other uses of sources of ionizing radiation in different spheres of human activity.

The advisability of giving examples of estimate of collective doses for the following cases in the second part of the document was recognized; from construction materials; from individual biologically active isotopes arriving into the organism through complex food chains; from transportation of irradiated fuel elements and other radioactive substances; from clouds of inert radioactive gases; from medicinal procedures.

Translated from *Atomnaya Energiya*, Vol.36, No.4, pp.335-336, April, 1974.

© 1974 Consultants Bureau, a division of Plenum Publishing Corporation, 227 West 17th Street, New York, N. Y. 10011. No part of this publication may be reproduced, stored in a retrieval system, or transmitted, in any form or by any means, electronic, mechanical, photocopying, microfilming, recording or otherwise, without written permission of the publisher. A copy of this article is available from the publisher for \$15.00.

BOOK REVIEWS

N. G. Gusev, L. R. Kimel',
E. E. Kovalev, V. P. Mashrovich,
B. G. Pologikh, and A. P. Suvorov

PROTECTION FROM IONIZING RADIATIONS VOLUME II. PROTECTION FROM RADIATIONS OF NUCLEAR ENGINEERING INSTALLATIONS

Reviewed by S. G. Tsypin

The book under review [for a review of Vol. I, see *Atomnaya Energiya*, 35, 151 (1973)] is a textbook. It includes eight chapters and two appendices.

The basic problems of protection from the radiations of real nuclear engineering installations and concrete radiation sources are discussed. Problems of protection of the active zone and the system of the coolant of the nuclear reactor, thermal calculation of protection, and the passage of radiations through inhomogeneities in the shielding, protection from the γ -radiation of fission products, problems of radiation safety in the production of uranium, radium, and fuel cells, and questions of the protection of accelerators and radiation safety during space flights are presented in detail.

The two examples of the calculation of shielding cited in the end of the book illustrate the use of the theoretical material of the book for the solution of one of the most complex problems of radiation protection.

The discussion is conducted at a rather high scientific and theoretical level. The systematic exposition of the problems of protection from the radiations of a wide assortment of sources of real nuclear engineering installations is cited for the first time not only in the textbook, but also in the monograph literature. This makes the book useful not only for students, but also for scientists, graduate students, engineers, and designers occupied with these problems.

Together with the "Collection of Problems in Dosimetry and Protection from Ionizing Radiations" (V. I. Ivanov and V. P. Mashkovich) and the handbooks "Protection from Ionizing Radiations" (L. R. Kimel' and V. P. Mashkovich) and "Protection from the γ -Radiation of Fission Products" (N. G. Gusev), recently published by Atomizdat, the textbook under review concludes the cycle of works essential for the study of a course in the physics of protection from ionizing radiation by students of physical engineering and physico-technical colleges of the country.

It is pleasant to note that the indicated textbooks, published by Atomizdat, are the first in world practice.

We should make some remarks about the second volume of the textbook under review:

- 1) the inclusion of problems of protection of the external environment – one of the most complex and acute problems of our time – in the book seems essential;
- 2) it would be advisable to discuss in this volume the general principles of the design of protection of nuclear engineering installations, problems of protection in the use of radiation sources in the national economy, and to take up the materials used in the construction of the shielding, organization and problems of the radiation safety service;

Translated from *Atomnaya Energiya*, Vol. 36, No. 4, p. 336, April, 1974.

© 1974 Consultants Bureau, a division of Plenum Publishing Corporation, 227 West 17th Street, New York, N. Y. 10011. No part of this publication may be reproduced, stored in a retrieval system, or transmitted, in any form or by any means, electronic, mechanical, photocopying, microfilming, recording or otherwise, without written permission of the publisher. A copy of this article is available from the publisher for \$15.00.

- 3) it would have been advisable to place chapters XI and XII ("Thermal Calculation of Shielding" and "Passage of Radiation Through Inhomogeneities in the Shielding") in the first volume;
- 4) the order of arrangement of the material in the book is not very successful; a good criterion for the placement of chapters IX, X, XII, and XIV might be the technological series, and the indicated chapters then should have followed the order: XIV, XIII, IX, X.

breaking the language barrier

WITH COVER-TO-COVER ENGLISH TRANSLATIONS OF SOVIET JOURNALS

in mathematics and information science

Title	# of Issues	Subscription Price
Algebra and Logic <i>Algebra i logika</i>	6	\$120.00
Automation and Remote Control <i>Avtomatika i telemekhanika</i>	24	\$215.00
Cybernetics <i>Kibernetika</i>	6	\$140.00
Differential Equations <i>Differentsial'nye uravneniya</i>	12	\$175.00
Functional Analysis and Its Applications <i>Funktsional'nyi analiz i ego prilozheniya</i>	4	\$110.00
Journal of Soviet Mathematics	6	\$135.00
Mathematical Notes <i>Matematicheskie zametki</i>	12 (2 vols./yr. 6 issues ea.)	\$185.00
Mathematical Transactions of the Academy of Sciences of the Lithuanian SSR <i>Litovskii Matematicheskii Sbornik</i>	4	\$150.00
Problems of Information Transmission <i>Problemy peredachi informatsii</i>	4	\$125.00
Siberian Mathematical Journal of the Academy of Sciences of the USSR Novosibirski <i>Sibirskii matematicheskii zhurnal</i>	6	\$215.00
Theoretical and Mathematical Physics <i>Teoreticheskaya i matematicheskaya fizika</i>	12 (4 vols./yr. 3 issues ea.)	\$160.00
Ukrainian Mathematical Journal <i>Ukrainskii matematicheskii zhurnal</i>	6	\$155.00

SEND FOR YOUR
FREE EXAMINATION COPIES

PLENUM PUBLISHING CORPORATION

Plenum Press • Consultants Bureau
• IFI/Plenum Data Corporation

227 WEST 17th STREET
NEW YORK, N. Y. 10011

In United Kingdom: 4a Lower John Street,
London W1R 3PD, England

Back volumes are available.

For further information, please contact the Publishers.

breaking the language barrier

WITH COVER-TO-COVER
ENGLISH TRANSLATIONS
OF SOVIET JOURNALS

in physics

SEND FOR YOUR
FREE EXAMINATION COPIES

PLENUM PUBLISHING CORPORATION

227 WEST 17th STREET
NEW YORK, N. Y. 10011

Plenum Press • Consultants Bureau
• IFI/Plenum Data Corporation

In United Kingdom: 4a Lower John Street,
London W1R 3PD, England

Title	# of Issues	Subscription Price
Astrophysics <i>Astrofizika</i>	4	\$120.00
Fluid Dynamics <i>Izvestiya Akademii Nauk SSSR mekhanika zhidkosti i gaza</i>	6	\$180.00
High-Energy Chemistry <i>Khimiya vysokikh energii</i>	6	\$155.00
High Temperature <i>Teplofizika vysokikh temperatur</i>	6	\$150.00
Journal of Applied Mechanics and Technical Physics <i>Zhurnal prikladnoi mekhaniki i tekhnicheskoi fiziki</i>	6	\$175.00
Journal of Engineering Physics <i>Inzhenerno-fizicheskii zhurnal</i>	12 (2 vols./yr. 6 issues ea.)	\$175.00 (\$87.50/vol.)
Magnetohydrodynamics <i>Magnitnaya gidrodinamika</i>	4	\$125.00
Mathematical Notes <i>Matematicheskie zametki</i>	12 (2 vols./yr. 6 issues ea.)	\$185.00
Polymer Mechanics <i>Mekhanika polimerov</i>	6	\$140.00
Radiophysics and Quantum Electronics (Formerly Soviet Radiophysics) <i>Izvestiya VUZ. radiofizika</i>	12	\$180.00
Solar System Research <i>Astronomicheskii vestnik</i>	4	\$ 95.00
Soviet Applied Mechanics <i>Prikladnaya mekhanika</i>	12	\$175.00
Soviet Atomic Energy <i>Atomnaya energiya</i>	12 (2 vols./yr. 6 issues ea.)	\$175.00 (\$87.50/vol.)
Soviet Physics Journal <i>Izvestiya VUZ. fizika</i>	12	\$180.00
Soviet Radiochemistry <i>Radiokhimiya</i>	6	\$165.00
Theoretical and Mathematical Physics <i>Teoreticheskaya i matematicheskaya fizika</i>	12 (4 vols./yr. 3 issues ea.)	\$160.00

Back volumes are available. For further information, please contact the Publishers.